

AN EVALUATION OF THE POTASSIUM
STEAM BINARY CYCLE

James Allen Pesar

LIBRARY
NAVAL POSTGRADUATE SCHOOL
MONTEREY, CALIFORNIA 93940

AN EVALUATION OF THE POTASSIUM-STEAM BINARY CYCLE

by

JAMES ALLEN PESAR

/

B.M.E., UNIVERSITY OF DAYTON
(1966)

M.S.M.E., PURDUE UNIVERSITY
(1968)

SUBMITTED IN PARTIAL FULFILLMENT OF
THE REQUIREMENTS FOR THE
DEGREE OF OCEAN ENGINEER AND THE
DEGREE OF MASTER OF SCIENCE IN
NAVAL ARCHITECTURE AND MARINE ENGINEERING

AN EVALUATION OF THE POTASSIUM-STEAM BINARY CYCLE

by

James A. Pesar

Submitted to the Department of Ocean Engineering on 7 May 1976, in partial fulfillment of the requirements for the degrees of Ocean Engineer and Master of Science in Naval Architecture and Marine Engineering.

ABSTRACT

A thermodynamic and economic analysis of the potassium-steam binary cycle is presented. The thermodynamic study includes an examination of the potassium cycle, and a first and second law analysis of the binary cycle. The investigation of two different sets of potassium turbine inlet conditions, with variable condensing potassium conditions, operating with a fixed steam cycle is presented. This analysis reveals that the single, most important parameter in the selection of potassium cycle design conditions is the condensing potassium-steam temperature difference. The cycle configurations with the smaller temperature difference are both less expensive to operate, as well as less expensive in total capital cost per unit electrical output.

The analysis was performed by implementation of a WATFIV computer program which evaluates the engineering properties of potassium using a virial form of the equation of state.

Thesis Supervisor: A. Douglas Carmichael

Title: Professor of Power Engineering

ACKNOWLEDGEMENTS

The author extends his appreciation to Professor A. Douglas Carmichael, under whose guidance this work was accomplished. His thoughtful suggestions and recommendations were invaluable in the preparation of this thesis.

I also wish to thank Elaine Govoni for her careful and thorough work in the typing of this thesis.

Finally, I wish to acknowledge the love, support, and understanding of my wife, Puring, and my daughter, Jennifer Ann, during the preparation of this thesis and during the past three years.

TABLE OF CONTENTS

| | |
|---|----|
| Title Page..... | 1 |
| Abstract | 2 |
| Acknowledgements..... | 3 |
| Table Of Contents | 4 |
| List Of Figures..... | 6 |
| List Of Tables..... | 10 |
| List Of Notations Used In Text | 11 |
| Chapter 1. Introduction | 13 |
| 1.1 Background..... | 13 |
| 1.2 Potassium As A Topping Cycle Fluid | 16 |
| Chapter 2. Literature Survey | 19 |
| Chapter 3. Thermodynamic Analysis | 26 |
| 3.1 First Law Analysis Of The Binary Cycle | 26 |
| 3.2 Rankine Cycle Potassium Plant..... | 31 |
| 3.3 Bottoming Cycle | 47 |
| 3.4 Second Law Analysis Of Binary Cycle Plant..... | 48 |
| Chapter 4. Power Plant Configuration | 65 |
| Chapter 5. Economic Analysis | 73 |
| 5.1 Background | 73 |
| 5.2 Capital Cost Determination..... | 73 |

TABLE OF CONTENTS (Continued)

| | | |
|------------|---|-----|
| Chapter 6. | Optimum Cycle | 83 |
| Chapter 7. | Conclusions | 87 |
| References | | 89 |
| Appendix A | Program Variable Listing | 92 |
| Appendix B | Properties Of Potassium..... | 98 |
| Appendix C | Potassium Condenser-Steam Boiler Sizing..... | 111 |
| Appendix D | Main Program..... | 116 |

LIST OF FIGURES

| NO. | TITLE | PAGE |
|------|---|------|
| 1-1 | Allowable Design Stress In Primary Combustor Materials | 14 |
| 1-2 | Binary Cycle Temperature Entropy Diagram | 15 |
| 3-1 | Major Components Of Potassium Steam Binary Cycle | 27 |
| 3-2 | Temperature Entropy Diagram For Potassium Steam Binary Cycle | 28 |
| 3-3 | Effect Of Topping Cycle Condensing Pressure On Potassium Steam Binary Cycle Overall Thermal Efficiency | 30 |
| 3-4 | Effect Of Turbine Inlet Temperature On Potassium Steam Binary Cycle Overall Thermal Efficiency | 33 |
| 3-5 | Simple Potassium Rankine Cycle Plant | 34 |
| 3-6 | Effect Of Boiler Pressure Of Simple Potassium Rankine Cycle Efficiency | 36 |
| 3-7 | Effect Of Superheating On Thermal Efficiency In The Potassium Rankine Cycle | 37 |
| 3-8 | Effect Of Condensing Pressure On Thermal Efficiency For The Simple Potassium Rankine Cycle | 38 |
| 3-9 | Simplified Potassium Regenerative Cycle With One Regenerative Feed Heater | 40 |
| 3-10 | Effect Of Regenerator Pressure Ratio On Thermal Efficiency For Simplified Potassium Regenerative Feed Heating Cycle | 42 |

LIST OF FIGURES (Continued)

| NO. | TITLE | PAGE |
|------|---|------|
| 3-11 | Effect Of Regenerator Pressure Ratio On Potassium Cycle Thermal Efficiency | 43 |
| 3-12 | Percent Extracted For Regeneration As A Function Of Pressure Ratio In The Potassium Regenerative Feed Heating Cycle | 45 |
| 3-13 | Effect Of Condensing Pressure On Thermal Efficiency Of Potassium Regenerative Cycle | 46 |
| 3-14 | Enthalpy-Entropy Diagram For Fixed Steam Bottoming Cycle | 49 |
| 3-15 | Major Heat Transfer Processes In Potassium Steam Binary Cycle | 52 |
| 3-16 | Potassium Condenser-Steam Boiler Available Energy For Potassium Steam Binary Cycle | 53 |
| 3-17 | Unavailable Energy Due To Potassium Steam Heat Transfer Process In The Potassium Binary Cycle | 54 |
| 3-18 | Potassium Cycle - Ideal Heat Engine Binary Cycle | 56 |
| 3-19 | Effect Of Condensing Temperature On Potassium Steam Binary Cycle Overall Efficiency | 60 |
| 3-20 | Effect Of Condensing Temperature On Percent Decrease In Ideal Thermal Efficiency For The Potassium Steam Binary Cycle | 61 |

LIST OF FIGURES (Continued)

| NO. | TITLE | PAGE |
|------|--|------|
| 3-21 | Effect Of The Dimensionless Temperature Ratio On Overall Thermal Efficiency For The Potassium Steam Binary Cycle | 62 |
| 3-22 | Effect Of Dimensionless Temperature Ratio On The Decrease In Thermal Efficiency For The Potassium Steam Binary Cycle | 63 |
| 4-1 | Vertical Section Through Potassium-Boiler Furnace Unit | 66 |
| 4-2 | Horizontal Cross Section Through Potassium-Boiler Furnace Unit | 67 |
| 4-3 | Tube Bundle Module For Potassium Boiler | 68 |
| 4-4 | Section Through A Re-Entry Tube For The Potassium Boiler Steam Condenser | 70 |
| 4-5 | Potassium Turbine - Condenser Arrangement | 71 |
| 5-1 | Capital Cost Per KW As A Function Of The Dimensionless Temperature Ratio | 71 |
| 5-2 | Operating Cost Per KW Hr As A Function Of The Dimensionless Temperature Ratio | 82 |
| 6-2 | Optimum Potassium-Steam Binary Cycle | 85 |
| B-1 | Flow Chart For Property Determination By Subroutine WET | 102 |
| B-2 | Mollier Diagram For Potassium Vapor | 105 |

LIST OF FIGURES (Continued)

| NO. | TITLE | PAGE |
|-----|---|------|
| C-1 | Flow Chart For Calculation Of Reheater Parameters | 113 |
| D-1 | Flow Chart For Determination Of Properties Of Potassium | 119 |
| D-2 | Illustration Of Searching Procedure Used To Determine Values Of Entropy and Enthalpy of Potassium | 125 |

LIST OF TABLES

| NO. | TITLE | PAGE |
|-----|--|------|
| 1-1 | Comparison Of Physical Properties Of Potassium And Water For Condens- ing Conditions | 18 |
| 3-1 | Performance Parameters Of Binary Cycle | 32 |
| 3-2 | Performance Parameters For Potassium Rankine Cycle Plant | 35 |
| 3-3 | Performance Parameters For Simplified Regenerative Feed Heating Cycle | 41 |
| 3-4 | Primary Points In Bottoming Cycle | 50 |
| 3-5 | Summary Of Power Output For Bottoming Cycle | 51 |
| 3-6 | Summary Of Second Law Analysis | 57 |
| 5-1 | Topping Cycle Unit Costs | 76 |
| 5-2 | Cost Distribution For 35.00psia 1700°F Topping Cycle Inlet Con- dition Binary Cycle | 79 |
| 5-3 | Cost Distribution For 30.86psia 1550°F Topping Cycle Inlet Condition Binary Cycle | 80 |
| 6-1 | Parameters Of Optimum Potassium Steam Binary Cycle | 86 |

LIST OF NOTATIONS USED IN TEXT

| | |
|-----------|--|
| A | Heat exchanger surface area (ft ²) |
| d | Tube diameter (in) |
| h | Potassium specific enthalpy (BTU/lbm) |
| J | 778 ft lbf/BTU |
| k | Thermal conductivity (BTU/hr ft°F) |
| L | Length (ft) |
| \dot{m} | Mass flow rate (lbm/hr) |
| N | Number of tubes in heat exchangers |
| P | Pressure (lbf/in ²) |
| P_e | Electrical power (MW) |
| PR | Regenerator to turbine inlet pressure ratio |
| \dot{Q} | Heat transfer rate (BTU/hr) |
| s | Potassium specific entropy (BTU/lbm °R) |
| T | Temperature (°F) |
| \bar{T} | Average temperature of heat addition |
| v | Potassium specific volume (ft ³ /lbm) |
| \dot{w} | Rate of output shaft work (BTU/hr) |
| x | Vapor quality |
| y | Ratio of mass flow extracted for regeneration to total boiler mass flow rate |
| η | Thermal efficiency |

Subscripts

| | |
|----|------------------------------|
| AV | Available energy (BTU/hr) |
| B | Quantity evaluated in boiler |

in Increase in unavailable energy
K Potassium property
KC Potassium property evaluated at condensing conditions
S Entropy averaged property
SC Property evaluated at condensing conditions of steam
t thermal efficiency
to Overall thermal efficiency

NOTE: (1) Numerical subscripts refer to properties evaluated at specific points;

(2) Notion for FORTRAN programming is found in Appendix A.

1. INTRODUCTION

1.1 BACKGROUND

During the past several years, there has been a steep increase in the cost of fuel. In an effort to increase the efficiency of central power generating stations, the peak temperatures and pressures of steam plants have been increased. However, these increases in peak temperature and pressure have caused serious problems since the strength of metal alloys available today falls off rapidly with increasing temperature. Figure 1-1, taken from Reference 1, shows this effect for some of the more conventional materials, as well as some of the exotic alloys. It is seen that for the conventional materials, the maximum allowable temperature is in the 1000 to 1200°F range.

One possible way to overcome the difficulty of increasing the peak cycle temperature while maintaining pressures at an acceptable level is to employ a two fluid or binary vapor system. In this system, a heat exchanger between the two fluids serves both as a condenser for the high temperature-low vapor pressure fluid as well as a boiler for the high vapor pressure-lower temperature fluid. A Temperature-Entropy diagram for a binary vapor system is shown in Figure 1-2.

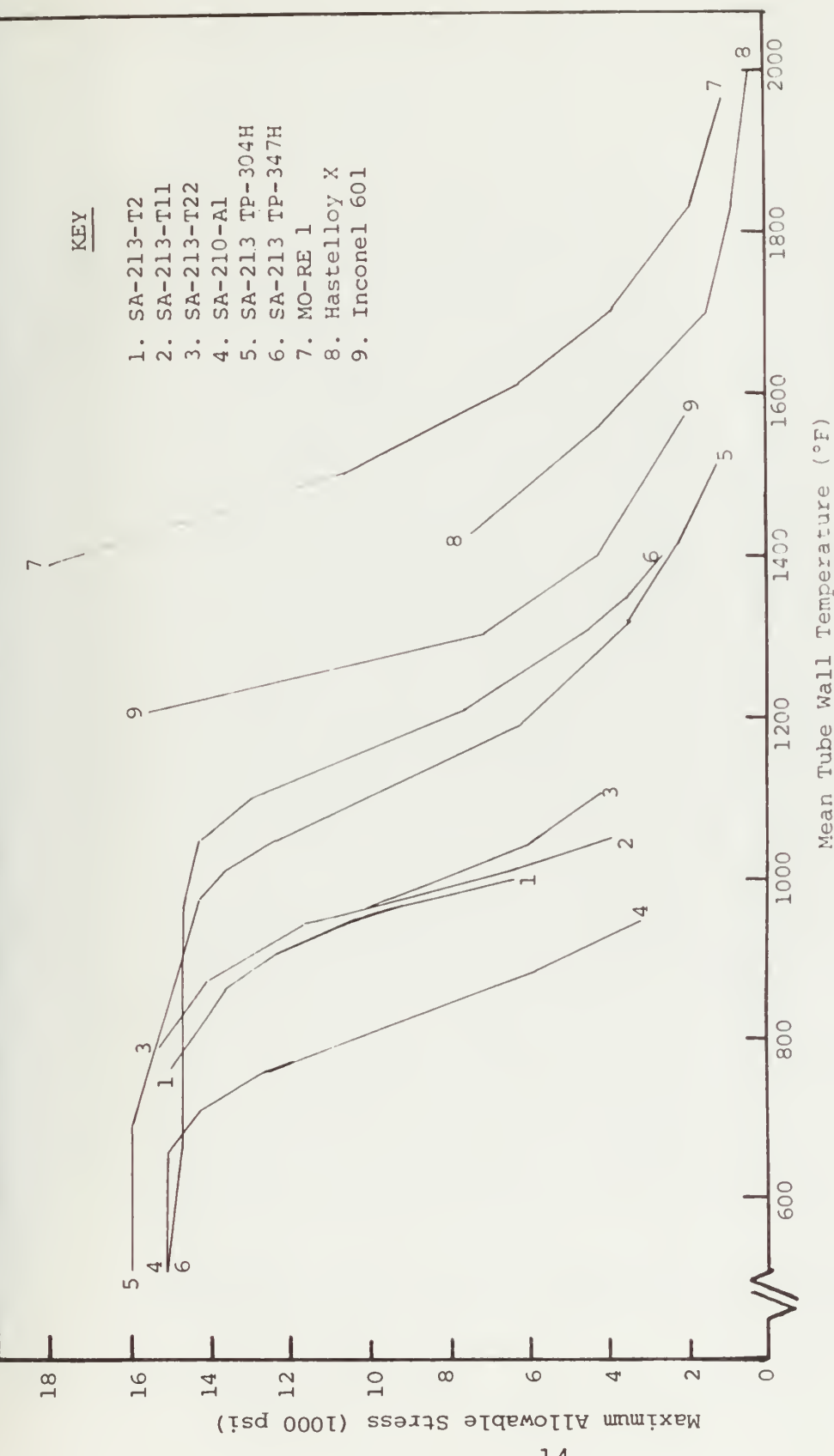


FIGURE 1-1 Allowable Design Stress In Primary Combustor Materials (Reference 1)

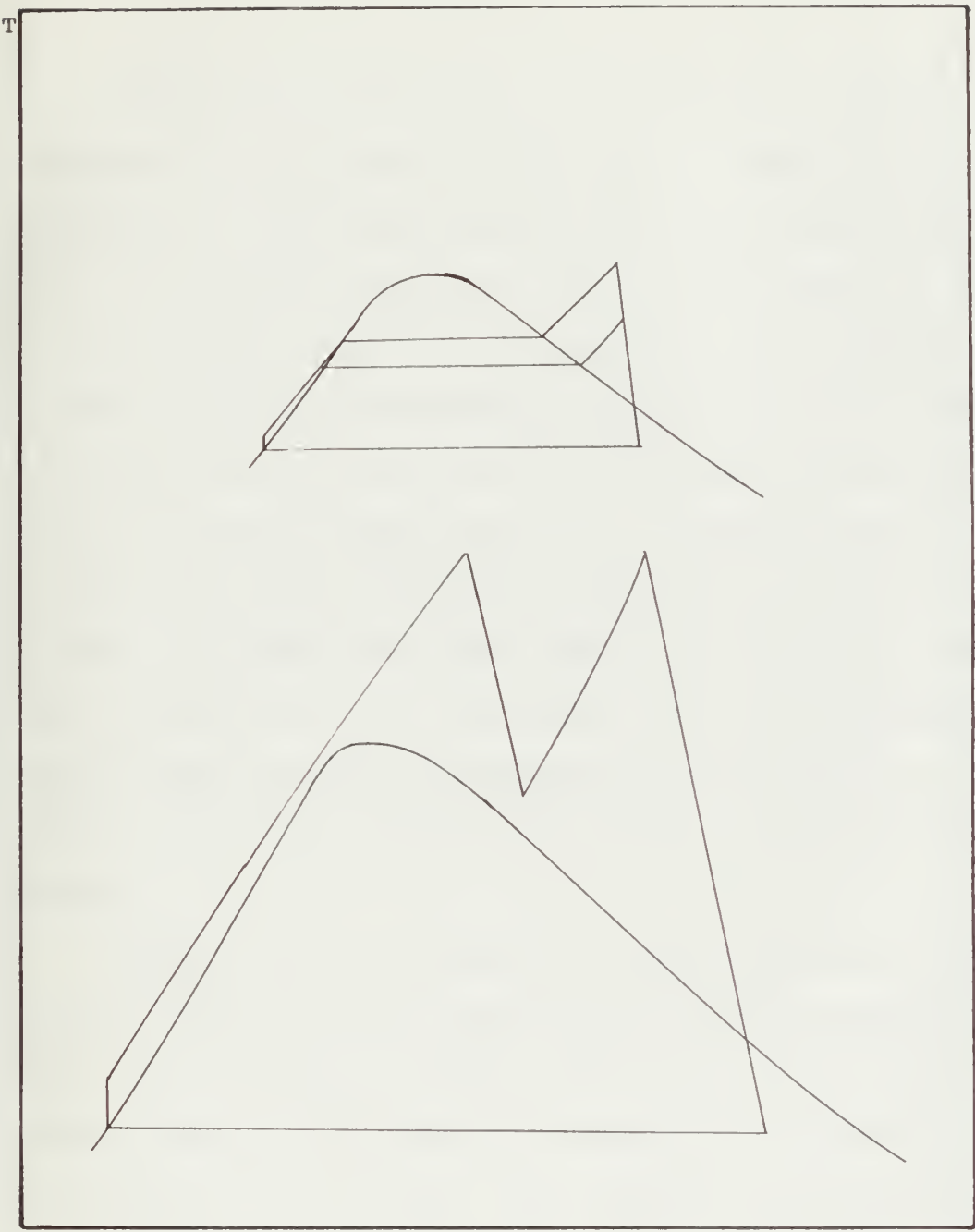


FIGURE 1-2 Binary Cycle Temperature Entropy Diagram

One of the first binary vapor cycles considered was the mercury-steam cycle. This cycle is described in Reference 2. The first plant of this type was built in 1917, and several others were built in the 1920's. At the time when these plants were constructed, the maximum steam conditions were approximately 450 psia, and 600°F. The low vapor pressure of mercury at this temperature made this fluid highly compatible with the steam cycle of this period. The peak temperature and pressure of these first binary cycle plants was about 900°F, and 125 psia. However, during the 1930's new steel alloys were developed which raised the peak temperature of steam cycles to 900°F, and thereby rendered the mercury steam plants obsolete.

Present day steam plants are metallurgically limited to the 1000°F to 1200°F range, with steam pressures in the 3000 to 4000 psia range. The use of mercury at these temperatures is not possible because it is highly corrosive above 950°F. In addition, the toxicity of mercury vapor in air is extremely serious.

1.2 POTASSIUM AS A TOPPING CYCLE FLUID

Just as mercury proved to be compatible with the peak steam conditions of the 1920's, potassium appears

to be compatible with the peak steam conditions of today. Its vapor pressure in the 1000°F to 1200°F range is of the order of 1.0 to 2.0 psia, and it has a heat of condensation of about 800 to 900 BTU/lbm. Table 1, taken from Reference 3, shows the properties of condensing potassium at 1.5 psia compared to water at 1.5 psia. The saturation pressures over the desired range are low enough so that stresses are not serious, and the vapor specific volume is low enough so that excessively large components will not be required. The only major difference in the two fluids is the thermal conductivity of potassium is about 60 times that of water. However, this is advantageous in improving the heat transfer coefficient, especially in the potassium condenser.

A survey of pertinent work in the use of potassium as a Rankine cycle working fluid, and the potassium-steam binary vapor cycle is presented. This is followed by a first and second law analysis of the potassium-steam cycle, a discussion of component configurations, and an economic analysis. Finally, an approximate optimum system is described.

| | Potassium | Water |
|--------------------------------------|-----------|---------|
| | Liquid | Vapor |
| Temperature, °F | 1040.0 | 115.6 |
| Pressure, psia | 1.50 | 1.50 |
| Specific volume, ft ³ /lb | 0.02269 | 267.15 |
| Enthalpy, Btu/lb | 283.0 | 1170.4 |
| Heat of Vaporization, Btu/lb | 887.4 | 1028.14 |
| Specific Heat, Btu/lb °F | 0.1823 | 0.1266 |
| Viscosity, lb/ft.hr | 0.37 | 0.0189 |
| Thermal Conductivity, Btu/hr.ft °F | 21.0 | 0.00363 |
| Prandtl No., $c_p \mu / k$ | 0.00321 | 0.659 |
| Surface Tension, lb/ft | 0.0041 | 0.00469 |

TABLE 1-1 Comparison Of Physical Properties Of Potassium
And Water For Condensing Conditions

2. LITERATURE SURVEY

Much of the technology related to the utilization of potassium is available as a result of the interest by NASA in the use of this fluid for use in small (300 to 1000kw) potassium Rankine cycle turbogenerators.

The engineering properties of potassium used here, as well as in much of NASA's work are given in Reference 4. These properties were experimentally determined for a temperature range from 1400° to 2525°F, and a pressure range of 0.2 to 35atm. The range of the properties was extended to 1.0 psia and 1000°F here, and in the NASA work. (See Appendix B.)

A series of experiments performed to determine the effect of potassium vapor on various component materials is reported in Reference 5. The heat transfer, corrosive and erosive characteristics of potassium were investigated in a test loop of Cb-1Zr. The effect of wet potassium vapor on a test loop of 316 stainless steel was also investigated. Tests were also conducted on a two stage turbine to determine the erosive effect of potassium on various turbine blading materials, as well as creep in rotor disks. These tests were conducted for 5000 hours with 1500°F, 99 percent vapor turbine inlet potassium. In the first test, the blading material was completely manufactured from Udimet-700. In the second

test, some of the second stage blading was replaced by TZC and TZM alloy blading. Upon completion of the test, the blading was removed and weighed. No significant erosion was observed as all blades were within 0.1 percent of their original weight. In Reference 6, the results of a two stage turbine test are presented. This test was conducted for 2000 hours to evaluate the effect of impacting droplets on erosion of turbine components. The materials tested were Udimet-700, TZM and TZC. Again, no significant blade damage was reported. However, specimens of the test material were installed so that they would be impacted by droplets leaving the second stage. While some indication of impact erosion was evident in the refractory metal alloys, only the Udimet-700 specimens indicated significant impact erosion. Metal transfer of potassium into the various blading materials was also investigated. In the case of all three alloys, the amount of potassium diffusion into the blading material was not considered significant. The results of an extensive 5000 hour test on a three stage potassium turbine are presented in Reference 7. This test was conducted with inlet vapor at 1500°F, inlet to exit static pressure ratio of 10, and vapor qualities of 99% (inlet) to 87% (exit). The primary

objective of this test was the determination of the effects of vapor wetness on impingement damage of rotor blading materials. The first stage blading was manufactured completely from René 77. The second and third stages contained blades of René 77, TZM and TZC. The condition of the blading was reported to be good after 5000 hours of operation. Some metal removal was observed, especially in the case of the molybdenum alloy blading. However, this metal removal was attributed to oxygen-accelerated washing corrosion. It has been reported that the mass transfer of molybdenum in potassium is increased with increasing oxygen concentration, and during the test a system failure had allowed oxygen to leak into the system. Because of this oxygen-accelerated mass transfer of molybdenum in potassium, so called "oxygen getters" were installed in the boiling potassium loop. These consisted of titanium sheets located in potassium dump tank, and zirconium sheets located in the condenser. In Reference 7 it was concluded that even with the excessive levels of oxygen in potassium, only minor impingement erosion damage was evident either in the molybdenum based alloys or the René 77. Molybdenum based alloys and René 77 were also recommended in Reference 1 for potassium

turbine blading.

Reference 8 provides an extensive treatment of information available on the superalloys such as the molybdenum based TZM, the tantalum based T-111 and Cb-12r. It contains information concerning the tensile properties, creep data, stress-rupture data, manufacturing experience such as forging methods and temperatures, heat treating procedures, forming, welding and machining processes, and the compatibility of candidate alloys with an alkali metal environment. It also provides a confidence index for the various alloys based on accumulated experience in manufacturing and use. A complete bibliography of over sixty references is provided.

The preliminary and final design of a 428kw potassium turbo-alternator is presented in References 9 and 10. The prime contractor for this study was the AiResearch Division of the Garrett Corporation. AiResearch was assisted in this study by the Westinghouse Electric Division in the design of the alternator, and by the Westinghouse Astronuclear Laboratory in the area of areothermodynamics and turbine blading material selection. The thermodynamic properties of potassium used in this study were those of Reference 4. The

design conditions of the potassium turbine which resulted from this study are as follows:

| | T (°F) | p (psia) |
|---------|--------|----------|
| Inlet | 2150 | 190.0 |
| Exhaust | 1220 | 5.44 |

The turbine is of the axial flow type with 10 stages, and is saddle mounted on potassium lubricated journal bearings. TZM alloy was selected for use in rotating hardware. In the high temperature first stage area, T-111 was selected for the turbine housing including the forward bearing, housing and inlet scroll. This material has the required strength level at 2150°F, and is easily fabricated. Cb-12r was recommended for the lower temperature sections.

Reference 11 provides a discussion of the possible materials for use in the potassium boiler, and the potassium condenser-steam generator. The material selected for the boiler must have good resistance to corrosion by combustion gas as well as good resistance to attack by boiling potassium. The potassium condenser-steam generator must also possess resistance to attack by potassium, resistance to chloride stress corrosion, and high strength in the 1000 to 1200°F range. The high nickel

alloys such as Iconel or Incoloy 800 are recommended for these components.

In Reference 12 it is reported that the condensing heat transfer coefficient for potassium in the range of temperatures from 1100 to 1400°F is on the order of 10000Btu/hr ft²°F. In Reference 3, a value of 3000Btu/hr ft²°F for boiling potassium at 1500°F is used.

References 1, 3, 11, 13, 14, and 15 are discussions of potassium steam vapor binary cycles of various configurations. Seventeen different potassium steam cycles are analyzed in Reference 1. Turbine inlet temperatures vary from 1400 to 1700°F while turbine exhaust conditions are fixed at 1100°F and 2.4 psia. For each case, efficiency, the capital cost and operating costs are presented. Recommendations as to the materials of construction are made. In all cases of Reference 1, the fuel is either coal or coal derived fuel. References 3 and 14 present a discussion of a nuclear powered potassium steam vapor cycle. These studies use turbine inlet conditions of 1540°F, and a condensing temperature of 1100°F. The bottoming cycle in these studies is a double reheat 1050°F, 4000 psia supercritical steam plant. An overall plant thermal efficiency of over 54 percent is

predicted. An analysis of the potassium-gas-steam cycle is presented in both References 11 and 13. The potassium and steam plant configurations are similar to those of References 3 and 15. These plants are fossil-fueled, with part of the heat input being the waste heat from a gas turbine. Again, a thermal efficiency of over 54 percent is predicted. References 3, 11, 13, and 15 also give detailed calculations methods which can be used to size a potassium boiler and the potassium condenser-steam generator. A disucssion of the Treble Rankine Cycle is presented in Reference 16. Here, the working fluids are potassium, diphenyl, and steam. It is reported that this cycle is even more thermally efficient than the potassium steam cycle. In addition, it is predicted that the Treble Rankine Cycle will be less expensive because the steam bottoming cycle will require much lower peak temperatures and pressures than would be required in the potassium steam cycle.

3. THERMODYNAMIC ANALYSIS

3.1 FIRST LAW ANALYSIS OF THE BINARY CYCLE

The major components of the potassium steam binary cycle are shown in Figure 3-1. Figure 3-2 is a Temperature-Entropy diagram representing the binary cycle. The main features of the binary cycle are that all heat addition is to the topping cycle, all heat rejected by the cycle is rejected by the condensing steam, and the topping and bottoming cycle are coupled in that the heat rejected by the topping cycle is the heat added to the bottoming cycle.

As given in Reference 3, the overall cycle efficiency of a binary plant may be evaluated by combining the individual cycle efficiencies for the topping and bottoming cycles. This results in the following relationship for the overall thermal efficiency.

$$\eta_{to} = \eta_K + (1-\eta_K)\eta_S \quad 3-1$$

This relationship may be established by considering the binary cycle in Figure 3-1. The overall plant efficiency is

$$\eta_{to} = \frac{\dot{W}_S + \dot{W}_K}{Q} \quad 3-2$$

For the topping cycle, the thermal efficiency is

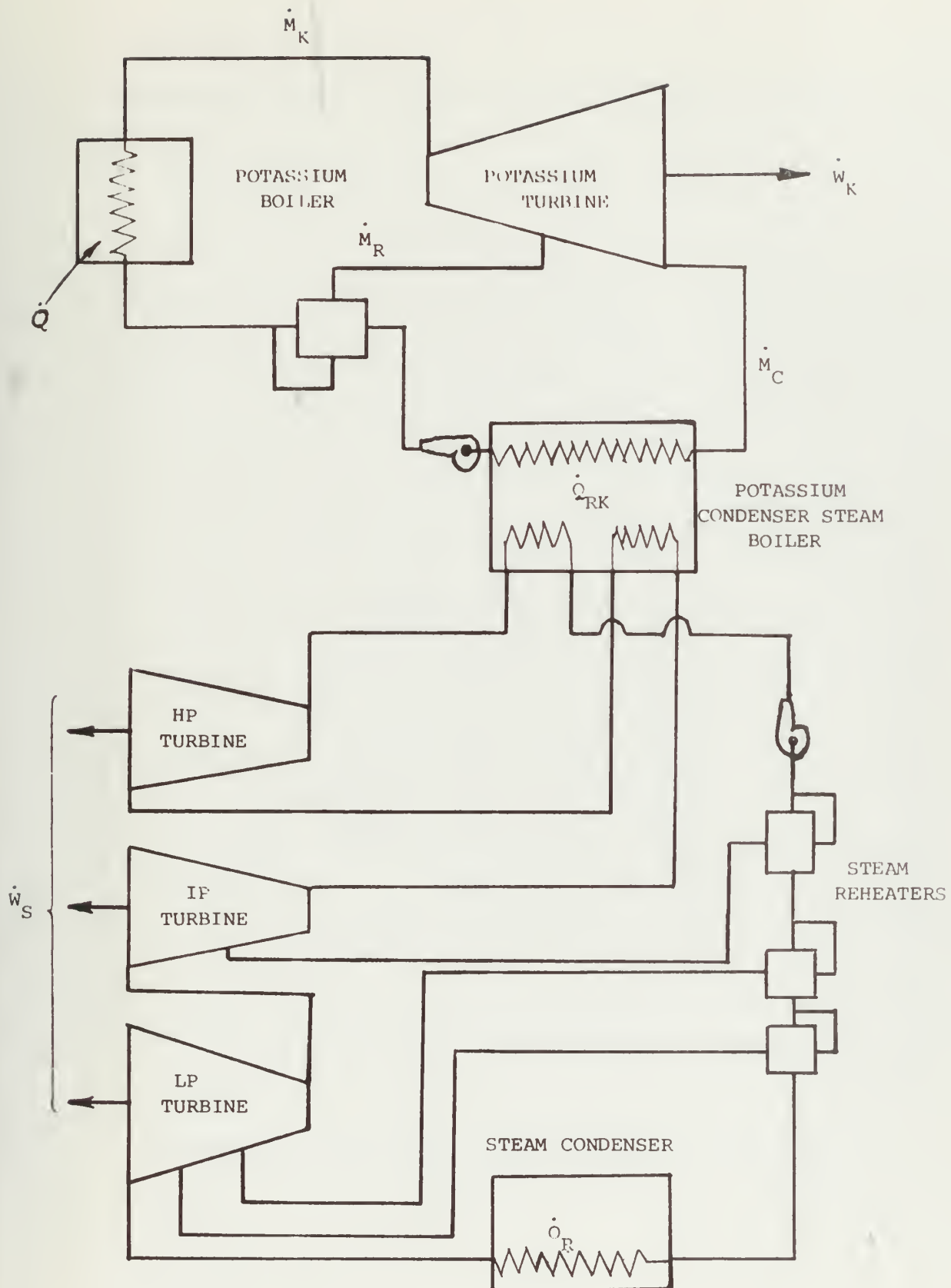
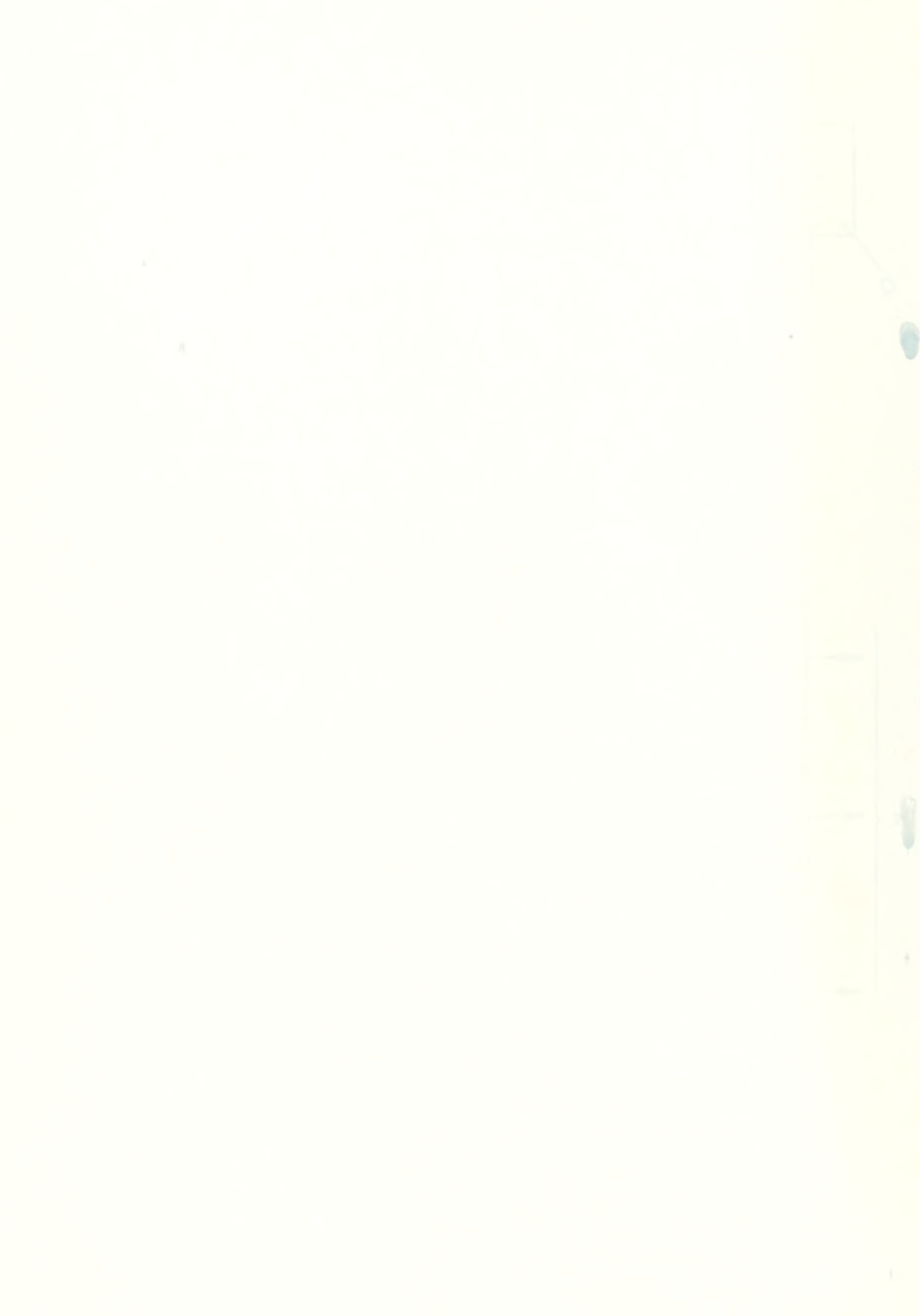


FIGURE 3-1 Major Components Of Potassium Steam Binary Cycle
-27-



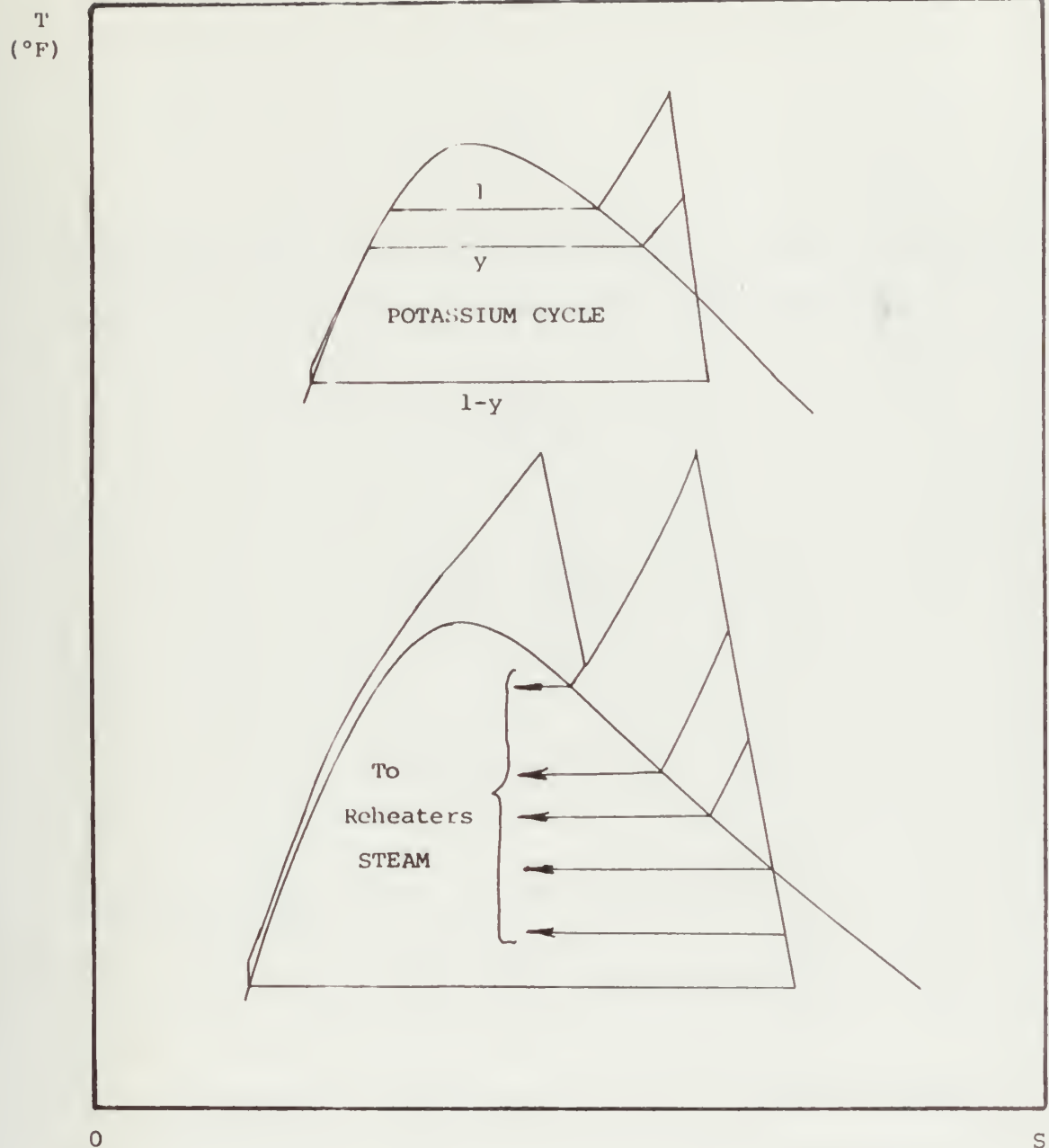


FIGURE 3-2 Temperature Entropy Diagram For Potassium Steam Binary Cycle

$$\eta_{to} = \frac{\dot{W}}{\dot{Q}}.$$

3-3

Since the heat rejected by the topping cycle is the heat input to the bottoming cycle, its efficiency is

$$\eta_S = \frac{\dot{W}_S}{\dot{Q}_{RK}}$$

or

$$\frac{\dot{W}_S}{\dot{Q}} = \eta_S \frac{\dot{Q}_{RK}}{\dot{Q}} \quad 3-4$$

But

$$\frac{\dot{Q}_{RK}}{\dot{Q}} = 1 - \eta_K .$$

Combining Equations 3-2, 3-3, and 3-4,

$$\eta_{to} = \frac{\dot{W}_K}{\dot{Q}} + \frac{\dot{W}_S}{\dot{Q}} = \eta_K + \eta_S(1 - \eta_K) .$$

Equation 3-1 indicates that for a given bottoming cycle efficiency, the overall binary cycle thermal efficiency may be increased by increasing the thermal efficiency of the topping cycle. Figure 3-3 shows the variation of topping cycle condensing pressure with the overall binary cycle efficiency for a fixed bottoming cycle, and two sets of topping cycle turbine inlet

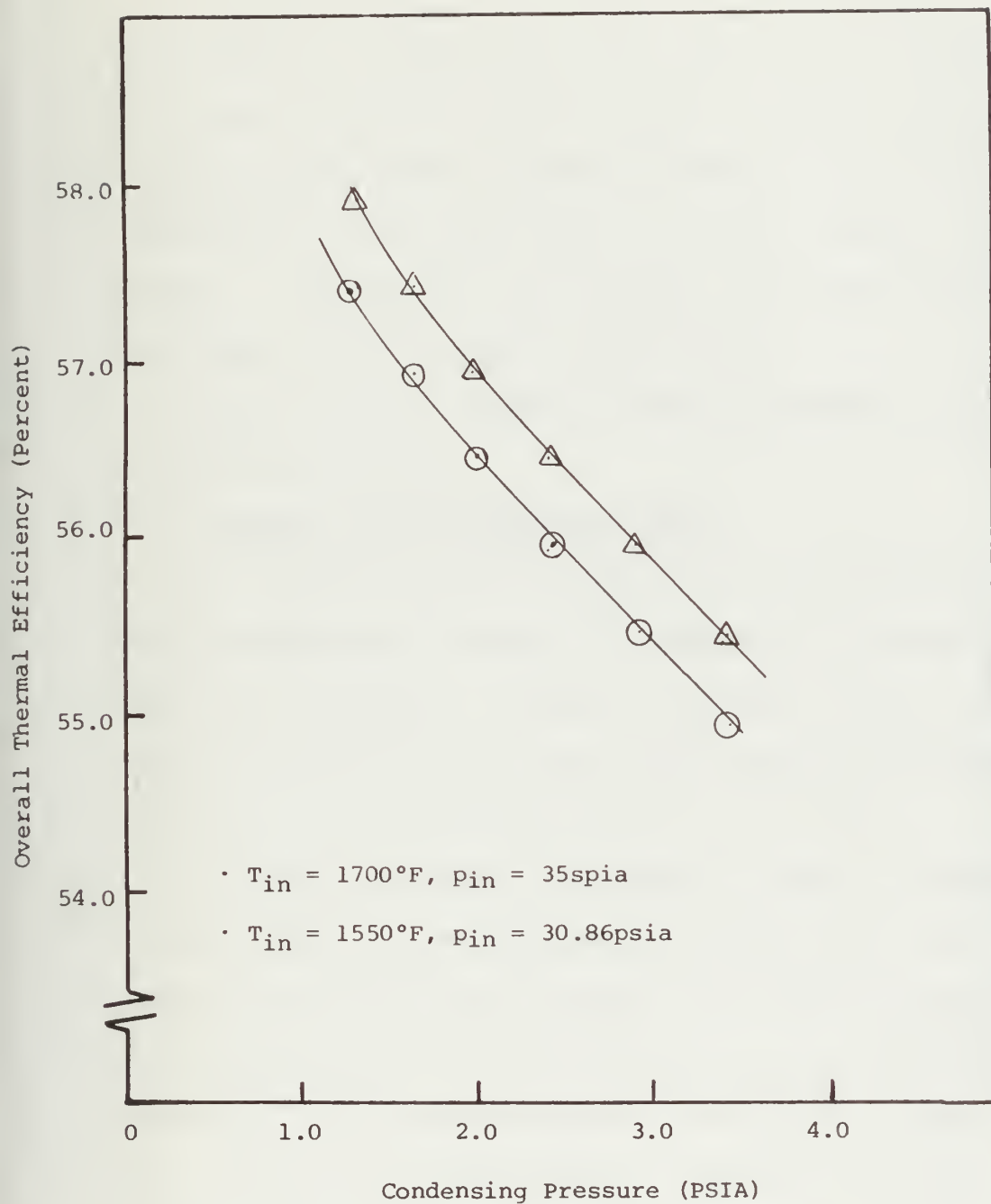


FIGURE 3-3 Effect Of Topping Cycle Condensing Pressure On Potassium Steam Binary Cycle Overall Thermal Efficiency

conditions. In each case, the overall plant thermal efficiency increases with decreasing topping cycle condensing pressure. Figure 3-4 shows the effect of superheating potassium vapor on overall thermal efficiency. In this case, the overall plant efficiency increases with increasing temperature.

Table 3-1 is a summary of the performance parameters of the binary cycle.

3.2 RANKINE CYCLE POTASSIUM PLANT

The Rankine cycle potassium plant consists of four major components: a boiler, a condenser, a boiler feed pump, and a turbine. Figure 3-5 shows the basic Rankine cycle potassium plant, along with Temperature-Entropy and Enthalpy-Enthalpy diagrams for the cycle.

As shown in Figure 3-5, heat is added to potassium in the boiler. Upon leaving the boiler, the high pressure potassium vapor enters the turbine where it produces positive work by expanding to the condenser pressure. The potassium vapor leaving the turbine is then condensed by transferring its heat of condensation to the steam, and leaves the condenser as saturated liquid. The low pressure liquid then enters the feed pump where its pressure is increased to that of the

| | |
|----------------------------|--|
| Heat Input | $\dot{Q}_{in} = \dot{M}_K(h_3 - h_6)$ |
| Power Output | $\dot{W}_T = \dot{W}_S + \dot{M}_K(h_3 - h_4) + \dot{M}_C(h_4 - h_5)$ $= \dot{W}_S + \dot{M}_C(h_2 - h_1)$ $= \dot{W}_S + \dot{W}_K$ |
| Overall Thermal Efficiency | $\eta_{to} = \frac{\dot{W}_S + \dot{W}_K}{\dot{Q}_{in}} = \eta_K + (1 - \eta_K)\eta_S$ |
| Heat Rejected | $Q_R = \dot{M}_{SC}(\Delta h_{SC})$ |
| Electrical Power | $P = \eta_{gen} \dot{W}_T$ |

TABLE 3-1 Performance Parameters Of Binary Cycle

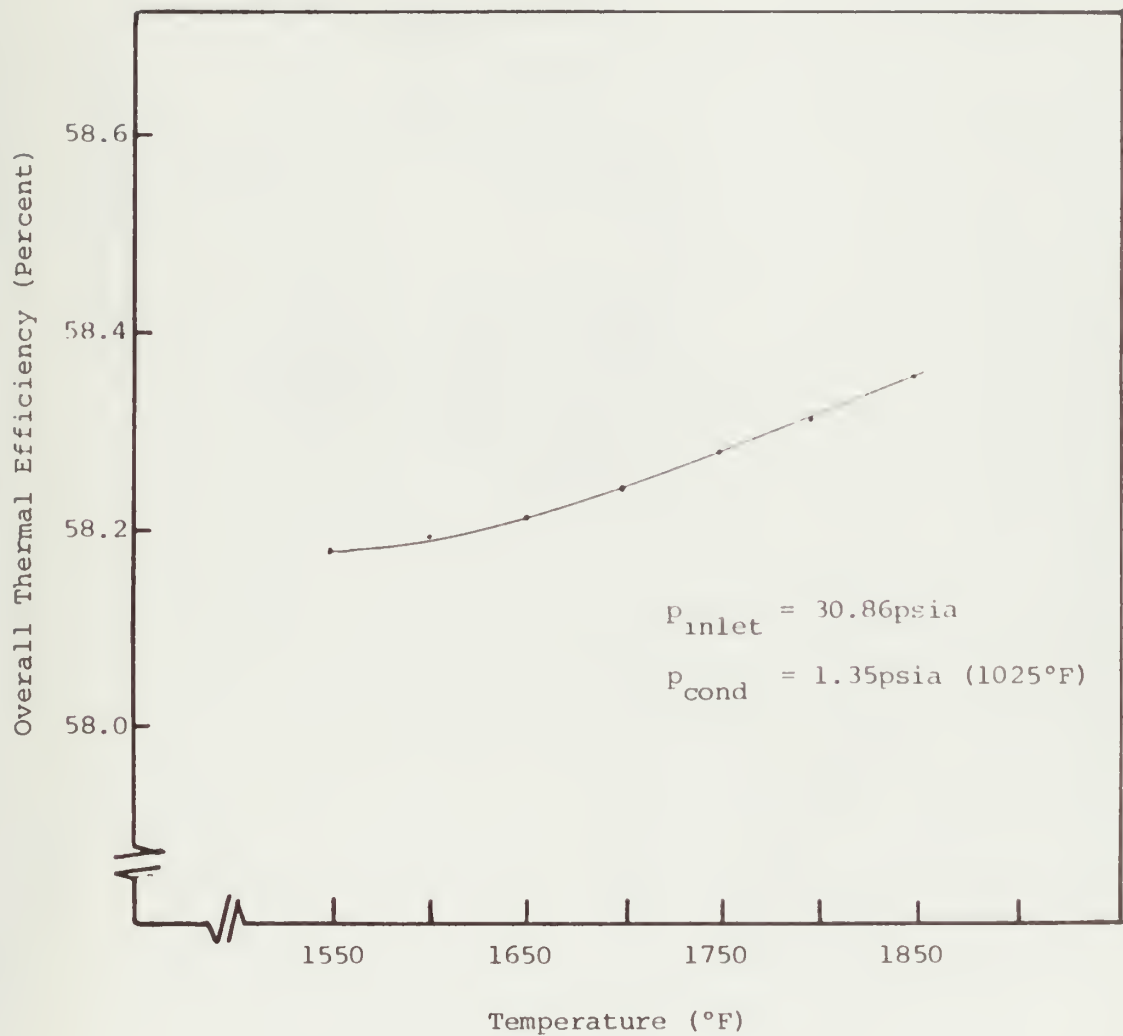


FIGURE 3-4 Effect Of Turbine Inlet Temperature
On Potassium Steam Binary Cycle
Overall Thermal Efficiency

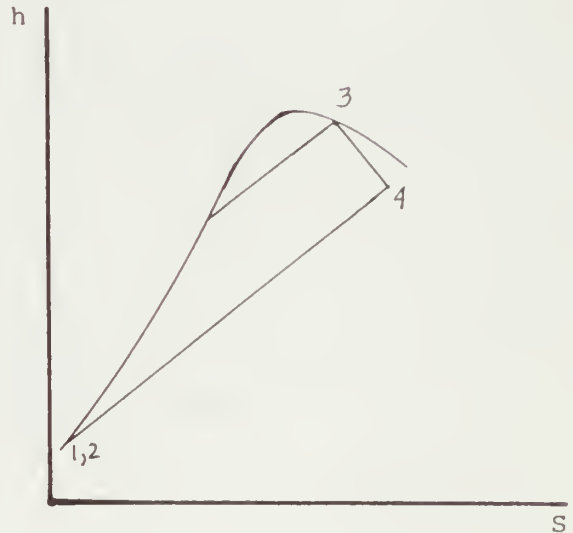
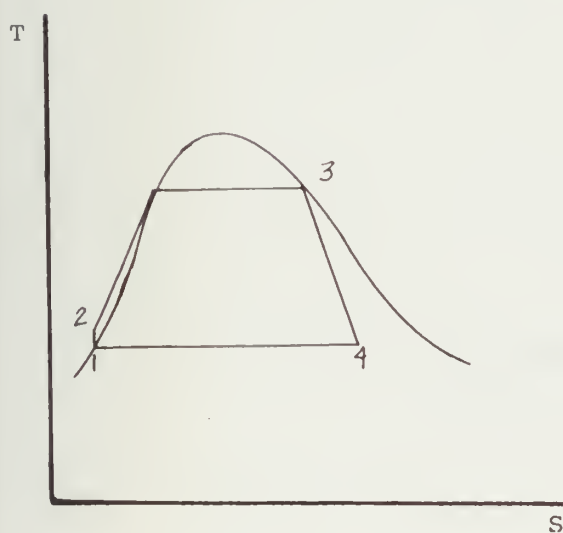
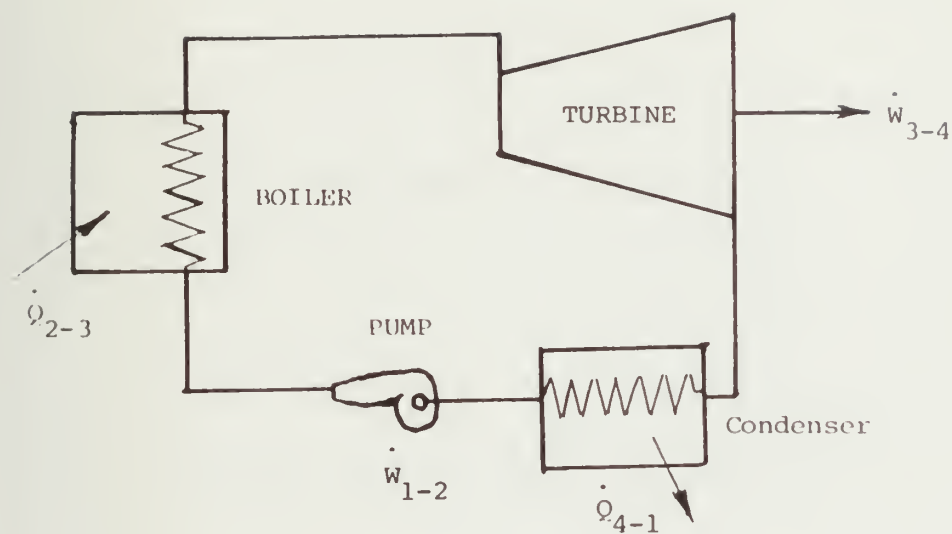


FIGURE 3-5 Simple Potassium Rankine Cycle Plant

| | |
|-------------------------|---|
| Boiler Heat Input | $\dot{Q}_{2-3} = \dot{M}(h_3 - h_2)$ |
| Turbine Power | $\dot{W}_{3-4} = \dot{M}(h_3 - h_4)$ |
| Pump Power | $\dot{W}_{1-2} = \dot{M}(h_1 - h_2)$ |
| Condenser Heat Transfer | $\dot{Q}_{4-1} = \dot{M}(h_4 - h_1)$ |
| Thermal Efficiency | $\eta_t = \frac{\dot{W}_{net}}{\dot{Q}_{2-3}} = \frac{h_3 - h_4 + h_1 - h_2}{h_3 - h_2}$ $\eta_t = \frac{\dot{Q}_{2-3} - \dot{Q}_{4-1}}{\dot{Q}_{2-3}} = 1 - \frac{h_4 - h_1}{h_2 - h_3}$ |

TABLE 3-2 Performance Parameters For
Potassium Rankine Cycle Plant

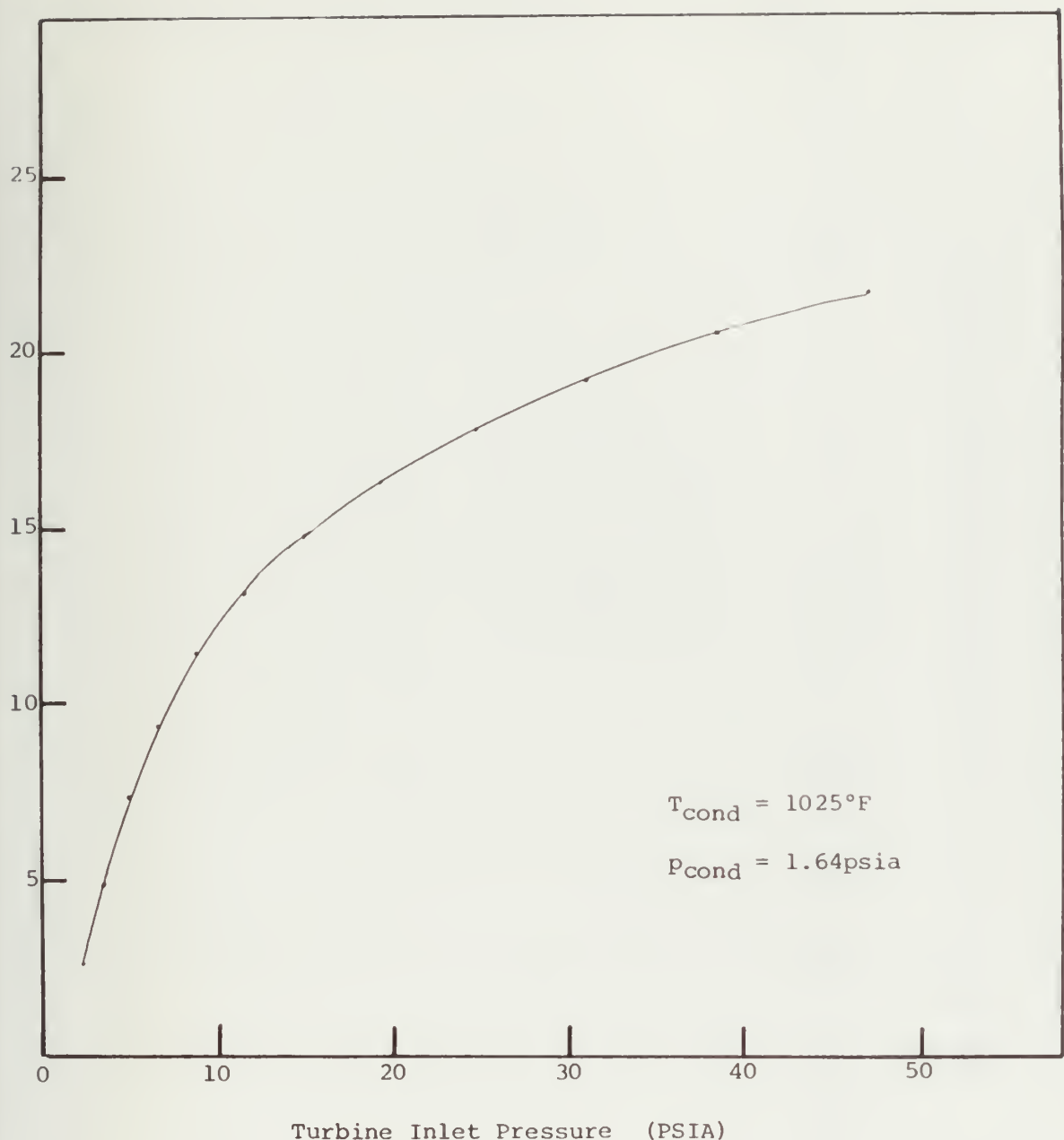


FIGURE 3-6 Effect Of Boiler Pressure Of
Simple Potassium Rankine
Cycle Efficiency

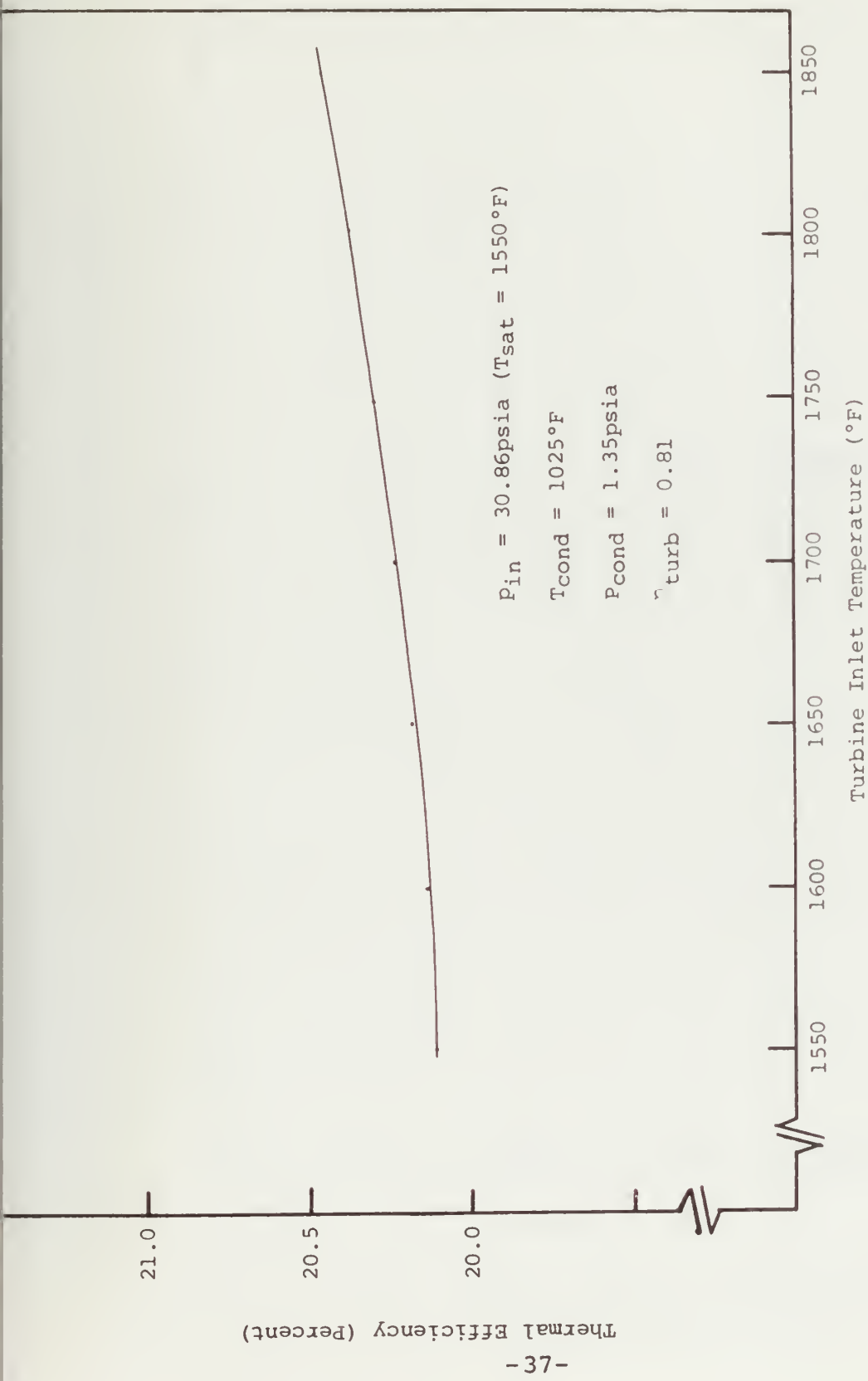


FIGURE 3-7 Effect Of Superheating On Thermal Efficiency
In The Potassium Rankine Cycle

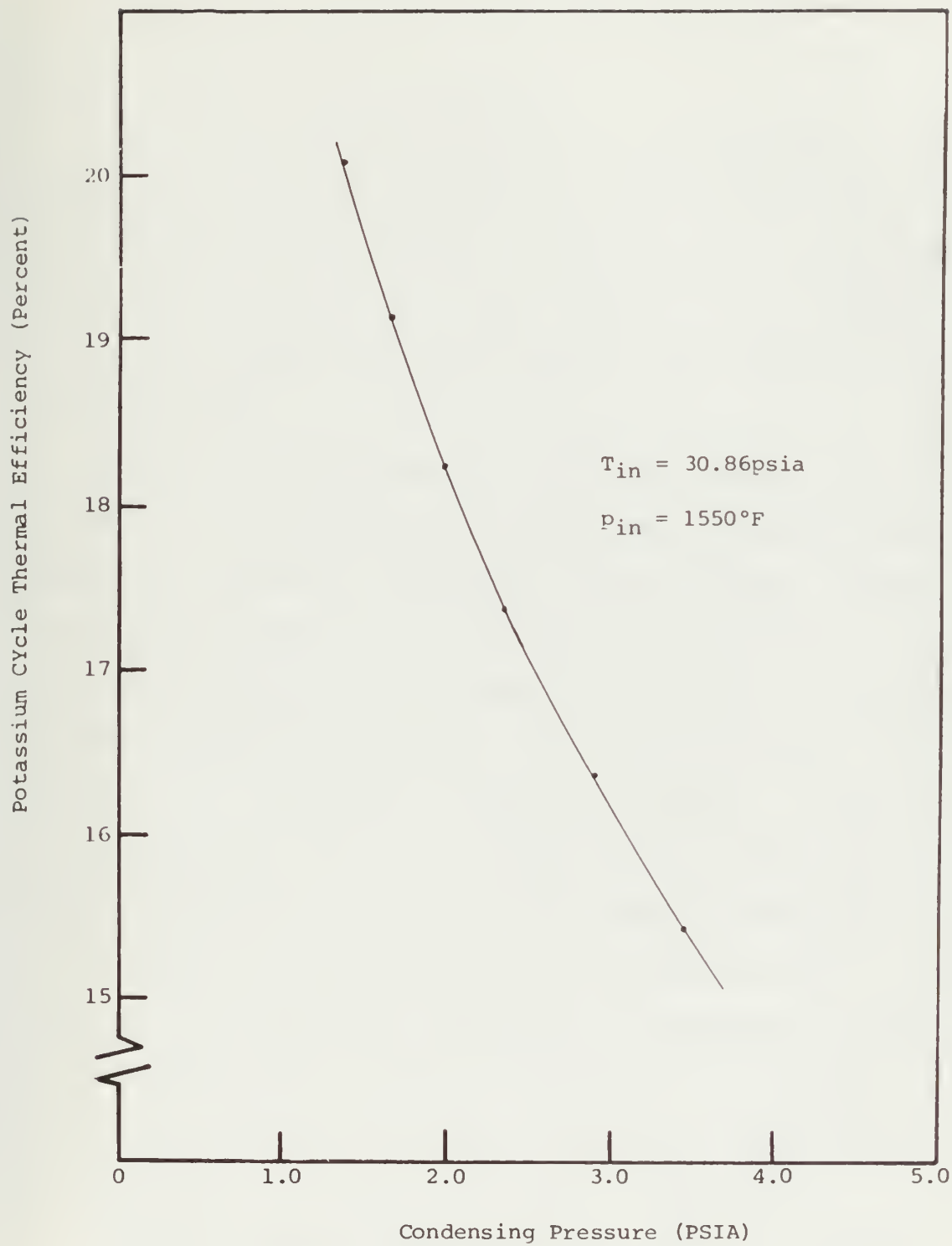


FIGURE 3-8 Effect Of Condensing Pressure On Thermal Efficiency For The Simple Potassium Rankine Cycle

boiler, and the cycle is complete.

The cycle produces net positive work when the positive work transfer produced by the expanding potassium vapor in the turbine is greater than the negative work required by the feed pump. Table 3-2 is a summary of the performance parameters of the simple Rankine cycle potassium plant.

There are two methods by which the thermal efficiency of the simple Rankine cycle can be improved, provided the condensing temperature remains fixed. Figure 3-6 shows the effect of increasing boiler pressure, while maintaining saturated vapor at turbine inlet and constant condensing pressure. The second of these methods is to superheat at constant pressure. Figure 3-7 shows this effect for a simple Rankine cycle condensing at a fixed pressure. The thermal efficiency for a simple Rankine cycle may also be improved by lowering the condensing temperature of potassium so that it approaches that of the top steam cycle temperature. Figure 3-8 indicates the effect on thermal efficiency of lowering the potassium condensing temperature.

There is still another method by which the thermal efficiency of a Rankine cycle may be improved. This method is known as regenerative feed heating, and has

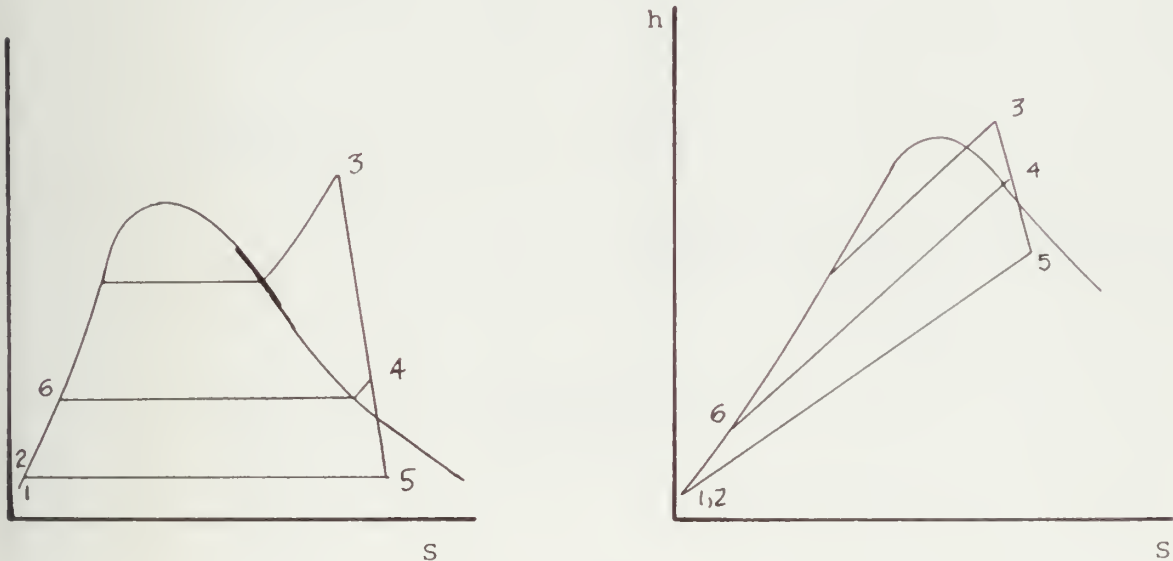
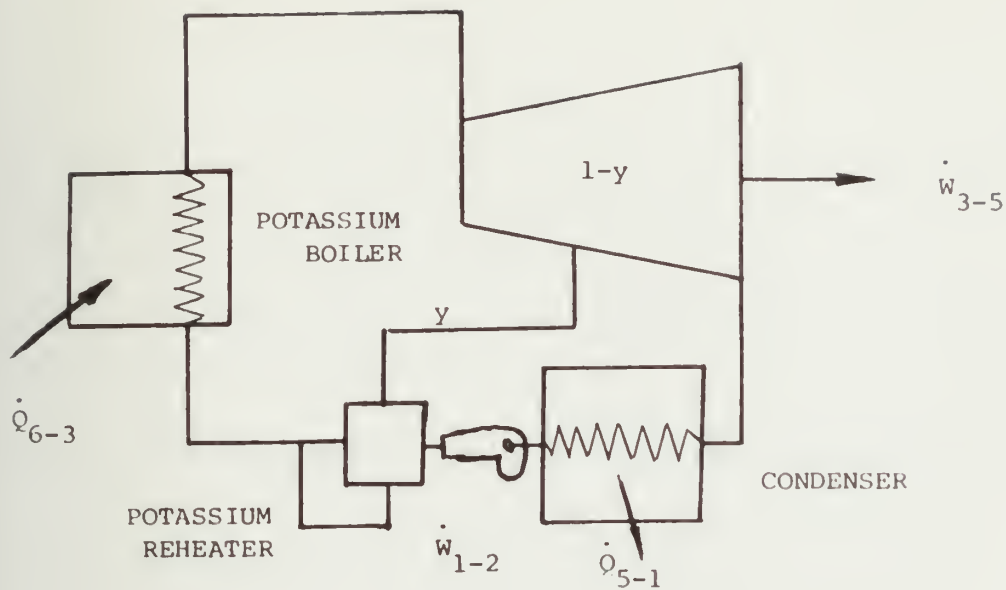


FIGURE 3-9 Simplified Potassium Regenerative Cycle With One Regenerative Feed Heater

$$\text{Extraction}^1 \quad y = \frac{h_6 - h_2}{h_4 - h_2}$$

$$\text{Turbine Power} \quad \dot{W}_{3-5} = \dot{M} [(h_3 - h_4) + (1-y) (h_4 - h_5)]$$

$$\text{Pump Power} \quad \dot{W}_{1-2} = \dot{M} (h_1 - h_2)$$

$$\text{Condenser Heat Transfer} \quad \dot{Q}_{5-1} = \dot{M} (1-y) (h_5 - h_1)$$

$$\text{Boiler Heat Input} \quad \dot{Q}_{6-3} = \dot{M} (h_3 - h_6)$$

$$\text{Thermal Efficiency} \quad \eta_t = \frac{\dot{W}_{\text{net}}}{\dot{Q}_{6-3}}$$

$$\eta_t = \frac{\dot{M} [(h_3 - h_4) + (1-y) (h_4 - h_5) + (1-y) (h_1 - h_2)]}{\dot{M} (h_3 - h_6)}$$

¹ Extraction is $\frac{\text{lbm extracted}}{\text{lbm boiler}}$

TABLE 3-3 Performance Parameters For
Simplified Regenerative
Feed Heating Cycle

Potassium Cycle Thermal Efficiency (percent)

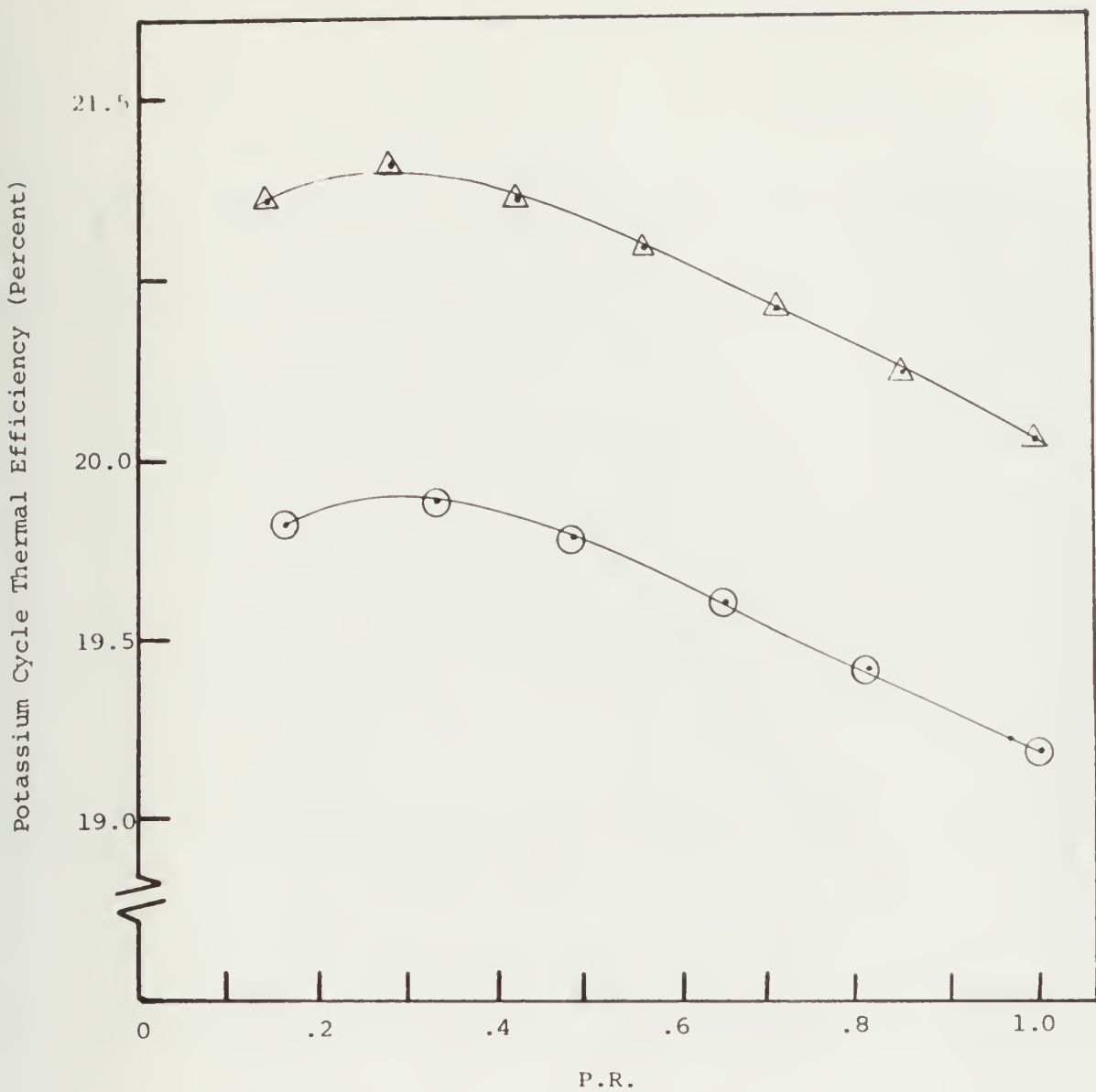


FIGURE 3-10 Effect Of Regenerator Pressure Ratio On Thermal Efficiency For Simplified Potassium Regenerative Feed Heating Cycle

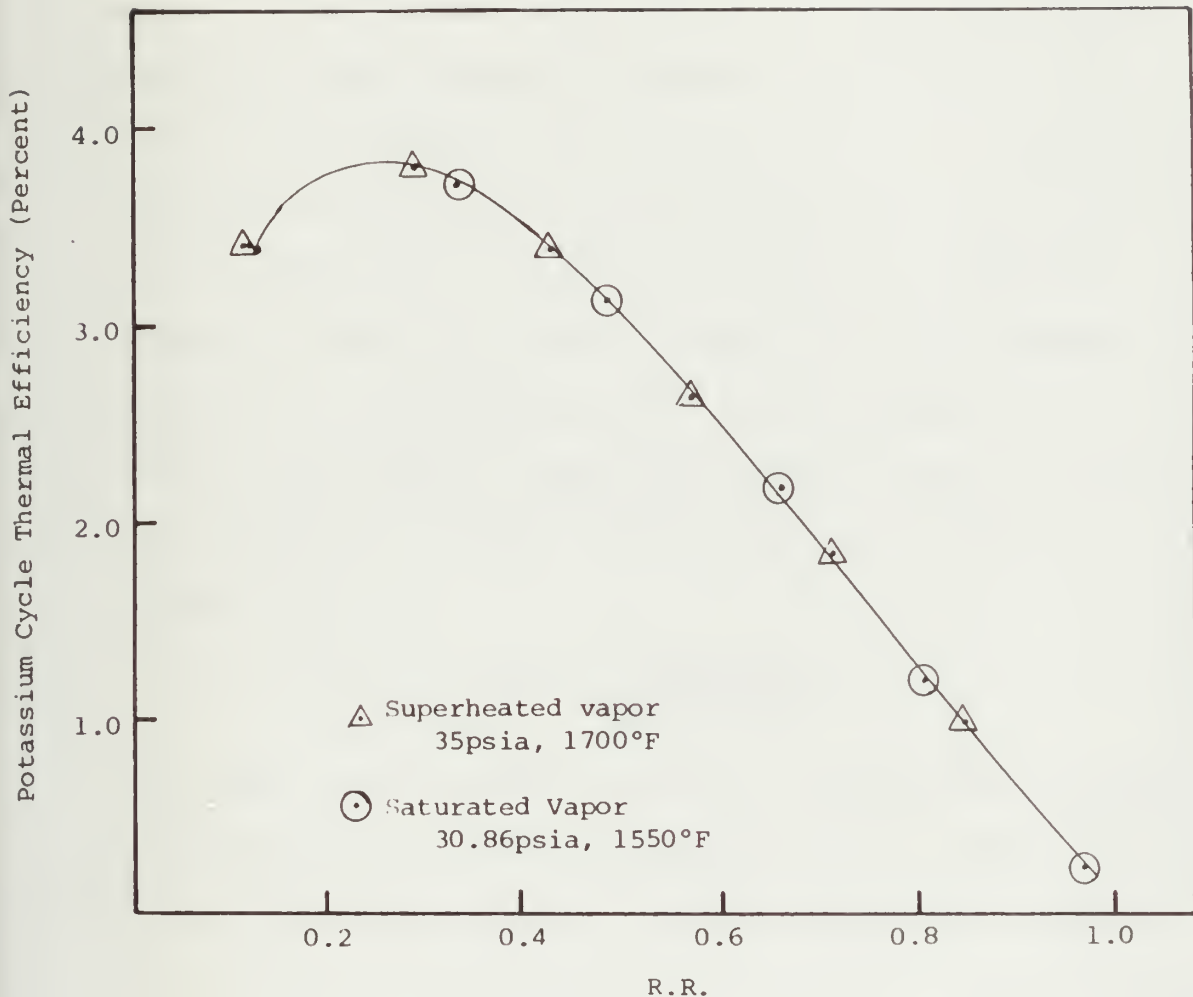


FIGURE 3-11 Effect Of Regenerator Pressure Ratio
On Potassium Cycle Thermal Efficiency

found extensive use in steam power plants. Figure 3-9 shows a regenerative feed system with one feed heater. Basically, the increase in thermal efficiency is the result of pre-heating the cool feed by using higher temperature fluid which has been extracted from the turbine prior to its complete expansion to condenser pressure. Table 3-3 gives a table of the performance parameters for the regenerative feed heating cycle. Figure 3-10 shows the effect on thermal efficiency of the regenerator pressure ratio, where this ratio is defined as

$$PR = \frac{P_{\text{regenerator}}}{P_{\text{turbine inlet}}}$$

This shows that the most effective regenerating pressure is approximately 30% of the maximum cycle pressure for a single feed heating plant. Figure 3-11 shows the percent increase in thermal efficiency over a simple Rankine cycle as a function of the regenerator pressure ratio. As in Figure 3-10, the most effective regenerating pressure ratio is approximately 0.30, and this ratio gives about a 3.8% increase in thermal efficiency over the simple Rankine cycle case. It should be noted that Chambers, et. al., in Reference 3, advised that an even more important reason for regenerative feed heating than

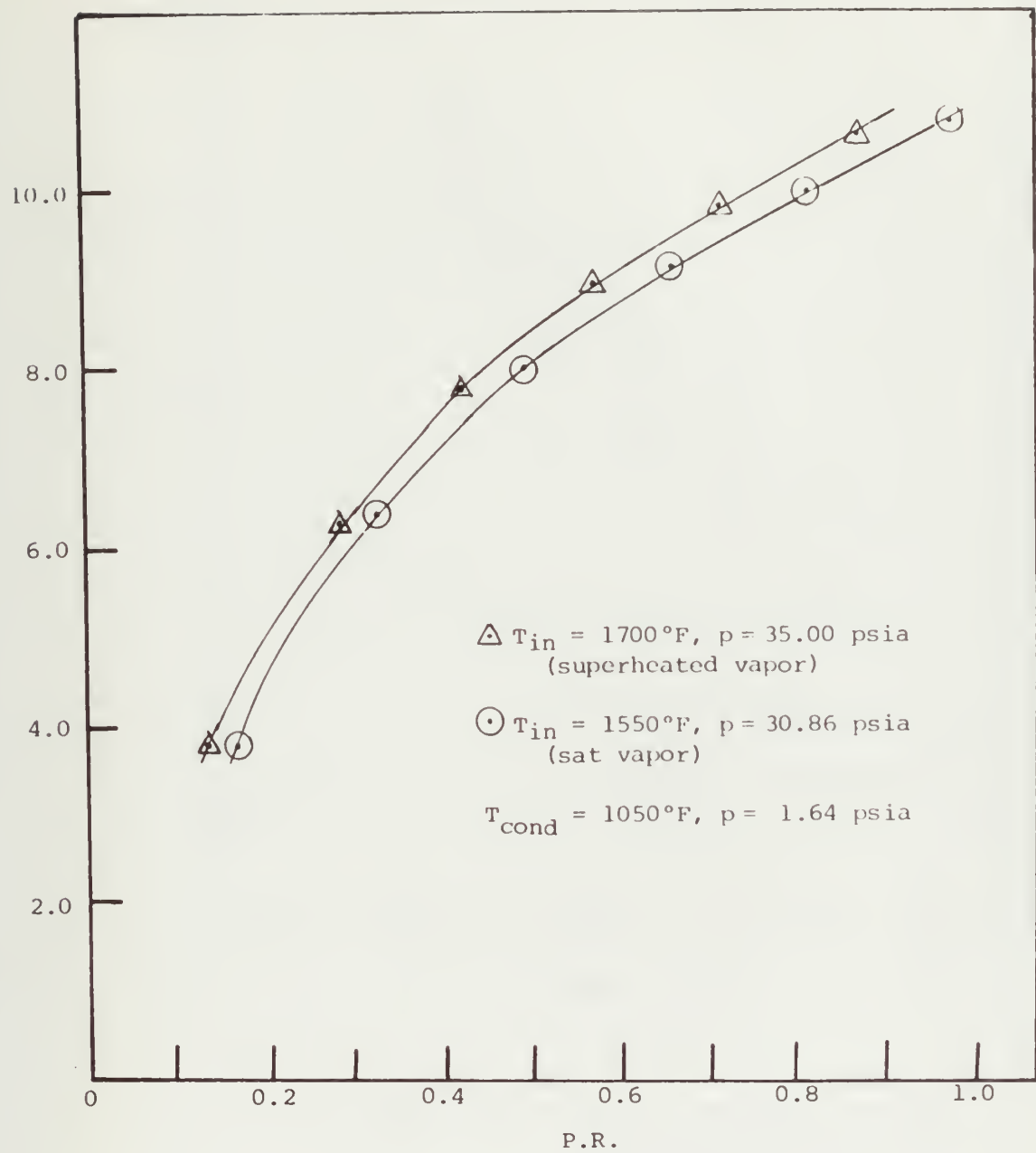


FIGURE 3-12 Percent Extracted For Regeneration
 As A Function Of Pressure Ratio In
 The Potassium Regenerative Feed
 Heating Cycle

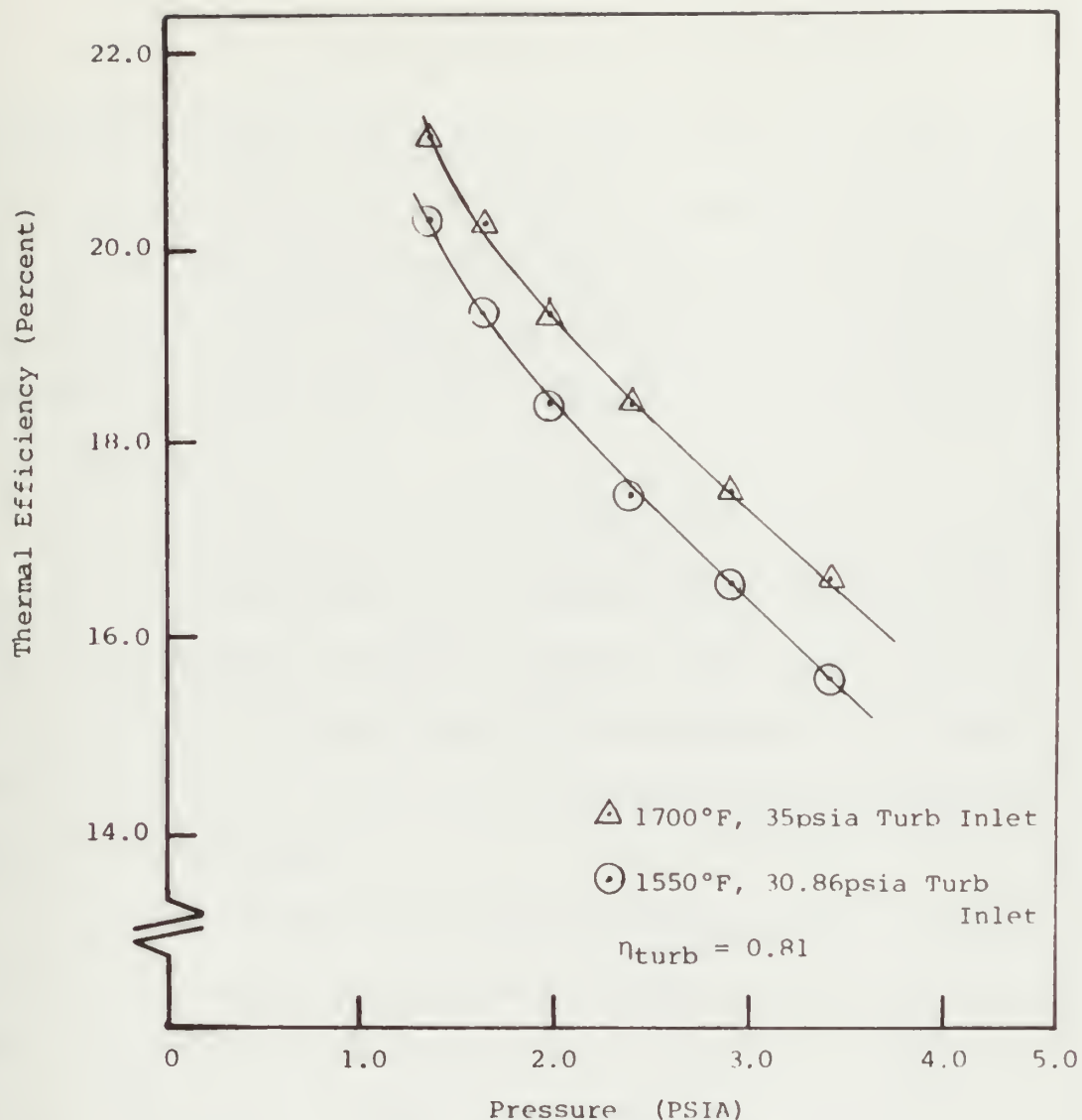


FIGURE 3-13 Effect Of Condensing Pressure
On Thermal Efficiency Of
Potassium Regenerative Cycle

increased thermal efficiency is the avoidance of thermal shock in the potassium boiler due to admission of liquid feed which is several hundred degrees below the boiler temperature. In the potassium topping cycle analyzed in Reference 3, the regenerator pressure ratio was approximately 0.90.

Figure 3-12 shows the relationship between the percent of the boiler mass flow extracted for regeneration, and the regenerator pressure ratio. Comparing Figures 3-11 and 3-12, the mass flow rate extracted at the best pressure ratio in terms of thermal efficiency is approximately 5.5 percent.

As in the case of the simple Rankine cycle, it is possible to increase the thermal efficiency of the regenerative cycle by lowering the pressure at which potassium condenses. Figure 3-13 shows the increase in thermal efficiency for the regenerative cycle as a function of condensing pressure.

3.3 BOTTOMING CYCLE

The bottoming cycle used to evaluate the Potassium-Steam Binary Cycle is the Bull Run Steam Plant described in Reference 19. The major reason for using this cycle is that it closely approximates the cycle that was used in the Liquid Metal Topping Cycle Plant Evaluation

of Reference 1, and a total bottoming cycle cost was available for this plant. This cost is used in later economic evaluations of various binary cycle plants.

The major parameters of the cycle are shown in Figure 3-14 and Tables 3-4 and 3-5.

3.4 SECOND LAW ANALYSIS OF BINARY CYCLE PLANT

Further insight into the energy conversion effectiveness of various topping cycle configurations over that provided by thermal efficiency (first law) considerations, may be gained by a second law analysis of the binary cycle plant. Consideration of Figures 3-3 and 3-4 suggests that the more reasonable method of increasing the thermal efficiency of the binary cycle plant is to lower the condensing temperature of the topping cycle rather than superheating since the former method yields approximately a 4 percent increase in thermal efficiency for a 125°F drop in condensing temperature, while superheating several hundred degrees results in less than a one percent increase.

The major heat transfer processes present in the binary cycle are shown in Figure 3-15. These processes are the heat transfer from the combustion gas to boiling potassium, the heat transfer from condensing potassium to boiling steam, and the heat transfer from condensing

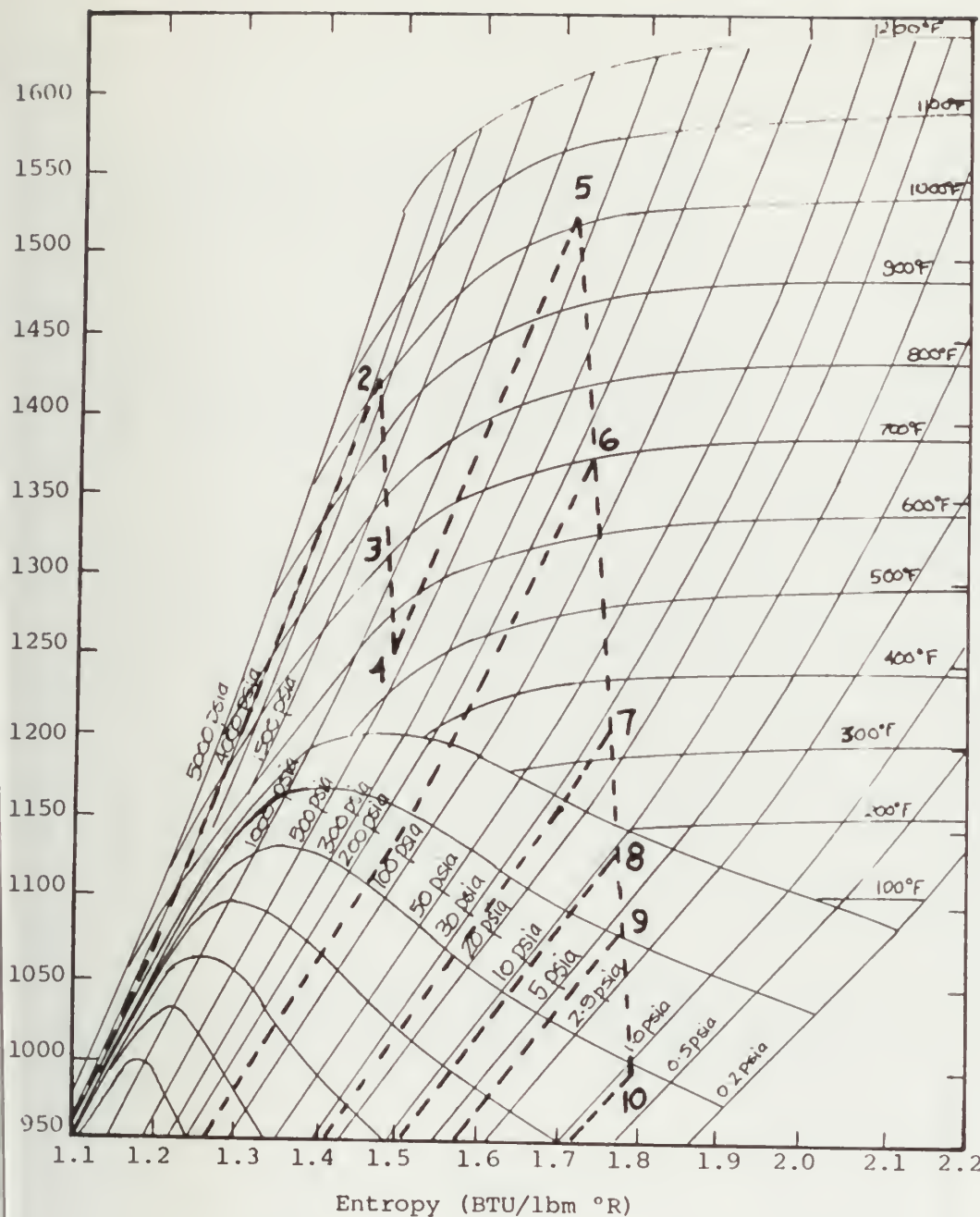


FIGURE 3-14 Enthalpy-Entropy Diagram
For Fixed Steam Bottoming
Cycle

| POINT | MASS FLOW | PRESSURE | TEMPERATURE | ENTHALPY | ENTROPY |
|-------------------------|-----------|----------|-------------|----------|---------|
| 1. Boiler In | 6.4574 | 4210.0 | 550.1° | 545.1 | 0.7333 |
| 2. Boiler Out | 6.4574 | 3515.0 | 1000.0° | 1421.7 | 1.4701 |
| 2. HP Turb Inlet | 6.4574 | 3515.0 | 1000.0° | 1421.7 | 1.4701 |
| 3. HP Turb Extraction | 1.3425* | 1137.0 | 697.7° | 1314.5 | 1.4927 |
| 4. HP Turb Exhaust | 5.1149 | 600.0 | 551.7 | 1256.8 | 1.5005 |
| 5. IP Turb Inlet | 4.7279 | 540.0 | 1000.0° | 1519.1 | 1.7280 |
| 6. IP Turb Exhaust | 4.7279 | 172.0 | 705.9° | 1378.7 | 1.7553 |
| 6. LP Turb Inlet | 4.5993 | 172.0 | 705.9° | 1378.7 | 1.7553 |
| 7. LP Turb Extraction 1 | 0.2673* | 26.7 | 328.7° | 1203.8 | 1.7670 |
| 8. LP Turb Extraction 2 | 0.1383* | 7.88 | 182.2° | 1124.8 | 1.7854 |
| 9. LP Turb Extraction 3 | 0.1912 | 3.45 | 147.0° | 1077.7 | 1.7970 |
| 10. LP Turb Exhaust | 4.0009 | 0.75 | 91.7° | 999.1 | 1.8183 |
| 4. Reheater In | 5.1149 | 600.0 | 551.7° | 1256.8 | 1.5005 |
| 5. Reheater Out | 5.1149 | 540.0 | 1000.0° | 1519.1 | 1.7280 |
| 10. Condenser Inlet | 4.0009 | 0.75 | 91.7° | 999.1 | 1.8183 |
| 11. Condenser Outlet | 4.0009 | 0.75 | 91.7° | 59.7 | 0.1147 |

NOTE: Mass Flow is in $\text{lbm/hr} \times 10^{-6}$
 Pressure is in psia
 Enthalpy is in BTU/lbm
 Entropy is in BTU/ $\text{lbm}^{\circ}\text{R}$
 Temperature is in $^{\circ}\text{F}$

*Indicates amount extracted for regenerators or auxiliary equipment operation.

TABLE 3-4 Primary Points In Bottoming Cycle

| | <u>Power (Btu/hr x 10⁻⁹)</u> | <u>Power (MW)</u> |
|---------|---|-------------------|
| HP Turb | 0.9874 | 289.28 |
| IP Turb | 0.6638 | 194.48 |
| LP Turb | 1.6582 | 485.81 |

Total Turbine Output = 969.57 MW(mech)

Total Power Output = 937.20 MW(e)

Power For Auxiliaries = 17.83 MW (Assuming a 1.5%
loss in generators)

TABLE 3-5 Summary Of Power Output For Bottoming Cycle

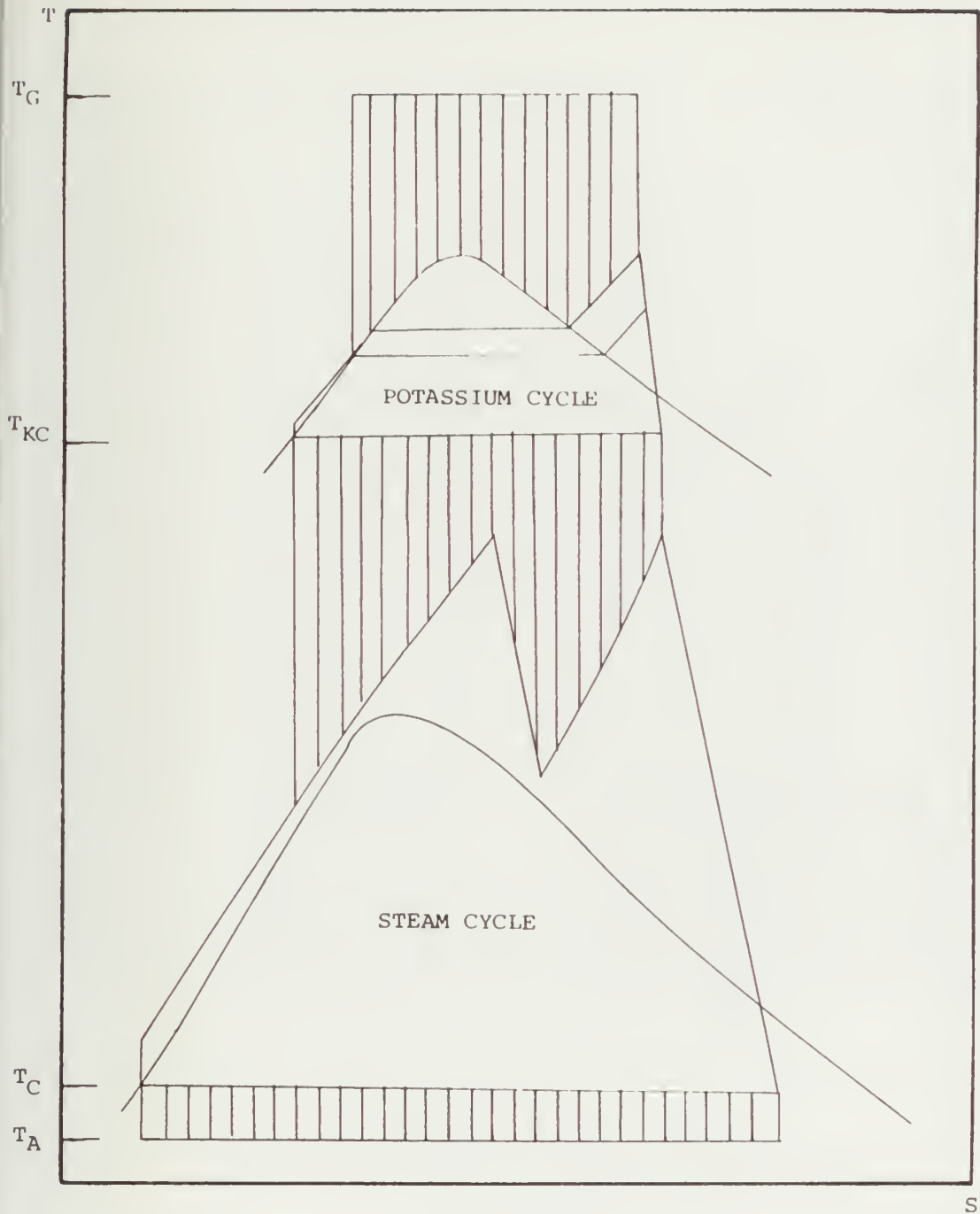


FIGURE 3-15 Major Heat Transfer Processes
In Potassium Steam Binary
Cycle

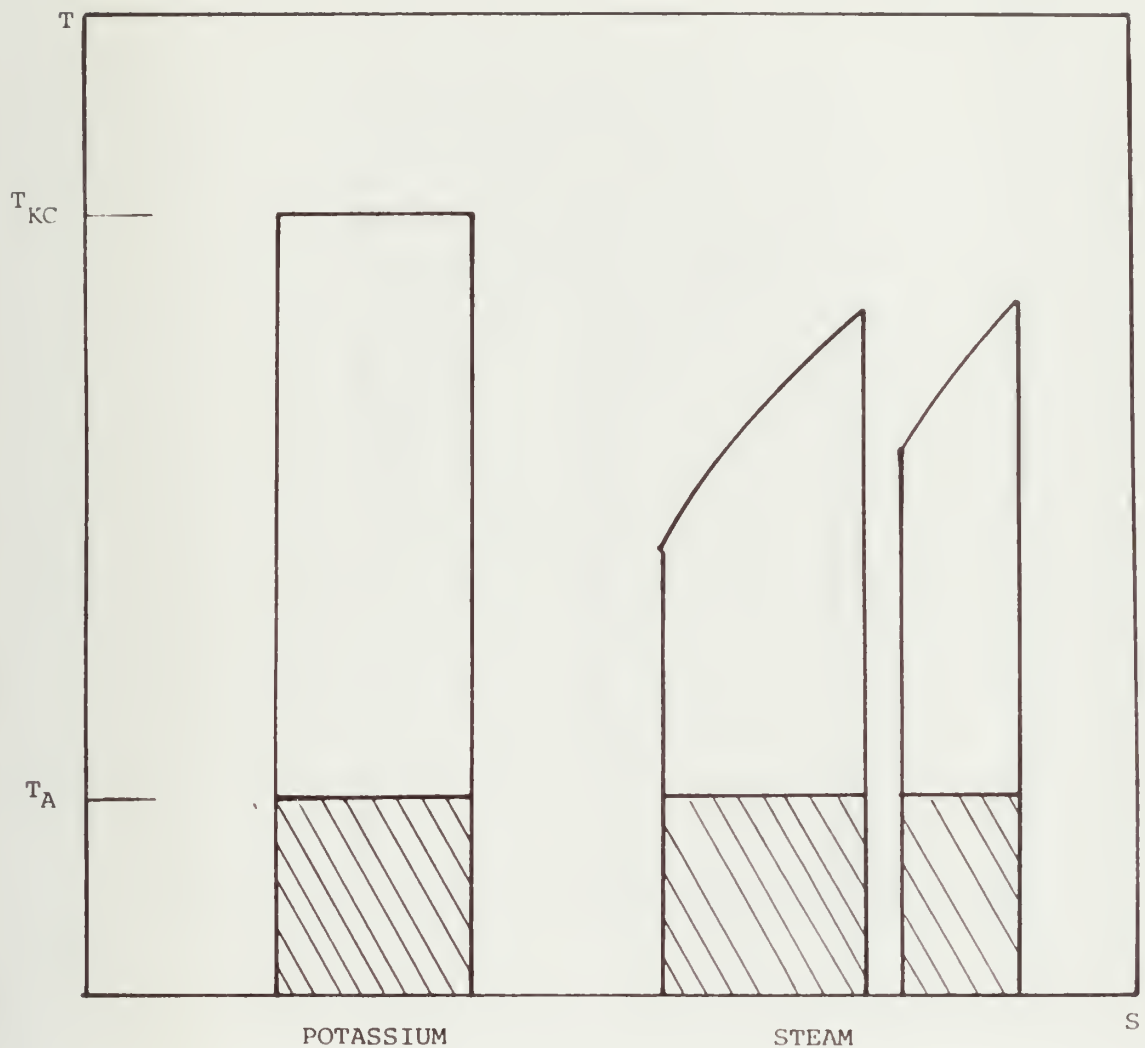


FIGURE 3-16 Potassium Condenser-Steam Boiler
Available Energy For Potassium
Steam Binary Cycle

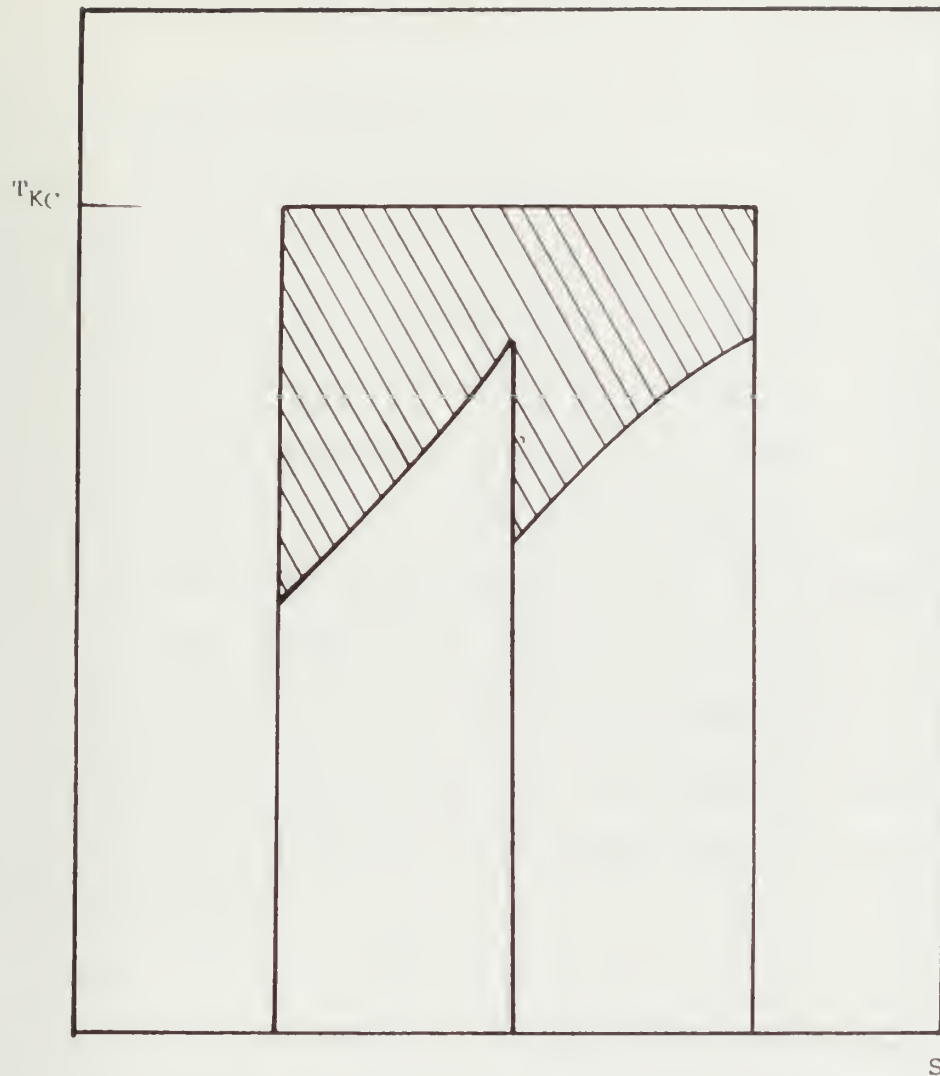


FIGURE 3-17 Unavailable Energy Due To Potassium-Steam Heat Transfer Process In The Potassium Binary Cycle

steam to the environment. During any heat transfer process from a high temperature system to a lower temperature system, there is a decrease in the available energy caused by the transfer of heat at the temperature of the lower temperature system. Two such systems are the condensing potassium and boiling steam. These are shown in Figure 3-16. The available energy for each system is given by the unshaded area. The shaded area is unavailable because its temperature is below that of the environment. Figure 3-17 again shows the two systems. The unavailable energy due to heat transfer from potassium to steam is given by the shaded area of this Temperature Entropy diagram.

In order to evaluate the effect of the heat transfer process from the condensing potassium to the steam, consider an ideal heat engine operating between the condensing potassium temperature and an environment temperature which is the condensing temperature of steam. Since it is of interest to evaluate the effect of the heat transfer from the potassium to steam, it is necessary to establish the environment at the steam condensing temperature in order to eliminate the effect of the condensing steam heat transfer. If the heat engine operating between the condensing potassium is an ideal engine, it

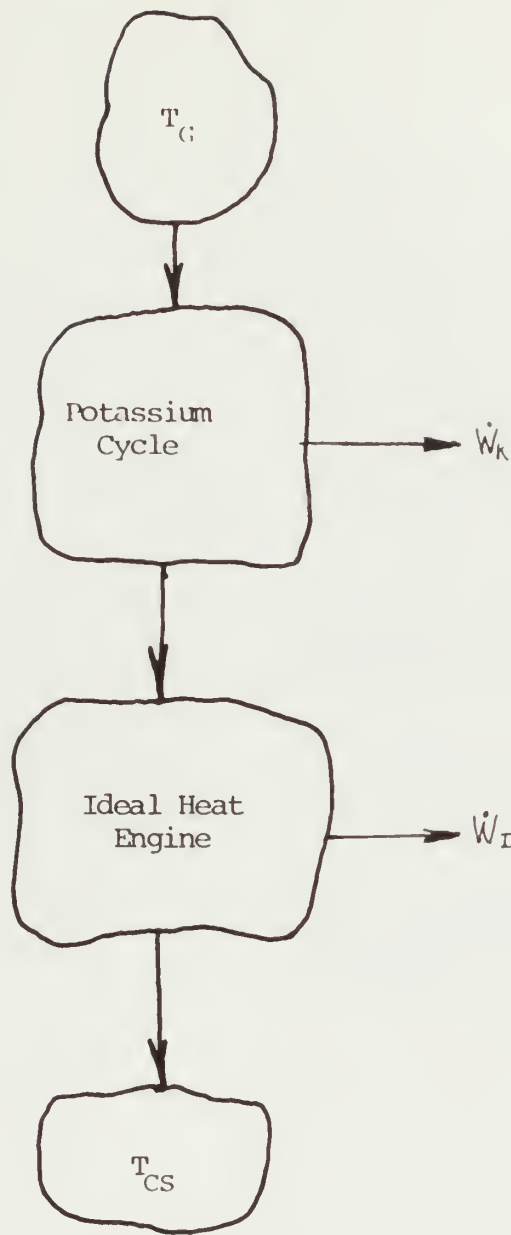


FIGURE 3-18 Potassium Cycle - Ideal Heat Engine Binary Cycle

| | | |
|--------------------|--|--|
| \dot{Q}_{RK} | $= \dot{m}_{KC} \Delta h_{KC}$ | Total heat rejected by topping cycle |
| \dot{w}_T | $= \dot{w}_S + \dot{w}_K$ | Total Turbine Power |
| \dot{Q}_{AV} | $= \dot{Q}_{RK} - \dot{m}_{KC} \dot{T}_{SC} (\Delta s_{KC})$ | Available Energy |
| \dot{Q} | $= \dot{m}_{KB} \Delta h_{KB}$ | Total Heat Input To Binary Cycle |
| \dot{Q}_{in} | $= \dot{Q}_{AV} - \dot{w}_S$ | Increase In Unavailable Energy |
| η_{ti} | $= \frac{\dot{Q}_{AV} + \dot{w}_K}{\dot{Q}} = \frac{\dot{w}_I + \dot{w}_K}{\dot{Q}}$ | Ideal Thermal Efficiency |
| $\% \Delta \eta_t$ | $= \frac{\eta_{ti} - \eta_{to}}{\eta_{ti}}$ | Percent Decrease In Thermal Efficiency |

TABLE 3-6 Summary Of Second Law Analysis

is capable of converting all the heat supplied to it into useful work. Now, if such an engine operated as a bottoming cycle plant with a potassium topping cycle, and rejected heat only at the temperature of condensing steam, an ideal thermal efficiency could be defined as

$$\eta_{ti} = \frac{\dot{W}_K + \dot{W}_I}{\dot{Q}} .$$

Such a system is shown in Figure 3-18.

The ideal engine work is the available energy, and is

$$\dot{Q}_{AV} = \dot{W}_I = \dot{M}_{KC} T_{KC} (S_5 - S_1) - \dot{M}_{KC} T_{SC} (S_5 - S_1) .$$

The entropy subscripts refer to Figure 3-9. The increase in unavailable energy due to the heat transfer in the potassium condenser is then

$$\dot{Q}_{IN} = \dot{Q}_{AV} - \dot{W}_S$$

where \dot{W}_S is evaluated for the fixed bottoming cycle plant. The percent decrease in ideal thermal efficiency is then

$$\% \Delta \eta_t = \frac{\eta_{ti} - \eta_{to}}{\eta_{ti}} .$$

A summary of these relationships is presented in Table 3-6.

Figure 3-19 shows the effect of potassium condensing temperature on the overall thermal efficiency for two topping cycles in combination with the fixed bottoming cycle. Figure 3-20 shows the effect of condensing temperature on the percent decrease in thermal efficiency. Both indicate that the potassium condensing temperature strongly influences thermal efficiency.

Since the heat addition to the steam cycle occurs, in two processes over a range of temperatures, it would seem useful to consider an average temperature of heat addition to the steam cycle. One such average temperature is the entropy average temperature which is defined as

$$\bar{T}_S = \frac{\dot{M}_B(h_2 - h_1) + \dot{M}_r(h_5 - h_4)}{\dot{M}_B(S_2 - S_1) + \dot{M}_r(S_5 - S_4)}$$

(The enthalpy and entropy subscripts refer to Table 3-4). It is then possible to define a dimensionless temperature ratio which corresponds to various condensing temperatures as

$$\frac{\Delta T_K}{T_{KC}} = \frac{T_{KC} - \bar{T}_S}{T_{KC}} .$$

Figures 3-21 and 3-22 illustrate the effect of the

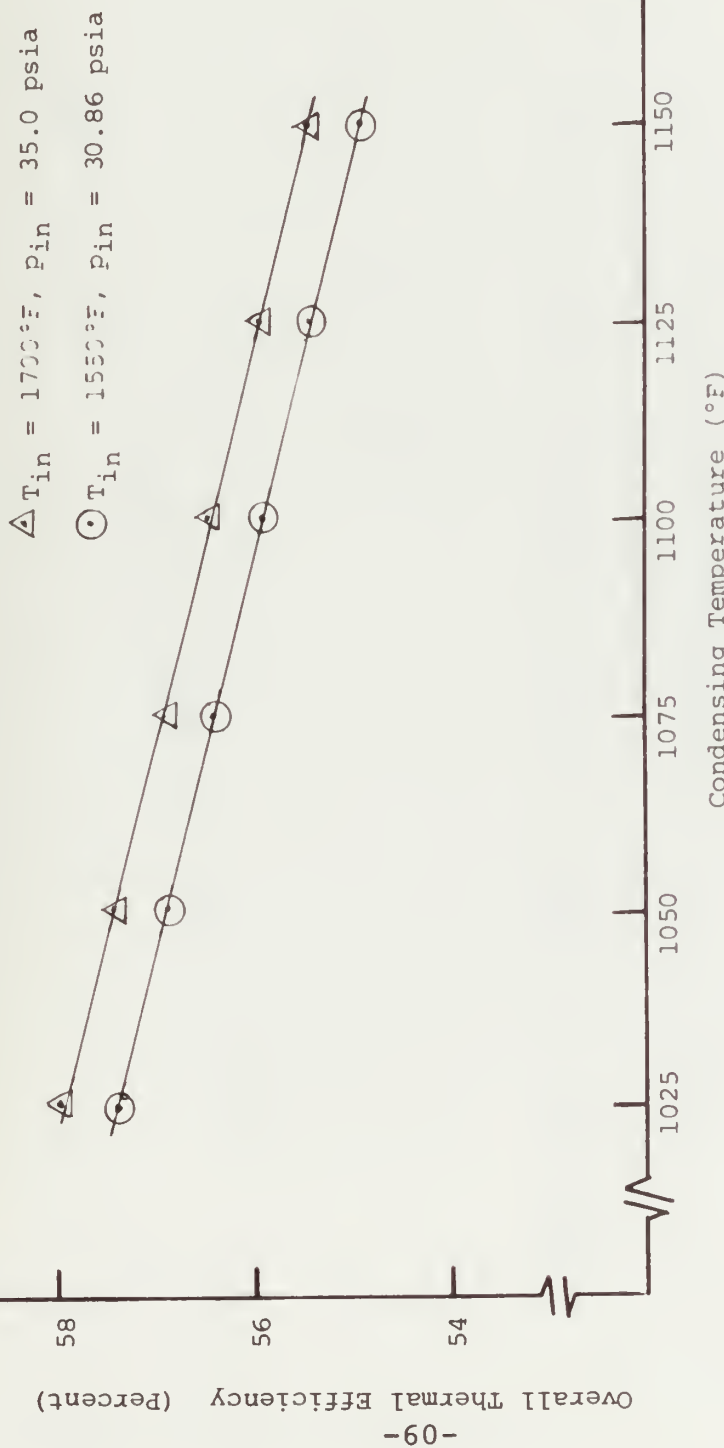


FIGURE 3-19 Effect Of Condensing Temperature On Potassium Steam Binary Cycle Overall Efficiency

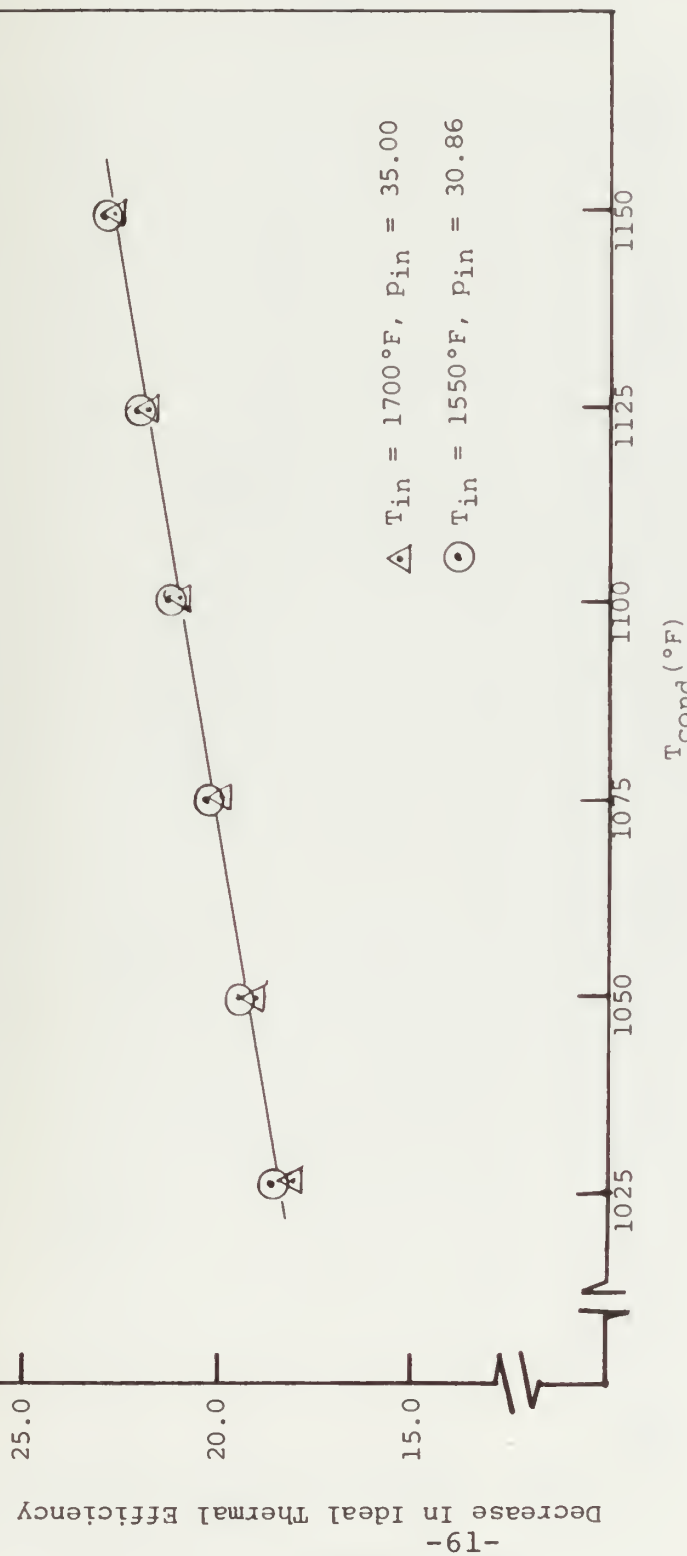


FIGURE 3-20 Effect Of Condensing Temperature On Percent Decrease
In Ideal Thermal Efficiency For
The Potassium Steam Binary Cycle

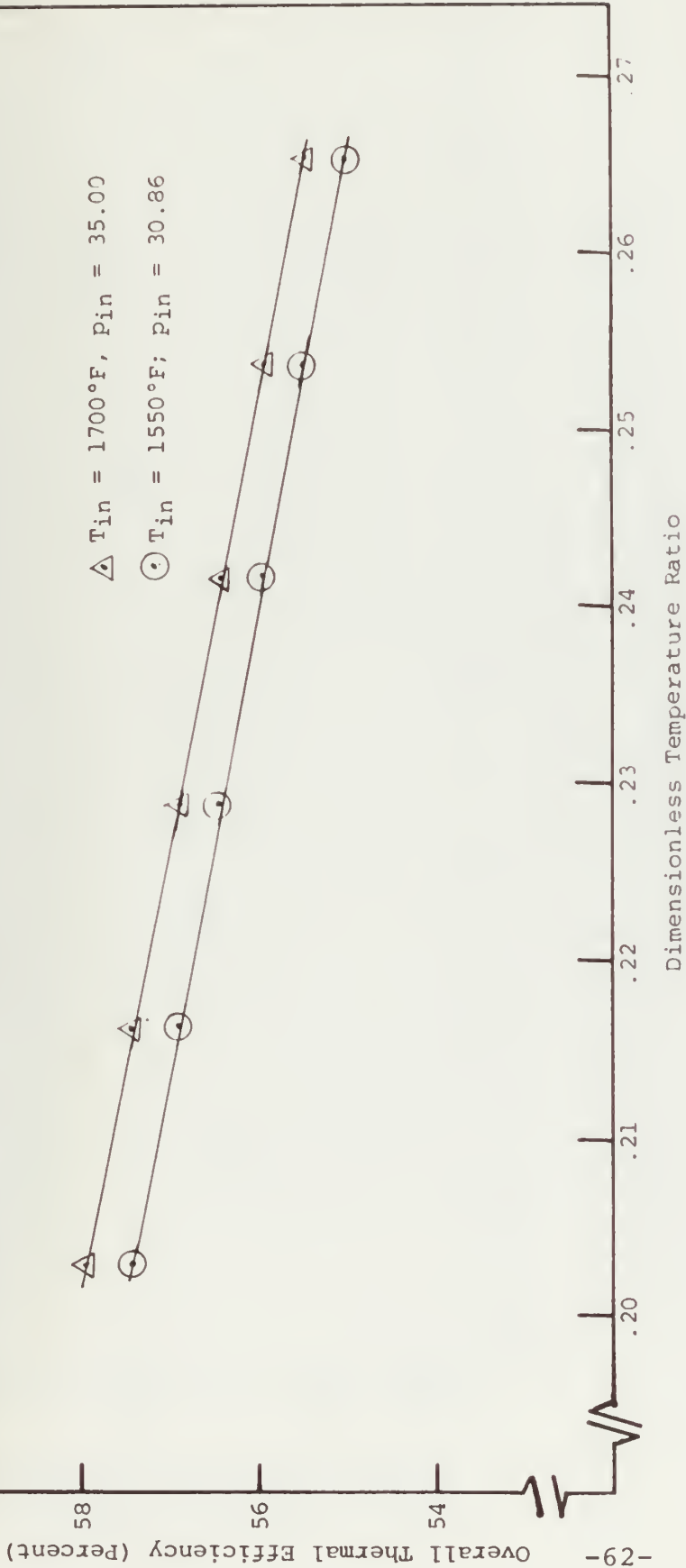


FIGURE 3-21 Effect Of The Dimensionless Temperature Ratio
On Overall Thermal Efficiency For
The Potassium Steam Binary Cycle



Decrease In Thermal Efficiency Due To
Increase In Unavailable Energy (Percent)

○ Sat Vapor Turbine Inlet ($p = 30.86\text{psia}$, $T = 1550^\circ\text{F}$)

△ Superheated vapor Turbine Inlet ($p = 35\text{psia}$, $T = 1700^\circ\text{F}$)

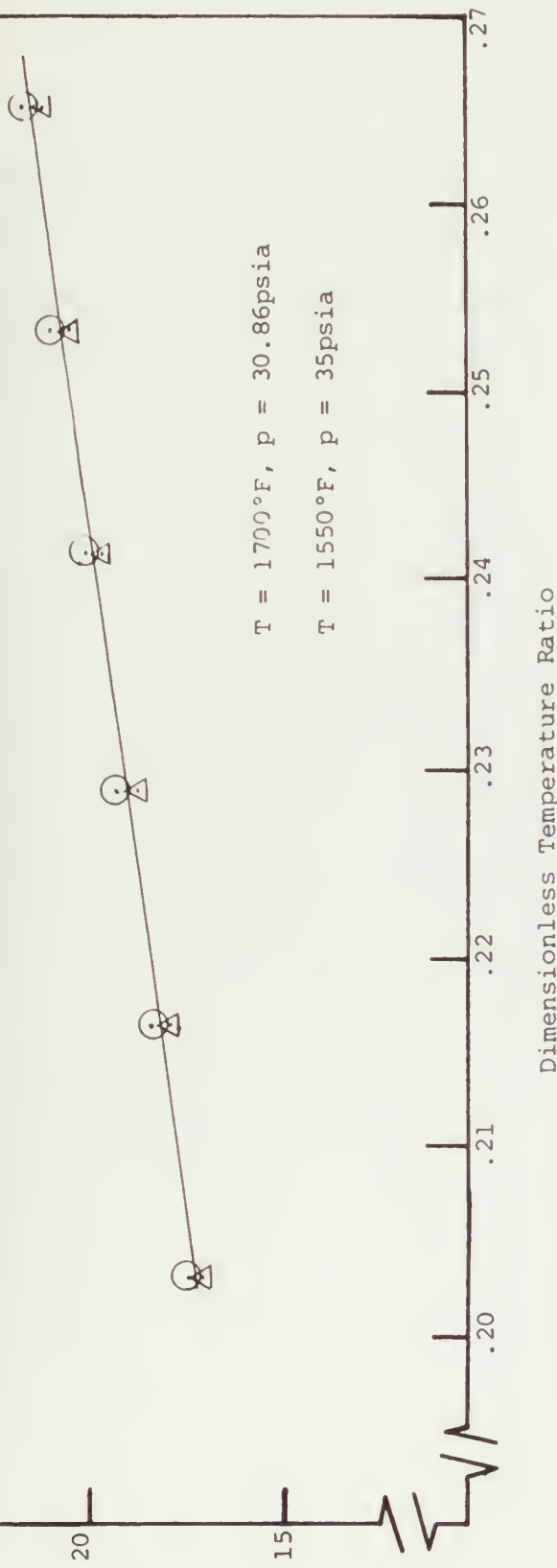


FIGURE 3-22 Effect Of Dimensionless Temperature Ratio On The Decrease In Thermal Efficiency For The Potassium Steam Binary Cycle

dimensionless temperature ratio on the overall thermal efficiency and the percent decrease in thermal efficiency. Once again, these quantities are seen to vary strongly with this ratio.

4. POWER PLANT CONFIGURATION

Several of the references discussed in Chapter 2 have made suggestions concerning possible plant layout and component design which might be used in the potassium-steam cycle. The major heat exchangers of the topping cycle are the potassium boiler and the potassium condenser-steam boiler.

Potassium Boiler and Furnace In References 11 and 14, a pressurized furnace manufactured from 316 stainless steel is proposed. The suggested pressure level in the furnace is approximately the top pressure of the potassium cycle. Figure 4-1 is the overall potassium furnace layout as suggested in Reference 14. A cross section of the furnace is shown in Figure 4-2. In this arrangement, the combustion gases flow upward through the combustion chamber, and return downward through the heat transfer matrix formed by the tube bundles.

A potassium boiler module is shown in Figure 4-3. It consists of a set of long parallel tubes. The actual combustion takes place in the space between the boiler tube modules. At the top of each module, the tubes flare outward before entering the header. This provides a space for the combustion gases to flow inward so that they can return downward through the boiler tube matrix. The potassium boiler is of the recirculating type. With this

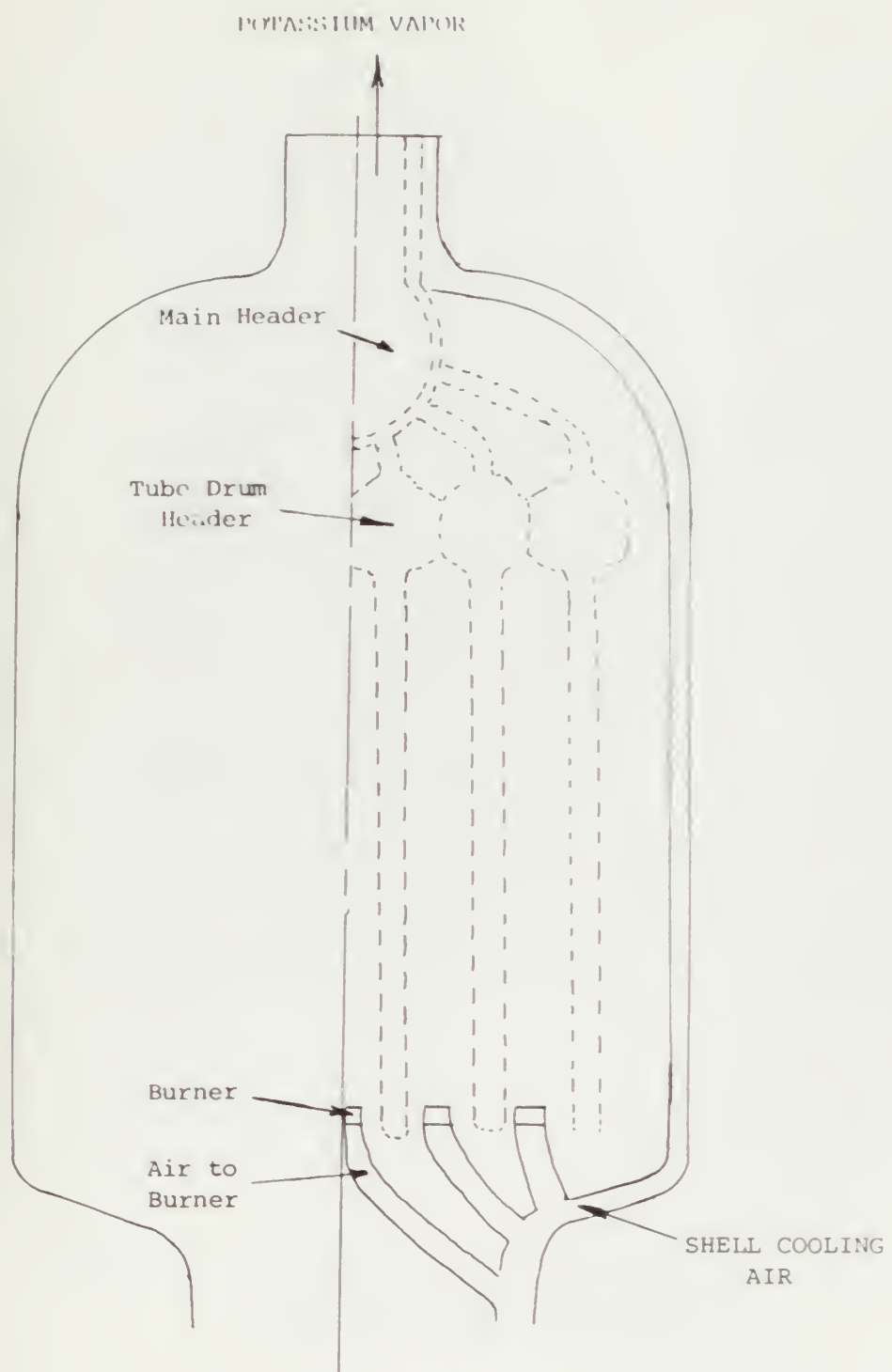


FIGURE 4-1 Vertical Section Through Potassium-Boiler Furnace Unit

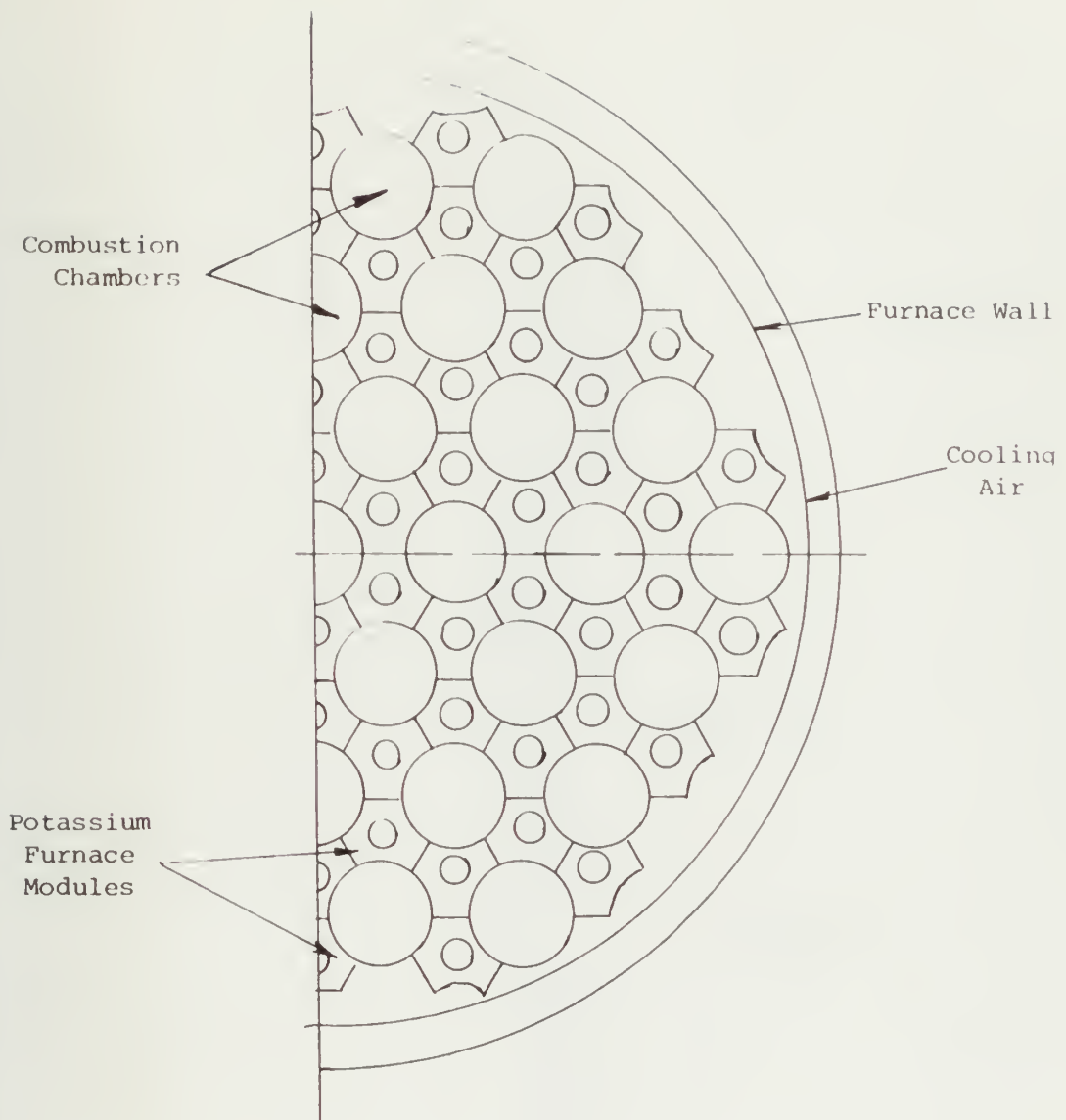


FIGURE 4-2 Horizontal Cross Section Through Potassium-Boiler Furnace Unit

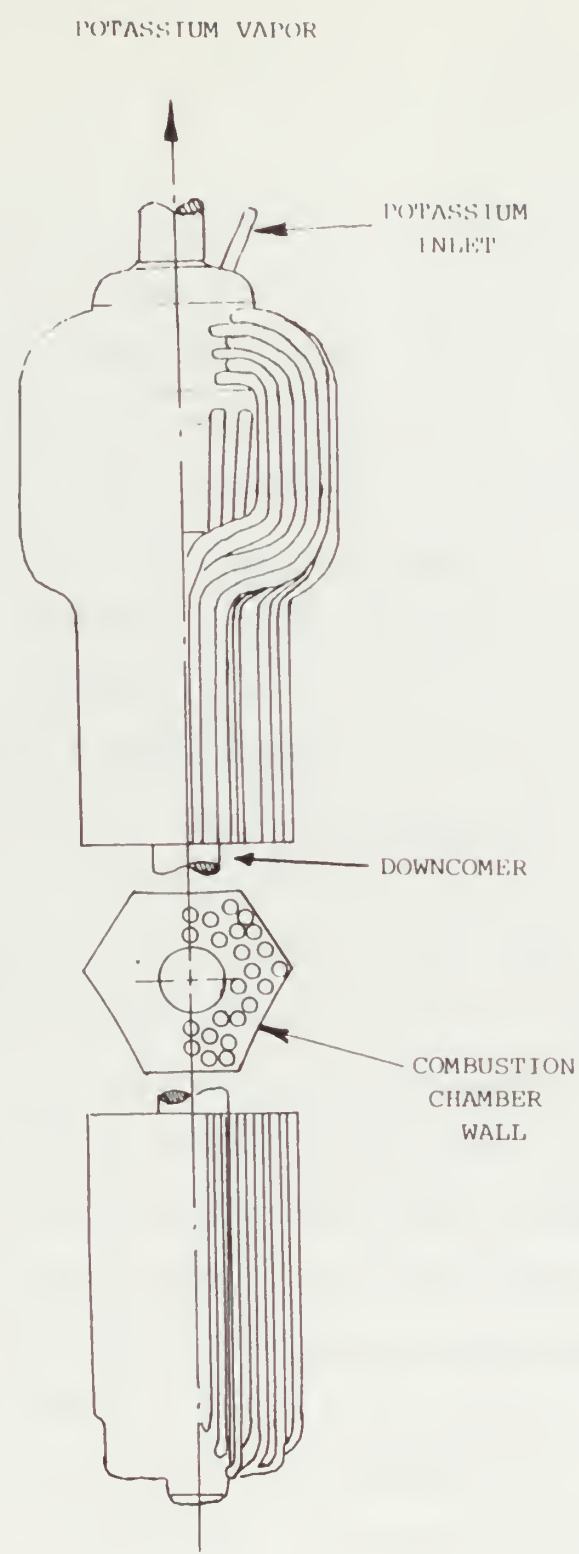


FIGURE 4-3 Tube Bundle Module For Potassium Boiler

design, it is possible to keep all of the metal surfaces from reaching temperatures which are very much higher than that of the boiling potassium, while at the same time maintaining a high heat flux throughout the entire heat exchanger surface. After evaporation, the potassium vapor flows upward into the module header. It then flows into the larger spheriodal header inside the furnace shell as shown in Figure 4-1.

Potassium Condenser - Steam boiler Since the heat transfer coefficient for condensing potassium is very high (a value of 10,000Btu/hr ft²°F is given in Reference 12) it is possible to operate with a very small temperature difference between condensing potassium and steam. Because of this high heat transfer coefficient, the total surface area required for steam generation is much smaller than that required in a conventional fossil-fueled steam plant of the same power output. In this component, an extremely high heat flux may be maintained since the peak metal temperature cannot reach a value greater than that of the condensing potassium. In Reference 14, a reentry tube steam boiler is proposed. A sketch of the reentry tube is shown in Figure 4-4. The reentry tube employs two vertical concentric tubes. Feed water enters through inner annulus, and flows vertically upward. Heating and

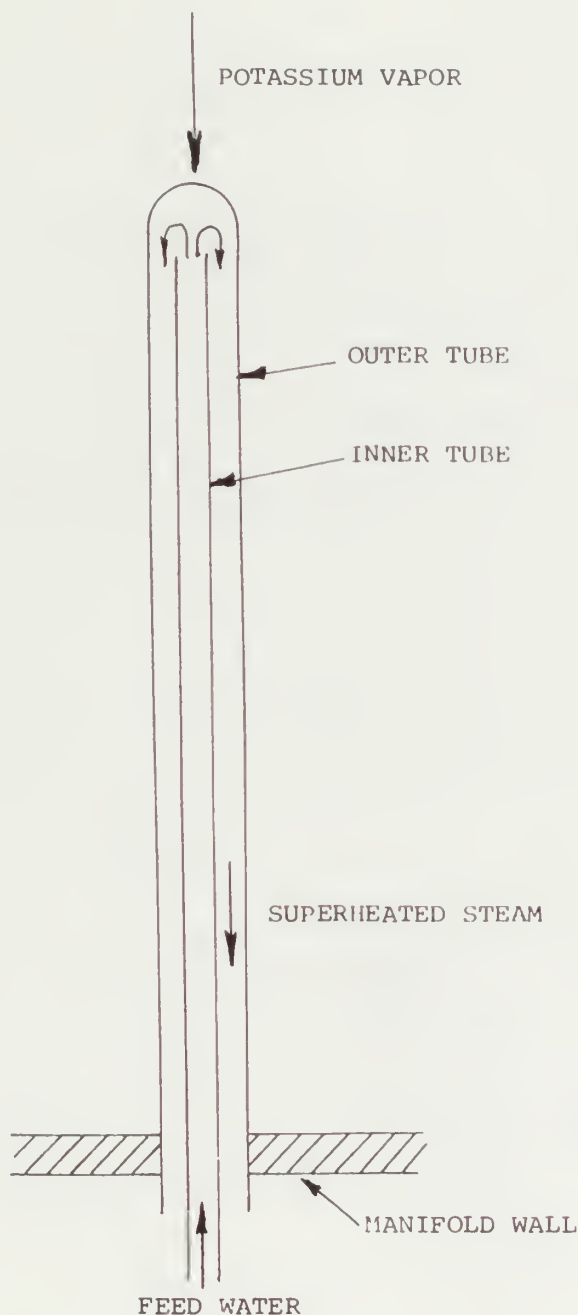


FIGURE 4-4 Section Through A Re-Entry Tube For The Potassium Boiler Steam Condenser

Potassium Turbine

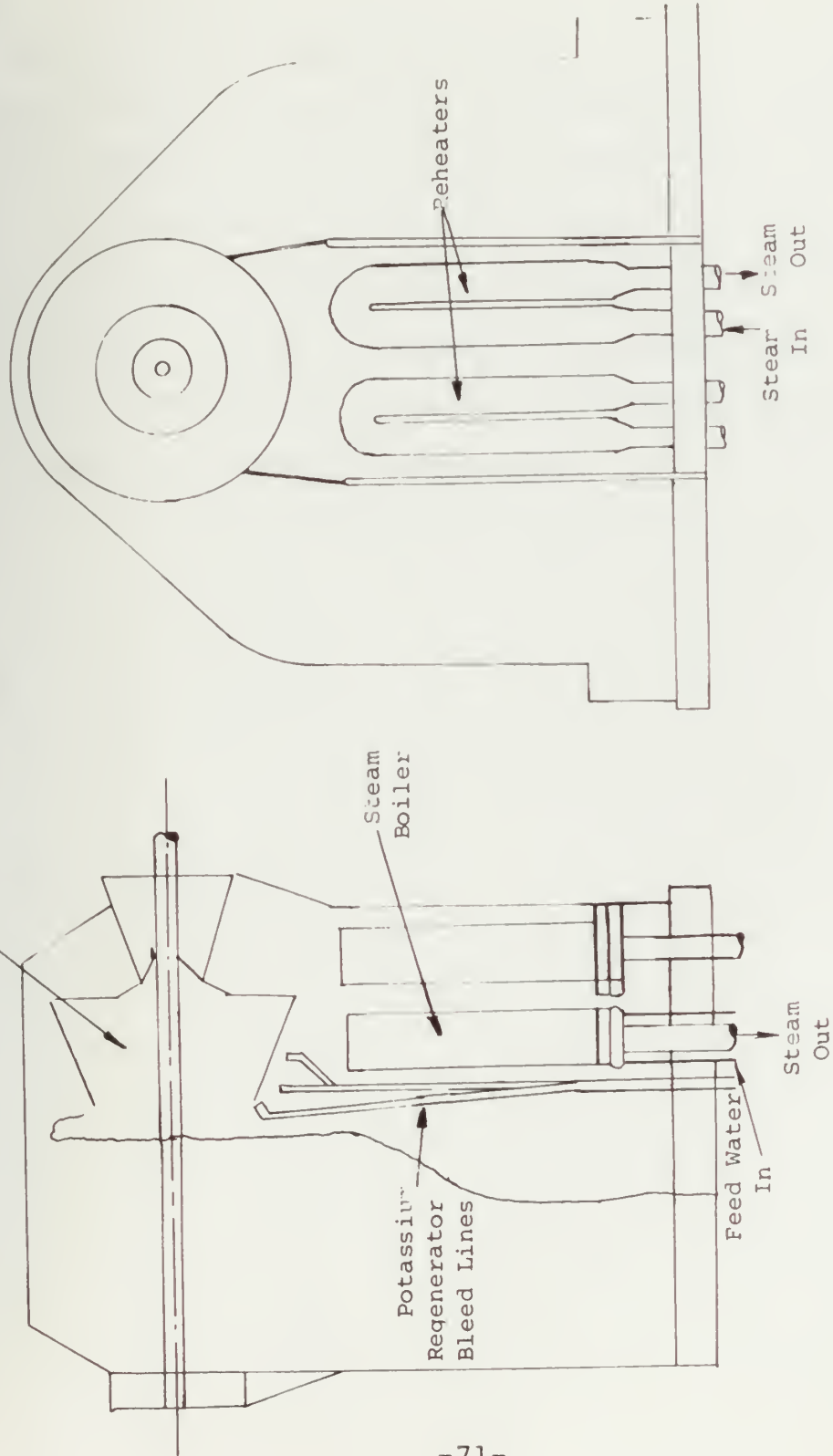


FIGURE 4-5 Potassium Turbine - Condenser Arrangement

evaporation occur in this section. Steam then emerges from the inner annulus and flows downward through the outer annulus. In this section, superheating takes place. Potassium vapor is condensed on the outer surface of the tube as it flows downward, and drains to the bottom of the condenser. Figure 4-5 shows the proposed layout of the potassium condenser located directly below the potassium turbine as given in Reference 14.

5. ECONOMIC ANALYSIS

5.1 BACKGROUND

The economic analysis consists of a capital cost determination of various topping cycle plant configurations in combination with the fixed bottoming cycle plant of Section 3.3. The capital cost is also found per unit plant output in kw. The operating cost is determined using a capacity factor of 0.65 as was done in Reference 1, and the cost data for Illinois Number 6 coal.

5.2 CAPITAL COST DETERMINATION

According to Reference 1, the major binary cycle cost components are:

- (1) Liquid Metal Pump
- (2) Liquid Metal Furnace
- (3) Air Preheater
- (4) Liquid Metal Turbogenerator
- (5) Liquid Metal Dump Tank
- (6) Liquid Metal Condenser
- (7) Bottoming Cycle (Fixed Cost)

In order to evaluate the cost of various topping cycle components for different configurations, it is necessary to determine a unit cost for the various components. A discussion of the assumptions under which these unit costs are obtained for various components follows.

Liquid Metal Pump

In Reference 1, an evaluation

of the cost of various topping cycle components for different cycle conditions is presented. However, only in one case was there enough detail to determine a unit cost. This configuration is referred to as base case number 1. The topping cycle operates between 1400°F (15.2 psia) and 1100°F (2.4 psia), and its net output is 296.6MW. The potassium mass flow rate in this cycle is 9.25×10^6 lbm/hr. The bottoming cycle in this case is a 937.2MW steam plant which is similar to that of Section 3.3. The pump cost in this case is 1.8 MM\$. Since the pressures for the topping cycles being evaluated are of the same order of magnitude, it is assumed that the pump cost is proportional to the potassium flow rate. Thus the unit cost for liquid metal pumps is assumed to be 0.1946 MM\$/ 10^6 lbm/hr.

Liquid Metal Furnace

A unit cost of 18.34 MM\$/

10^9 Btu/hr is given in Reference 1 for the liquid metal topping cycle furnace.

Air Preheater

A unit cost for liquid metal

furnace air preheaters is not given in Reference 1. However, for the cases analyzed in Reference 1, the air preheater cost is approximately 10.5 percent of the liquid metal furnace cost, with less than 1 percent deviation

from this value. Therefore, it is assumed that the air preheater cost is 1.93 MM\$/ 10^9 Btu/hr.

Liquid Metal Turbogenerator In reference 11, it is estimated that the cost of a potassium vapor turbine will be approximately 30% higher than a gas turbine of the same power output. Reference 20 provides an estimated cost of industrial gas turbines of 20 \$/kw(e) (1970 dollars). Reference 21 provided a cost index for this type of machinery of 1.222 for 1970, and 1.758 for 1974 based on an index of 1.00 in 1967. Using these indices, and the 30 percent additional cost predicted in Reference 11, the unit cost for the turbine is 37.46 \$/kw(e). In Reference 20, the cost of electrical generators is estimated to be approximately 10 \$/kw(e) (1970 dollars). Using similar cost indices for electrical generators available in Reference 21, the unit cost of generators is 14.18 \$/kw. Thus the unit cost for turbogenerators is 51.65 \$/kw(e).

Liquid Metal Dump Tank As in the case of the liquid metal pump, the unit cost for this component is assumed to be proportional to the mass flow rate. For the base case of Reference 1, the cost of this component is 7.1MM\$, with a flow rate of 9.25×10^6 lbm/hr. Thus the unit cost is 0.7676MM\$/ 10^6 lbm/hr.

| <u>COMPONENT</u> | <u>UNIT COST</u> |
|-----------------------------|------------------------------------|
| Liquid Metal Pump | 0.1946 MM\$/ 10^6 lbm/hr |
| Liquid Metal Furnce | 18.34 MM\$/ 10^9 Btu/hr |
| Air Preheater | 1.93 MM\$/ 10^9 Btu/hr |
| Liquid Metal Turbogenerator | 51.65 \$/kw (e) |
| Liquid Metal Dump Tank | 0.7676 MM\$/ 10^6 lbm/hr |
| Liquid Metal Condenser | 3.189 MM\$/ 10^5 ft ² |

Note: Costs are in 1974 dollars

TABLE 5-1 Topping Cycle Unit Costs

Liquid Metal Condenser

The cost of this component is assumed to be proportional to the total heat exchanger surface area. The cost for the base case of Reference 1 is 2.6MM\$, and the total heat exchanger surface area as evaluated by the computer program of Appendix A is $81532 \cdot 13 \text{ ft}^2$. Thus the unit cost is $3.189 \text{ MM\$} / 10^5 \text{ ft}^2$.

Bottoming Cycle

The bottoming cycle as estimated by Reference 1 is 354.3MM\$. Table 5-1 lists the above unit costs.

5.3 OPERATING COSTS

The operating costs for various binary cycle plants is determined for Illinois Number 6 Coal. The cost of this fuel is 0.85\$/MM Btu and its higher heating value is 10788Btu/lbm (Reference 1). If a furnace efficiency of 92.5 percent (Reference 16), and a capacity factor of 0.65 (Reference 1) is assumed, then the actual heat input required by the binary cycle is given by

$$\dot{Q}_{act} = \left(\frac{\text{Capacity}}{\text{Factor}} \right) \times \left(\frac{\dot{Q}}{\eta_F} \right) .$$

Here \dot{Q} is the heat input calculated from the enthalpy changes in the potassium boiler. The cost in mills per kw-hr(e) is then

$$\text{Cost} = \left(\frac{\dot{Q}_{\text{act}}}{\text{Power In Kw}} \right) \left(\text{Cost of Fuel} \right).$$

The yearly fuel cost is found by

$$\left(\frac{\text{Yearly Fuel}}{\text{Cost}} \right) = [\dot{Q}_{\text{act}}] \left[8760 \frac{\text{hr}}{\text{yr}} \right] [\text{Cost}]$$

Tables 5-2 and 5-3 present the capital cost distributions as determined by the unit costs of Section 5-2, and the operating costs as determined by this section. These costs are determined for the binary cycle plants analyzed in Chapter 3. Figure 5-1 shows the variation of capital cost per unit electrical output as a function of the dimensionless temperature ratio. Comparison of Tables 5-2 and 5-3, and Figure 5-1 show that although the superheated plants are more expensive in total capital cost, they are less expensive per unit output since they are more efficient for a given volume of the dimensionless temperature ratio. Figure 5-2 shows the operating cost as a function of the dimensionless temperature ratio. Once again, the superheated plants are less expensive because of their higher efficiency.

| <u>CONDENSING LIQUID</u> | <u>1025</u> | <u>1050</u> | <u>1075</u> | <u>1100</u> | <u>1125</u> | <u>1150</u> |
|------------------------------|-------------|-------------|-------------|-------------|-------------|-------------|
| Liquid Metal Turbo Gen | 27.85 | 26.34 | 24.86 | 23.41 | 22.00 | 20.00 |
| Liquid Metal Dump Tank | 8.13 | 8.03 | 7.94 | 7.83 | 7.76 | 7.70 |
| Liquid Metal Pump | 2.06 | 2.04 | 2.01 | 1.99 | 1.97 | 1.95 |
| Liquid Metal Furnace | 162.86 | 161.03 | 159.19 | 157.36 | 155.71 | 153.87 |
| Air Preheater | 17.14 | 16.95 | 16.75 | 16.56 | 16.39 | 16.19 |
| Liquid Metal Condenser | 4.68 | 3.60 | 3.00 | 2.60 | 2.31 | 2.09 |
| Bottoming Cycle | 354.30 | 354.30 | 354.30 | 354.30 | 354.30 | 354.30 |
| Acquisition Cost | 577.02 | 572.29 | 568.05 | 564.05 | 560.44 | 556.70 |
| Power [MW(e)] | 1476.45 | 1447.21 | 1418.59 | 1390.40 | 1363.05 | 1336.10 |
| Capital Cost [\$/KW(e)] | 390.82 | 395.44 | 400.43 | 405.67 | 411.17 | 416.65 |
| Operating Cost [mills/kw hr] | 3.592 | 3.624 | 3.655 | 3.686 | 3.720 | 3.751 |
| Yearly Fuel Cost | 46.46 | 45.94 | 45.42 | 44.90 | 44.42 | 43.90 |

Note: Costs are in millions of dollars (1974)

TABLE 5-2 Cost Distribution For 35.00psia, 1700°F Topping Cycle
Inlet Condition Binary Cycle

CONDENSING TEMPERATURE

| | <u>1025</u> | <u>1050</u> | <u>1075</u> | <u>1100</u> | <u>1125</u> | <u>1150</u> |
|-----------------------------|-------------|-------------|-------------|-------------|-------------|-------------|
| Liquid Metal Turbo·Gen | 26.33 | 24.83 | 23.34 | 21.92 | 20.52 | 19.14 |
| Liquid Metal Dump Tank | 8.32 | 8.23 | 8.14 | 8.04 | 7.95 | 7.87 |
| Liquid Metal Pump | 2.11 | 2.09 | 2.06 | 2.04 | 2.02 | 1.99 |
| Liquid Metal Furnace | 161.03 | 159.19 | 157.36 | 155.42 | 153.87 | 152.04 |
| Air Preheater | 16.95 | 16.75 | 16.56 | 16.37 | 16.19 | 16.00 |
| Liquid Metal Condenser | 4.98 | 3.60 | 3.00 | 2.60 | 2.31 | 2.08 |
| Bottoming Cycle | 354.30 | 354.30 | 354.30 | 354.30 | 354.30 | 354.30 |
| Acquisition Cost | 573.72 | 568.99 | 564.76 | 560.69 | 557.16 | 533.42 |
| Power [MW(e)] | 1447.00 | 1418.00 | 1389.63 | 1361.69 | 1334.57 | 1307.84 |
| Capital Cost [\$/kW(e)] | 369.49 | 401.26 | 406.41 | 411.76 | 417.48 | 423.16 |
| Operating Cost [cents/kWhr] | 3.624 | 3.656 | 3.688 | 3.720 | 3.755 | 3.786 |
| Yearly Fuel Cost | 45.94 | 45.41 | 44.89 | 44.37 | 43.90 | 43.37 |

Note: Costs are in millions of dollars (1974)

TABLE 5-3 Cost Distribution For 30.86psia, 1550°F Topping Cycle
Inlet Condition Binary Cycle Plant

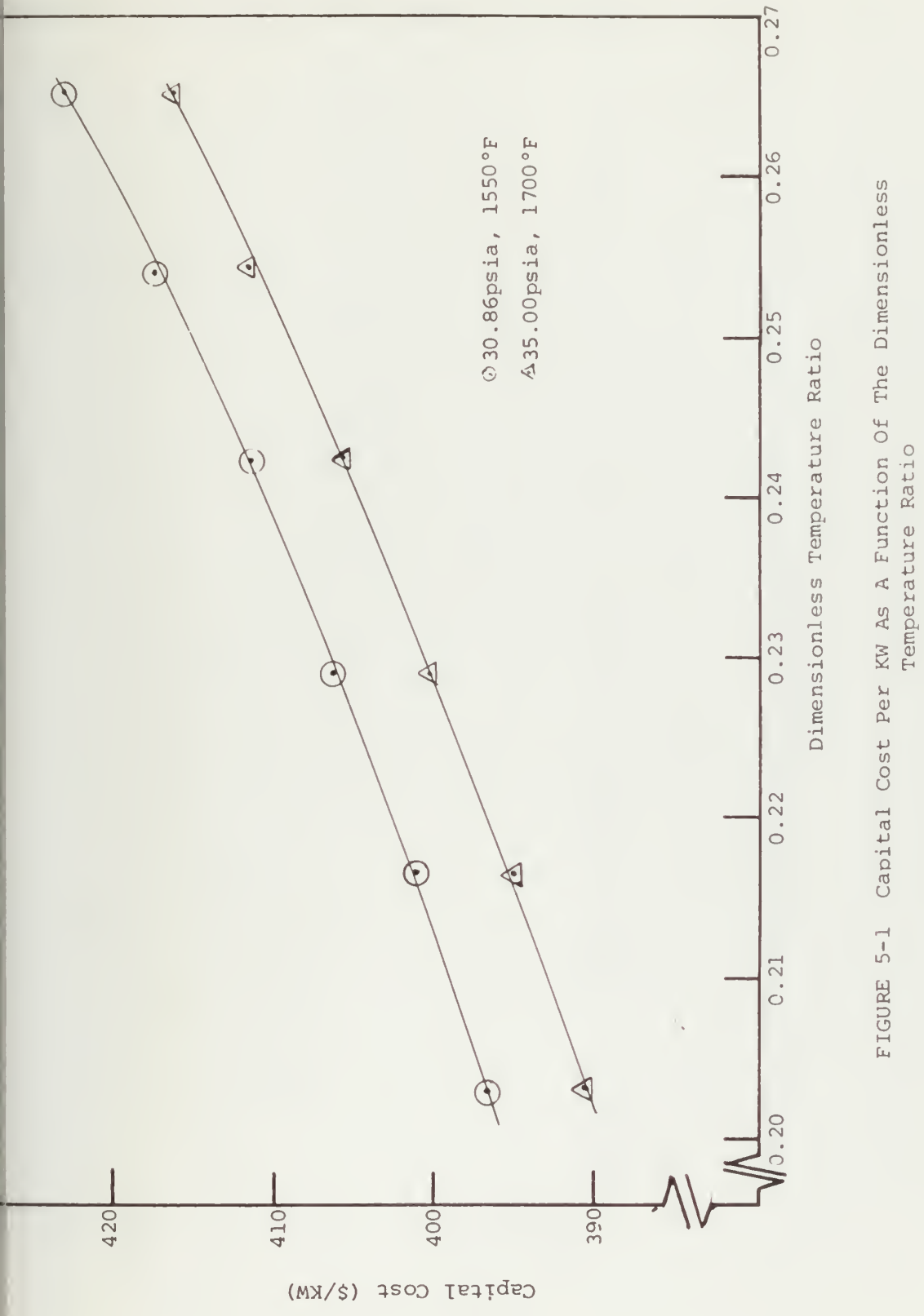


FIGURE 5-1 Capital Cost per KW As A Function Of The Dimensionless Temperature Ratio

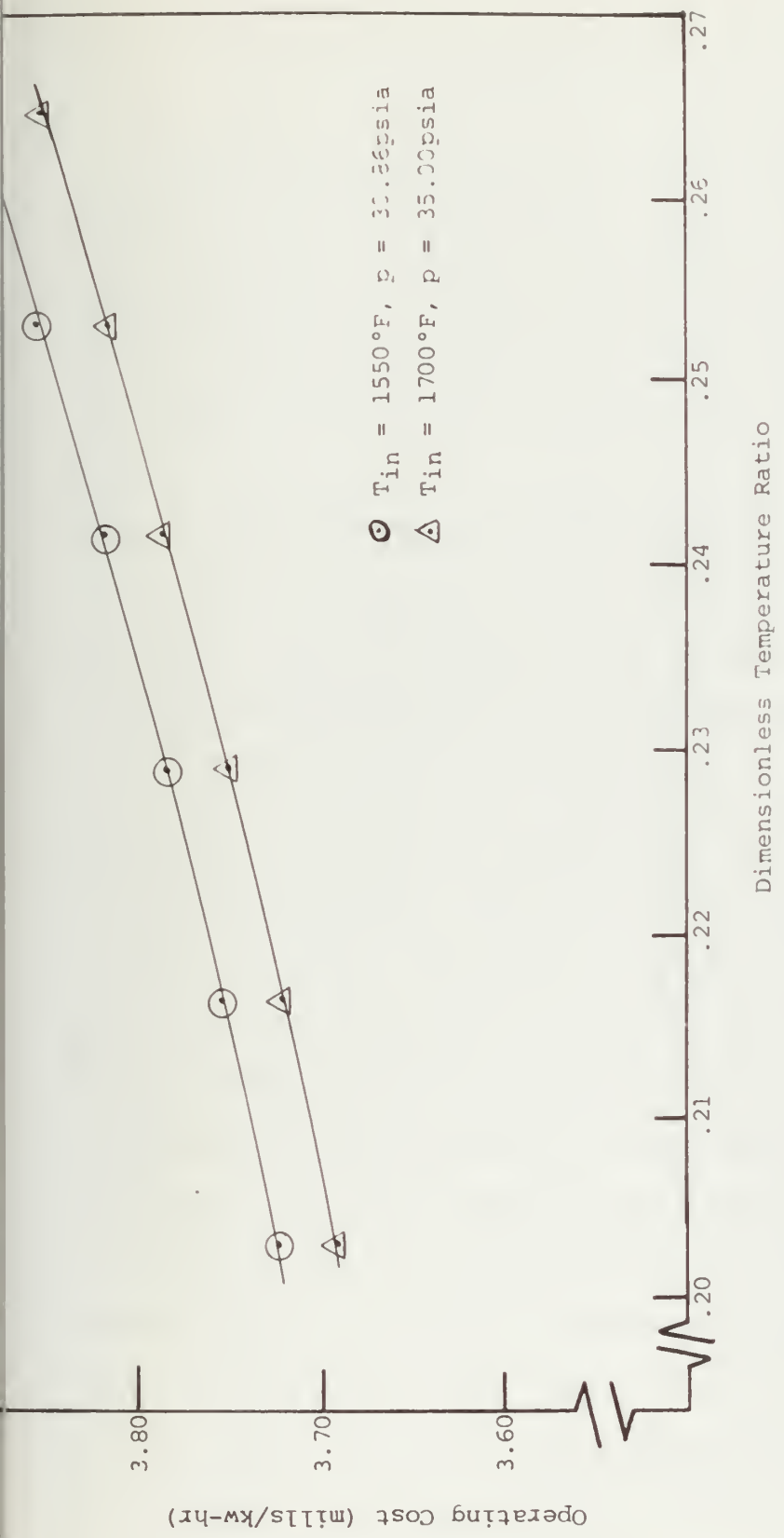


FIGURE 5-2 Operating Cost Per KW Hr As A Function Of The Dimensionless Temperature Ratio

6. OPTIMUM CYCLE

There are several major considerations in the selection of the optimum cycle. Among these are the cost, both operating and capital, the materials selected especially those used in the potassium cycle, and the thermal efficiency. Each of the above considerations is discussed below.

COST The economic analysis of Chapter 5 has indicated that the best operating cost and capital cost per unit electrical output is obtained for topping cycle plant configurations which have the smallest temperature difference in the potassium condenser.

MATERIALS The work accomplished by NASA in the area of potassium turbines indicates that, although there may be some problems in this area, there is a good deal of experience in the use of potassium as a turbine working fluid. However, all of the work of NASA has been accomplished using electrical resistance heating to boil potassium, with the eventual heat source for space use to be nuclear power. No experimental work in the area of the combustion gas-boiler tube-potassium interaction is reported, although in Reference 14, the use of high nickel alloy steels has been suggested for potassium boiler tubes. It appears that in this area there is a lack of experience upon which a decision regarding boiler

tube materials might be made. In Reference 14 it is stated that superheating potassium is likely to cause local hot spots in boiler tubes, and has recommended that it is not necessary to superheat since potassium is much less likely to cause erosion damage than water.

THERMAL EFFICIENCY The analysis of Chapter 3 has indicated that the most efficient plants are those which have the smallest potassium condenser-steam boiler temperature differences.

Based on the above considerations, the optimum cycle of those analyzed in Chapter 3 and Chapter 5 is the saturated vapor turbine inlet (1550°F), 1025°F condensing temperature topping cycle operating with the fixed steam cycle. A cycle diagram, with the important pressures, temperatures, enthalpies and flow rates is shown in Figure 6-1. Table 6-1 lists the major heat transfer rates, power outputs, and the efficiency for this cycle.

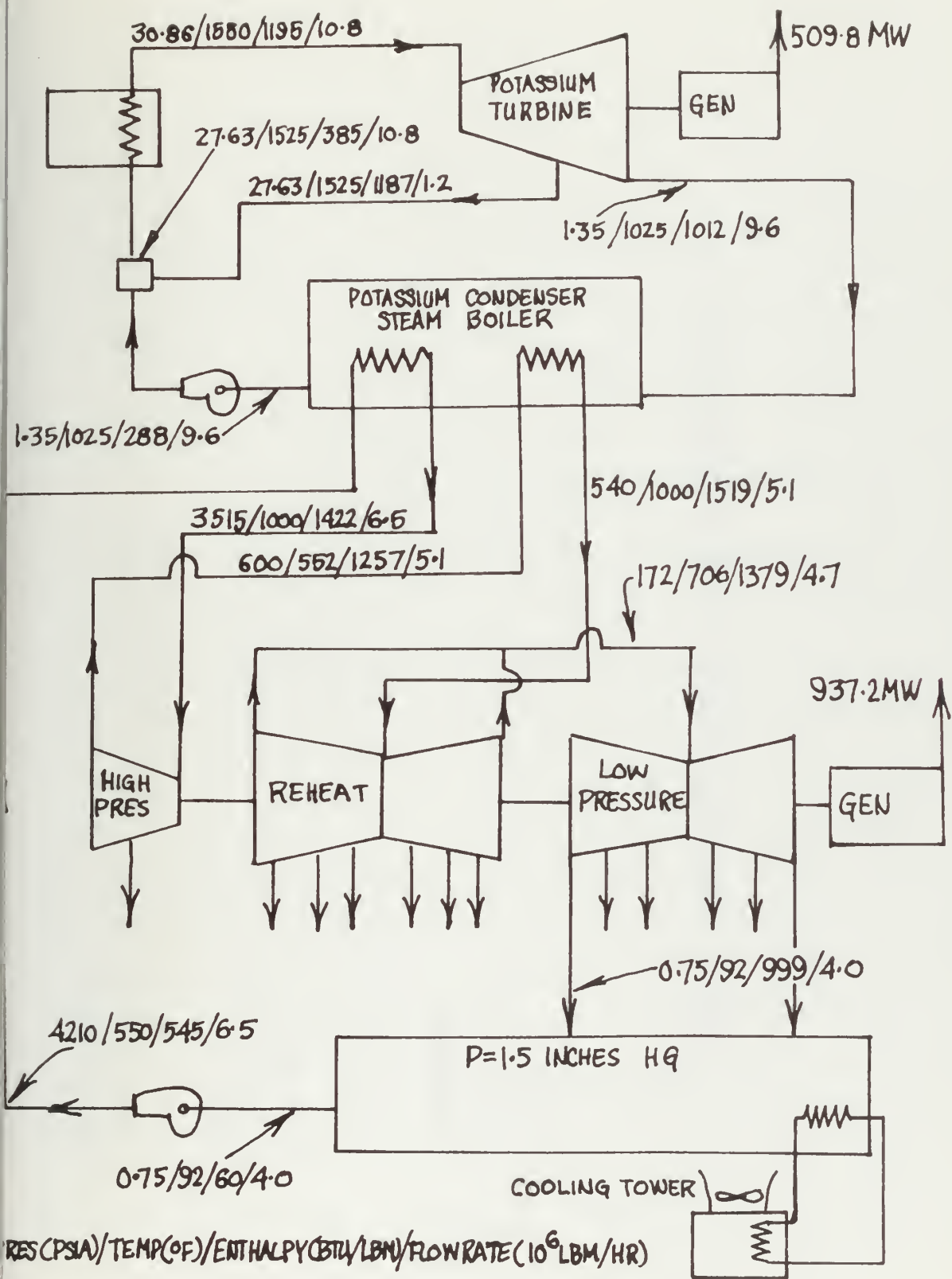


FIGURE 6-2 Optimum Potassium-Steam Binary Cycle

| <u>HEAT TRANSFERS</u> | | | | |
|---------------------------------------|-----------------------|---------------|------------------------|--|
| Potassium Boiler. | 8.753 x 10^9 BTU/hr | 1525°F inlet, | 1550°F outlet | |
| Steam Condenser | 3.756 x 10^9 BTU/hr | 92°F | Condensing Temperature | |
| <u>POWERS</u> | | | | |
| Potassium Cycle | | 509.83W | | |
| Steam Cycle | | 937.21W | | |
| Maximum Cycle Temperature | | 1550°F | | |
| Steam Condenser Temperature | | 92°F | | |
| <u>EFFICIENCIES</u> | | | | |
| Overall Cycle | | 57.06% | | |
| Potassium Cycle | | 19.93% | | |
| Steam Cycle | | 46.37% | | |

TABLE 6-1 Parameters Of Optimum Potassium Steam Binary Cycle



7. CONCLUSIONS

An analysis of the potassium steam binary vapor cycle has been presented. The computer program presented here provides a quick and accurate method which may be used to evaluate various potassium cycle design conditions.

A review of the literature on the utilization of potassium as a turbine working fluid indicates that there is a good deal of experience in this field. However, this work has dealt with turbines of very small output. No work has been done in the design and testing of large power output turbines in the range of several hundred megawatts. In addition, these small turbine tests were performed with the ultimate heat input source for boiling potassium being a nuclear reactor. Also, in these tests, the potassium waste heat was rejected to molten salt or liquid metal. There has been no experimental work in the area of combustion gas-boiler tube-potassium compatibility. Since the potassium steam cycle is to be fueled by coal or coal derived fuels, material selection for this purpose is an area of uncertainty which requires further investigation. Similarly, since the potassium cycle rejects heat to the steam cycle and a potassium steam reaction would be catastrophic, extremely reliable methods of sealing the

potassium condenser and materials must be developed.

The first and second law analysis indicates that the most important potassium cycle design parameter influencing overall cycle thermal efficiency is the temperature difference between condensing potassium and steam. The highest thermal efficiencies are obtained in those plants with the smalles temperature difference in the condenser. The economic analysis indicates that those plants with the smaller condenser temperature difference are higher in total captial cost. However, the more thermally efficient plants are less expensive both in operating cost and in capital cost per unit electrical output.

The potassium steam binary vapor cycle is a possible solution to the problem of more economical and efficient electrical power production. However, before construction of such plants, further work is required in the area of large scale potassium turbines, and in the area of materials for use in the potassium boiler, and the potassium condenser-steam boiler.

REFERENCES

1. "Study of Advanced Energy Conversion Techniques For Utility Applications Using Coal and Coal Derived Fuels," Volumes I and II, Corporate Research and Development, General Electric Company, Schenectady, New York, Contract NAS 3-19406, 1975.
2. Hacket, H. N., and Douglass, D. "Modern Mercury-Unit Power Plant Design," Trans, ASME, 72: 89, 1950.
3. Chambers, W. R., Fraas, A. P., and Ozisik, M. N. "A Potassium Steam Binary Vapor Cycle For Nuclear Power Plants," Oak Ridge National Laboratory, Oak Ridge, Tennessee, ORNL-3584.
4. Ewing, C. T., Stone, J. P., and Steinkuller, E. W. "High Temperature Properties of Potassium," Naval Research Laboratory, Washington, D.C., NRL Report 6233, 24 September 1965.
5. English, R. E., Wetmann, R. N. "Experience in the Investigation of Components of the Alkali Metal Vapor Space Power Program," Lewis Research Center, Cleveland, Ohio, December 1968.
6. Zimmerman, W. F., Hand, R. B., Engleby, D. S., and Samuel, J. W. "Two Stage Potassium Test Turbine," General Electric Company, Cincinnati, Ohio, NASA CR-925.
7. Moor, B. L. and Schnetzer, E. "Three-Stage Potassium Vapor Turbine Test," General Electric Company, Cincinnati, Ohio, NASA CR-1815.
8. Lessmann, G. G., Gold, R. E., Arcella, F. G., and Reed, F. "Turbine Materials," Westinghouse Astro-nuclear Laboratory, WANL-TME-1889, 1969.
9. Rackley, R. A. (Editor) "Potassium Turboalternator (KTA) Preliminary Design Study," Volume I, AiResearch Corporation, NASA CR-1498, April 1970.
10. Rackley, R. A. (Editor) "Potassium Turboalternator (KTA) Preliminary Design Study," Volume III, AiResearch Corporation, NASA CR-1500, April 1970.

REFERENCES (Continued)

11. Fraas, A. P. "A Preliminary Assessment of a Potassium-Steam-Gas Vapor Binary Cycle For Better Fuel Economy and Reduced Thermal Pollution," Oak Ridge National Laboratory, Oak Ridge, Tennessee, ORNL-NSF-EP-6, August 1971.
12. Sawochka, S. G. "Forced Convection Heat Transfer Properties of Potassium," General Electric Company Cincinnati, Ohio, NASA CR 851.
13. Wilson, A. J. "Space Power Spinoff Can Add 10+ Points of Efficiency to Fossil-Fueled Power Plants," Seventh Intersociety Energy Conversion Engineering Conference, San Diego, California, September 1972.
14. Fraas, A. P. "A Potassium Steam Binary Vapor Cycle For Better Fuel Economy and Reduced Thermal Pollution," ASME Journal For Power Engineering, January 1973.
15. Fraas, A. P. "A Potassium-Steam Binary Vapor Cycle For Molten-Salt Reactor Power Plants," ASME Journal for Power Engineering, October 1966.
16. Rajakovics, G. E. "Energy Conversion Process With About 60% Efficiency for Central Power Stations," Ninth Intersociety Energy Conversion Engineering Conference, San Francisco, California, August 1974.
17. Hatsopoulos, G. N. and Keenan, J. H. "Principles of General Thermodynamics," John Wiley and Sons, Inc., New York, 1965.
18. Cravalho, E. G., and Smith, J. L. "Thermodynamics An Introduction," Holt, Rinehart, and Winston, Inc., New York, 1971.
19. Palo, G. P., Emmons, W. F., and Gardner, R. M. "Symposium On TVA's Bull Run Plant - General Design Features," American Power Conference, XXV: 331, 1963.
20. "Advanced Nonthermally Polluting Gas Turbines In Utility Applications," United Aircraft Research Laboratories of United Aircraft Corporation, East Hartford, Connecticut, March 1971 .

REFERENCES (Continued)

21. "Department Of Labor Statistics, Wholesale Price Index," Department of Labor, 1970 and 1974.
22. Meyer, C. A., et. al., "Thermodynamic and Transport Properties of Steam," American Society of Mechanical Engineers, 1967.
23. Rohsenow, W. M. and Choi, H. "Heat, Mass, and Momentum Transfer," Prentice-Hall, Inc., Englewood Cliffs, New Jersey, 1961.

APPENDIX A
PROGRAM VARIABLE LISTING

The following is a list of variables used in the main computer program and its subprograms. Intermediate variables which are used only for ease of calculation are not listed. Unless otherwise indicated, variable names are of the default REAL or INTEGER type.

| | |
|-------|--|
| AT | Total heat transfer area in potassium condenser (ft ²) |
| BFAC | Reciprocal of the boiler efficiency |
| BST | Boiler steam flow rate (lbm/sec) |
| CF | Constant relating MW to 10 ⁹ Btu/hr |
| DB | Steam boiler tube diameter (in) |
| DELHK | Enthalpy change of potassium in condenser (Btu/lbm) |
| DRL | Steam reheater tube diameter (in) |
| EFF | Potassium turbine efficiency |
| EFFK | Potassium cycle thermal efficiency |
| ETAI | Overall binary cycle thermal efficiency |
| GB | Mass flow rate of steam in boiler (lbm/ft ² sec) |
| GRL | Mass flow rate of steam in reheater (lbm/ft ² sec) |
| H1 | Enthalpy at point 1 of the potassium cycle, other subscripts indicate enthalpy at other points of the cycle. (Btu/lbm) |
| HFG | Enthalpy of condensation of potassium (Btu/lbm) |
| HL | Enthalpy of saturated liquid (Btu/lbm) |

| | |
|-------|---|
| I | Integer which indicates whether the potassium cycle is a simple Rankine cycle or a regenerative feed cycle. (If I=1, then the cycle is regenerative feed.) |
| KIM | Integer which indicates whether to perform only an analysis of the potassium cycle or the complete analysis of the binary cycle. (If KIM=1, only analysis of potassium cycle is performed.) |
| MDOT | Potassium flow rate. For a simple cycle MDOT is the cycle flow rate. For a regenerative cycle, MDOT is the boiler flow rate. (lbm/hr) (REAL) |
| MDOTC | Potassium condenser mass flow rate in regenerative cycle (lbm/hr) (REAL) |
| MDOTR | Potassium regenerator flow rate (lbm/hr) (REAL) |
| NB | Number of tubes in steam boiler |
| NR1 | Number of tubes in reheater |
| PR | Steam Prandtl Number |
| PWK | Potassium cycle electrical output (MW) |
| QB | Heat required by fixed bottoming cycle (Btu/hr) |
| QIN | Heat input to binary cycle (Btu/hr) |
| QUAV | Total available energy provided by condensing potassium (Btu/hr) |
| QUIN | Increase in unavailable energy due to condensing potassium (Btu/hr) |
| S1 | Entropy at point 1 of the potassium cycle; other subscripts indicate entropy at other points of the cycle (Btu/lbm °R) |
| SFG | Entropy of condensation of potassium (Btu/lbm °R) |
| SL | Entropy of saturated liquid (Btu/lbm °R) |

| | |
|-------|--|
| T1 | Temperature at point 1 of potassium cycle; other subscripts indicate temperature at other points of the cycle ($^{\circ}$ F) |
| TENAV | Entropy average temperature of heat addition to the steam cycle ($^{\circ}$ R) |
| V1 | Vapor or liquid specific volume at point 1 of the potassium cycle; other subscripts indicate the specific volume at other points of the cycle (ft^3/lbm) |
| X5 | Potassium vapor quality at point 5 of the cycle; other subscripts indicate quality at other points of the cycle |
| YY | Percent of boiler mass flow rate extracted for regeneration in potassium cycle (lbm/hr) |

Subroutine: PRES

| | |
|----|--|
| A | Test pressure calculated to determine if temperature is within a specified tolerance |
| C1 | Constant used in evaluating saturation temperature corresponding to a specified pressure; C2 and C3 are similar. |
| T | Temperature (F) |
| P | Pressure (psia) |

Subroutines: WET and SUPER

| | |
|------|---|
| AHG1 | Constant used to evaluate the ideal gas enthalpy. AHG2, AHG3, and AHG4 are similar. |
| B | Second virial coefficient |
| B1 | Constant used to evaluate second virial coefficient. B2 is similar. |

Subroutines: WET and SUPER (Continued)

| | |
|------|---|
| C | Third virial coefficient |
| C1 | Constant used to evaluate third virial coefficient. C2 is similar. |
| CH1 | Constant used to evaluate the saturated liquid enthalpy. CH2, CH3, CH4, and CH5 are similar. |
| CS1 | Constant used to evaluate the ideal gas entropy. CS2, CS3, and CS4 are similar. |
| D | Fourth virial coefficient |
| D1 | Constant used to evaluate the fourth virial coefficient. D2 is similar. |
| DB | Derivative of second virial coefficient with respect to temperature. DC and DD are similar derivatives of the third and fourth virial coefficients. |
| DEN | Denominator used in solving for the vapor specific volume by Newton's iterative method. |
| FUNC | Numerator used in solving for the vapor specific volume by Newton's iterative method. |
| H | Vapor specific enthalpy (Btu/lbm) |
| HFG | Specific enthalpy of condensation (Btu/lbm) |
| HIDG | Ideal gas specific enthalpy (Btu/lbm) |
| HL | Saturated liquid specific enthalpy (Btu/lbm) |
| P | Pressure (psia) |
| R | Universal gas constant (1545.3ft lbf/lb mole °R) |
| S | Vapor specific entropy (Btu/lbm °R) |
| SFG | Specific entropy of condensation (Btu/lbm °R) |
| SIDG | Ideal gas specific entropy (Btu/lbm °R) |

Subroutines: WET and SUPER (Continued)

SL Saturated liquid specific entropy (Btu/lbm °R)
T Temperature (°F)
V Vapor specific volume (ft³/lbm)
VL Test value of vapor specific volume used in
Newton's iterative method.
WTM Molecular weight of potassium (39.10 lbm/lb
mole)
Z First vapor specific volume estimate in
iterative solution.

Subroutines: SIM and REGEN

CMDOT Condenser potassium flow rate (lbm/hr)
DOTM Boiler potassium flow rate (lbm/hr)
EFF Potassium turbine isentropic efficiency
EFFK Potassium cycle thermal efficiency
H1 Enthalpy at point 1 of potassium cycle, other
subscripts indicate enthalpy at other points
of the cycle. (Btu/lbm)
OVEFF Binary cycle overall efficiency
PWK Potassium cycle electrical output (MW)
RMDOT Regenerator potassium flow rate (lbm/hr)
TKW Binary cycle electrical output (MW)
YY Percent of boiler mass flow rate extracted
for regeneration (lbm/hr)

Subroutines: BOILER and REHEAT

A Heat exchanger area (ft²)
AL Tube length (ft)
DI Tube inside diameter (in)
DTLOG Log mean temperature difference (F)
G Steam flow rate (lbm.ft² sec)
H Overall heat transfer coefficient (Btu/hr ft²
°F)
N Number of tubes
RE Reynold's number
T Temperature (°F)
TK Condensing potassium temperature (°F)
WI Total steam flow rate (lbm/sec)

APPENDIX B

PROPERTIES OF POTASSIUM

The engineering properties of potassium used in the analysis of various topping cycle conditions are those as determined by Ewing, et. al. in Reference 4. In this work two forms of the equation of state are presented; one of the quasi-chemical form, and one of the virial form. Since the authors considered the virial form as the more accurate form, this form is used in the present analysis.

The virial equation of state used to derive the engineering properties of potassium was reduced from experimental PVT data in the range from 2.35atm to 27.4atm. Therefore, all saturation properties below 1575°F and above 2375°F require an extension of the virial equation outside its experimentally determined range. According to Ewing, et. al., properties computed for states outside of the measured range may be of reduced accuracy, especially those at pressure states above 27atm. Since the present analysis was carried out either within or slightly below both the experimental temperature and pressure range, the possible error in property determination was not considered significant.

The properties of potassium were programmed and

evaluated using the subroutines SUPER and WET listed at the end of this appendix. P and T (pressure and temperature) are the inputs to both subroutines. All other variables are outputs. The subroutine SUPER is used to evaluate properties in the superheated region, and the subroutine WET is used to evaluate properties in the two-phase region.

The basic equations used to evaluate the properties of potassium are as follows:

$$V_v = \frac{R_0 T}{144 p M} \left[1 + \frac{B(T)}{V_v} + \frac{C(T)}{V_v^2} + \frac{D(T)}{V_v^3} \right] \quad (1)$$

$$B(T) = B_1 T \exp [B_2/T] \quad (2)$$

$$B_1 = 3.38156 \times 10$$

$$B_2 = 11261.3$$

$$\frac{d}{dT} B(T) = \left[1 - \frac{B_2}{T} \right] \left[\frac{B(T)}{T} \right] \quad (3)$$

$$C(T) = C_1 \exp [C_2/T] \quad (4)$$

$$C_1 = 2.52903 \times 10^{-3}$$

$$C_2 = 14703.7$$

$$\frac{d}{dT} C(T) = - \frac{C_2}{T^2} C \quad (5)$$

$$D(T) = D_1 \exp - D_2/T \quad (6)$$

$$D_1 = 4.81912 \times 10^{-$$

$$D_2 = 18107.2$$

$$\frac{d}{dT} D(T) = - \frac{D_2}{T^2} D_2 \quad (7)$$

$$V_L = \left[VL_1 + VL_2 \left(\frac{T}{1000} \right) + VL_3 \left(\frac{T}{1000} \right)^2 + VL_4 \left(\frac{T}{1000} \right)^3 \right]^{-1} \quad (8)$$

$$VL_1 = 56.099$$

$$VL_2 = 6.9828$$

$$VL_3 = 0.5942$$

$$VL_4 = 0.0498$$

$$h_L = CH_1 + CH_2 T + CH_3 T^2 + CH_4 T^3 + CH_5 T^4 \quad (9)$$

$$CH_1 = 394.2209$$

$$CH_2 = 0.609266$$

$$CH_3 = 6.05836 \times 10^{-4}$$

$$CH_4 = 2.009 \times 10^{-7}$$

$$CH_5 = 2.481349 \times 10^{-11} \quad (9)$$

$$h^0 = AHG_1 + AHG_2 T + AHG_3 \exp \left[-AHG_4/T \right] \quad (10)$$

$$AHG_1 = 998.95$$

$$AHG_2 = 0.127$$

$$AHG_3 = 24836.0$$

$$AHG_4 = 39375.0$$

$$s^0 = CS_1 + CS_2 n(T) + CS_3 \exp \left[-CS_4/T \right] \quad (11)$$

$$CS_1 = 0.18075$$

$$CS_2 = 0.127$$

$$CS_3 = 0.7617$$

$$CS_4 = 31126.0$$

$$h_v = h + \left[\frac{R_o T}{M J} \right] \left\{ \frac{1}{V_v} \left[B - T \frac{dB}{dT} \right] + \frac{1}{V_v^2} \left[C - \frac{T}{2} \frac{dC}{dT} \right] + \frac{1}{V_v^3} \left[D - \frac{T}{3} \frac{dD}{dT} \right] \right\} \quad (12)$$

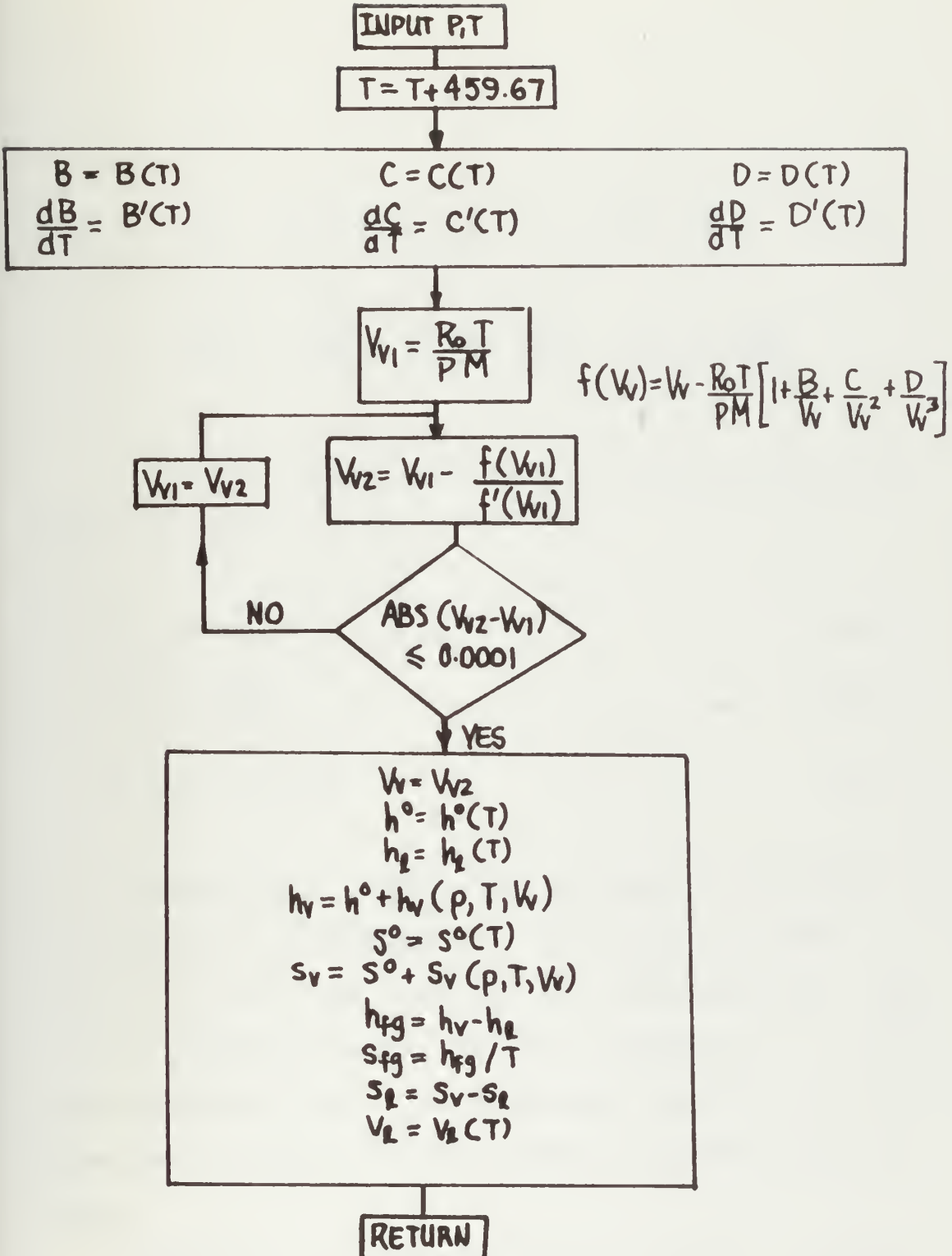


FIGURE B-1 Flow Chart For Property Determination By Subroutine WET
 -102-

$$s_v = s_o - \left| \frac{R_o}{Mj} \right| \left\{ \ln \left[\frac{p}{p_{atm}} \right] - \ln \left[\frac{144 p V_v^M}{R_o T} \right] + \left(\frac{1}{V_v} \left[B + T \frac{dB}{dT} \right] + \frac{1}{2V_v^2} \left[C + T \frac{dC}{dT} \right] + \frac{1}{3V_v^3} \left[D + \frac{dD}{dT} \right] \right) \right\} \quad (13)$$

For the two phase region, the following additional equations apply.

$$h_{fg} = h_v - h \quad (14)$$

$$s_{fg} = \frac{h_{fg}}{T} \quad (15)$$

$$s_l = s_v - s_{fg} \quad (16)$$

Equations (1) through (13) are present in SUPER, and equations (1) through (16) are present in WET.

Figure B-1 is a flow chart for the subroutine WET. The calling program provides the input pressure (in lb_f/in^2) and temperature ($^{\circ}F$). The functional relationships represented in Figure B-1 are those of the previous equations.

Figure B-2 is an Enthalpy-Entropy diagram for potassium vapor for the region of interest. This diagram was

plotted using the IBM-370 Computer, and the CALCOMP plotting routines available. In addition to the subroutines SUPER and WET, the following equation and the subroutine PRES (listed at the end of this appendix) were used to obtain this plot.

$$P_{\text{sat}} = CPS_1 T^{CPS_2} \exp(CPS_3/T)$$

$$CPS_1 = 1.9712 \times 10^7$$

$$CPS_2 = 0.53299$$

$$CPS_3 = 18717.22$$

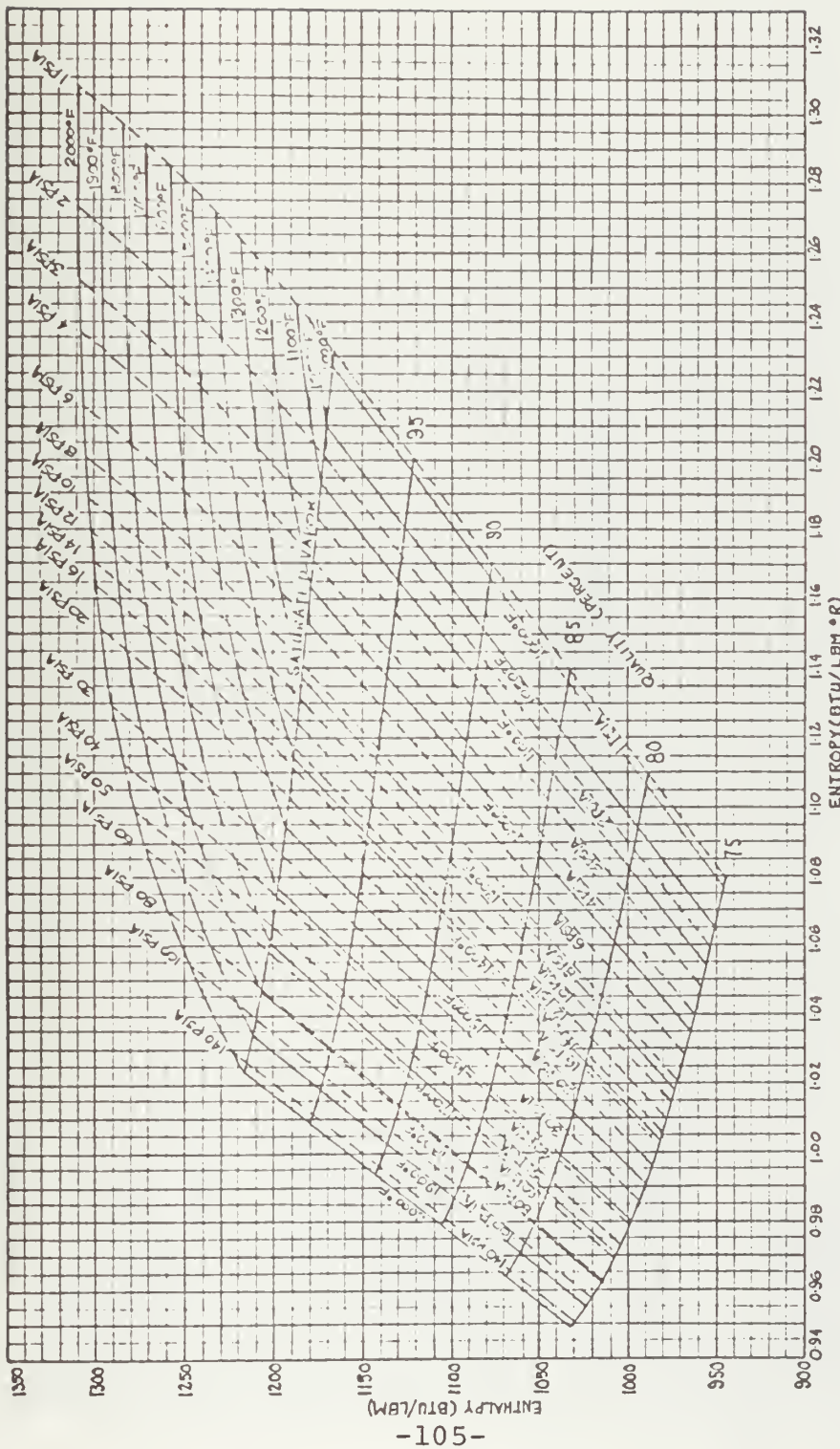


Figure B-2 Mollier Diagram For Potassium Vapor

C SUBROUTINE SUPER(P,T,H,S,V)
 C THE SUBROUTINE WET EVALUATES THE ENGINEERING PROPERTIES OF POTASSIUM
 C IN THE SUPERHEATED REGION. THE TEMPERATURE AND PRESSURE ARE THE INPUTS
 C TO THE SUBROUTINE.
 R=1545.3

```

    B1=-3.38156E-6
    B2=11261.3
    C1=2.52903E-3
    C2=14707.7
    D1=-4.81912E-4
    D2=18107.2
    T=T+459.67
    B=B1*T*EXP(B2/T)
    DB=(1.0-B2/T)*B/T
    C=C1*EXP(C2/T)
    DC=-C2*C/T**2.0
    D=D1*EXP(D2/T)
    DD=-D2*D/T**2.0
    HTM=39.10
    Z=R/(144.0*HTM)
    V=Z*(T/P)
    10 FUNC=V-Z*(T/P)*(1.0+B/V+C/V**2.0*D/V**3.0)
    DBN=1.0-Z*(T/P)*(-B/V**2.0-2.0*C/V**3.0-3.0*D/V**4.0)
    V1=V-FUNC/DEN
    IP(ABS(V-V1).LT.0.0001) GC TO 11
    V=V1
    GO TO 10
  11 V=V1
    AHG1=998.95
    AHG2=0.127
    AHG3=24836.0
    AHG4=39375.0
    HIDG=AHG1+AHG2*T+AHG3*EXP(-AHG4/T)
    W1=(B-DB*T)/V
    W2=(C-0.5*T*DC)/V**2.0
  
```



```
H=H1*DG+R*T*(W1+W2+W3)/(WTB*778.0)
CS1=0. 18075
CS2=0. 127
CS3=0. 7617
CS4=31126.0
SIDG=CS1+CS2* ALOG(T) +CS3* EXP (-CS4/T)
U1=ALOG(P/14.696)
U2=ALOG(P*V*144.0*WTB/(R*T))
U3=(B*T*DB)/V
U4=(C+T*DC)/(2.0*V**2.0)
U5=(D+T*DD)/(3.0*V**3.0)
S=SIDG-R*(U1-U2+U3+U4+U5)/(WTB*778.0)
T=T-459.67
RETURN
END
```


SUBROUTINE WET(P,T,H,S,HFG,SPG,HL,SL,V)

C THE SUBROUTINE WET EVALUATES THE ENGINEERING PROPERTIES OF POTASSIUM
 C IN THE TWO PHASE REGION. THE PRESSURE AND TEMPERATURE ARE INPUT TO
 C THE SUBROUTINE.

R=1545.3

B1=-3.38156E-6

B2=11261.3

C1=2.52903E-3

C2=14707.7

D1=-4.81912E-4

D2=18107.2

T=T+459.67

B=B1*T*EXP(B2/T)

DB=(1.0-B2/T)*B/T

C=C1*EXP(C2/T)

DC=-C2*C/T**2.0

D=D1*EXP(D2/T)

DD=-D2*D/T**2.0

WTM=39.10

Z=B/(144.0*WTM)

V=Z*(T/P)

10 FUNC=V-Z*(T/P)*(1.0+B/V+C/V**2.0*D/V**3.0)

DEN=1.0-Z*(T/P)*(-B/V**2.0-2.0*C/V**3.0-3.0*D/V**4.0)

V1=V-FUNC/DEN

IP(ABS(V-V1).LT.0.0001) GC TO 11

V=V1

GO TO 10

11

V=V1

AHG1=998.95

AHG2=0.127

AHG3=24836.0

AHG4=39375.0

HIDG=AHG1+AHG2*T+AHG3*T*EXP(-AHG4/T)

W1=(B-DB*T)/V

W2=(C-0.5*T*DC)/V**2.0


```

W3=(D-T*DD/3.0)/V**3.0
H=H1DG+R*T*(W1+W2+W3)/(WTN*778.0)
CS1=0.18075
CS2=0.127
CS3=0.7617
CS4=31126.0
SIDG=CS1+CS2**ALOG(T)+CS3*EXP(-CS4/T)
U1=ALOG(P/14.696)
U2=ALOG(P*V*144.0*WTN/(R*T))
U3=(B+T*DB)/V
U4=(C+T*DC)/(2.0*V**2.0)
U5=(D+T*DD)/(3.0*V**3.0)
S=SIDG-R*(U1-U2+U3+U4+U5)/(WTN*778.0)
CH1=394.2209
CH2=-0.609266
CH3=6.05836E-4
CH4=-2.009E-7
CH5=2.481349E-11
HL=CH1+CH2*T+CH3*T**2.0+CH4*T**3.0+CH5*T**4.0
HFG=H-HL
SPG=HFG/T
SL=S-SPG
T=T-459.67
RETURN
END

```


PGM 2

C THE SUBROUTINE PRES DETERMINES THE VALUE OF SATURATION TEMPERATURE
C CORRESPONDING TO A PRESSURE. BOTH ARGUMENTS ARE INPUT TO PRES.
C THE TEMPERATURE VALUE INPUT IS AN ESTIMATE OF THE SATURATION TEMPERATURE.
C NEWTON'S ITERATIVE METHOD IS USED TO DETERMINE THE EXACT VALUE.
SUBROUTINE PRES (P, T)

C1=1.9714E7

C2=.53299

C3=18717.22

1 A1= ALOG (P/C1) + C2* ALOG (T+459.67) + C3 / (T+459.67)

A2=C2/(T+459.67) - C3/(T+459.67) ** 2.0

T1=T-A1/A2

T=T1

A=C1*(T+459.67)**(-C2)*EXP(-C3/(T+459.67))
IF (ABS (P-A) .GT. 0.001) GO TO 1

RETURN

END

APPENDIX C

POTASSIUM CONDENSER - STEAM BOILER SIZING

The Potassium Condenser - Steam Boiler Size was determined by the computer program in the Subroutines BOILER and REHEAT listed in this appendix. The steam property data was taken from Reference 21. The mass flux of steam into the boiler and reheater are those as used in Reference 3. These values are respectively $70. \frac{\text{lbm}}{\text{ft}^2 \text{sec}}$ and $100. \frac{\text{lbm}}{\text{ft}^2 \text{sec}}$. The McAdams correlation

(Reference 22) was used to determine the length of tubes required. The inputs to the subroutines are steam flow rate, steam mass flux, the properties of steam, the inside diameter of the tubes, and the inlet and outlet temperatures of steam. The outputs of the subroutines are the total number of tubes, the length of tubes, and the total surface area of tubes required. A flow diagram of the subroutine REHEAT is shown in Figure C-1. In Reference 12, a heat transfer coefficient of $10000 \text{ Btu/hr ft}^2 \text{ }^\circ\text{F}$ was found for condensing potassium. This value is assumed, and its effect is neglected in the calculation of the overall heat transfer coefficient for the inside of the tube. The rate of potassium condensation on the main boiler is calculated in the main program using the

following relation:

$$\dot{M}_{KC} = \frac{\dot{M}_S (\Delta h_S)}{\Delta h_K} \quad .$$

INPUT $W_i, G_i, d_i, \mu, T_k, T_{is}, T_{os}, Pr, \Delta H_k, k$

$$N = \frac{4 W_i}{\pi d_i^2 G_i}$$

$$144$$

$$Re = \frac{G_i d_i}{12 \mu}$$

$$h_s = 0.023 \frac{k}{d_i/12} [Re]^{0.8} [Pr]^{0.4}$$

$$\Delta T_{ln} = \frac{(T_k - T_{is}) + (T_k - T_{os})}{\ln \left[\frac{T_k - T_{is}}{T_k - T_{os}} \right]}$$

$$A = \frac{W_i \Delta H_k}{h_s \Delta T_{ln}}$$

$$L = \frac{12 A}{N \pi d_i}$$

RETURN

FIGURE C-1 Flow Chart For Calculation of Reheater Parameters

SUBROUTINE REHEAT(WI,DI,G,VIS,TK,TIN,TOUT,PR,HD,N,A,AL,THCON)
C THE SUBROUTINE REHEAT DETERMINES THE CHARACTERISTICS OF THE STREAM
C REHEATER.
PI=3.14159
N=1PIX(576.0*WI/(PI*DI**2.0*G))
RE=G*DI/(12.0*VIS)
H=0.276*THCCN*RE**0.8*PR**0.4/DI
DEN=ALOG((TK-TIN)/(TK-TOUT))
DTLOG=(TK-TIN-TK*TOUT)/DEN
A=WI*HD*3600.0/(H*DTLOG)
AL=12.0*A/(FLOAT(N)*PI*DI)
RETURN
END

PGM8

SUBROUTINE BOILER(WI,DI,G,VIS,TK,TIN,TOUT,PR,THCON,HI,HO,N,A,AL)
C THE SUBROUTINE BOILER DETERMINES THE CHARACTERISTICS OF THE STEAM
C BOILER.
TO=TOUT

PI=3.14159
N=IPIX(576.0*WI/(PI*DI**2.0*G))
RE=G*DI/(12.0*VIS)
H=0.276*THCON*RE**0.8*PR**0.4/DI
TC=705.0
DEN= ALOG((TK-TIN)/(TK-TC))
DTLOG=(TK-TIN-TK+TC)/DEN
HCK=3000.0
U=(H*BCK)/(H+BCK)
A1=WI*(763.0-HI)*3600.0/(U*DTLOG)
H=10.4*G**0.8
DEN= ALOG((TK-TC)/(TK-TO))
DTLOG=(TK-TC-TK+TO)/DEN
A2=WI*(HO-763.0)*3600.0/(H*DTLOG)
A=A1+A2
AL=12.0*A/(FLCAT(N)*PI*DI)
RETURN
END

APPENDIX D

MAIN PROGRAM

The main program is used to calculate the parameters of the potassium topping cycle, and the binary cycle. The major inputs required by the program are the pressures and temperatures of the various points in the topping cycle, and the parameters of the fixed bottoming cycle. The properties (entropy, enthalpy, and specific volume) for the potassium cycle are calculated by calling the subroutines SUPER and WET which are discussed in Appendix B.

The basic path of calculation is to provide the pressure and temperature at the turbine inlet, the regenerator pressure and temperature (in the case of simple cycle evaluation this input is not required) and the condensing pressure and temperature. With these parameters as input, the program then evaluates the engineering properties at the points of the potassium cycle. Since the basic parameter relating the two cycles is that the heat rejected by the potassium cycle is the heat added to the bottoming cycle, the mass flow rate of potassium in the condenser is found. For a simple Rankine Cycle potassium plant, this mass flow is the mass flow in the boiler. For a regenerative feed cycle potassium

plant, the condenser mass flow rate is related to the boiler flow rate as is indicated in Table 3-3. Once the condenser mass flow rate is known, the topping cycle efficiency, power output for potassium plant, binary cycle efficiency, boiler and regenerator mass flow rates, and total plant output are calculated. These quantities are evaluated by the subroutines SIM and REGEN for simple and regenerative feed cycles respectively.

The program is capable of analyzing the parameters of the binary cycle for the following topping cycle cases:

(1) Simple Rankine Cycle with saturated vapor turbine inlet conditions and final expansion into the two phase region.

(2) Simple Rankine Cycle with superheated conditions at inlet, isentropic expansion and actual expansion into the two phase region.

(3) Simple Rankine Cycle with superheated conditions at inlet, isentropic expansion into the two phase region, and final expansion into superheated region.

(4) Simple Rankine Cycle with superheated conditions at turbine inlet, and isentropic and actual expansion into the superheated region.

(5) Regenerative feed heating cycle with saturated vapor inlet condition, extraction in the two phase region

and final expansion in two phase region.

(6) Regenerative feed heating cycle with superheated vapor inlet conditions, actual extraction in the superheated vapor inlet conditions, extraction in the two phase region and final expansion in the two phase region.

(7) Regenerative feed heating cycle with superheated vapor inlet conditions, extraction in the two phase region and final expansion in the two phase region.

Figure D-1 illustrates the path of calculation for the regenerative feed heating case. The case for a simple Rankine Cycle is quite similar and is not illustrated. The first inputs to the calculation are the conditions at turbine inlet. With these values for pressure and temperature, the main program calls the subroutine SUPER and the values of h_3 and S_3 are returned. (The subscripts refer to Figure 3-5.) If the values of pressure and temperature are for a saturated vapor state, the values for h_3 and S_3 are still returned correctly by SUPER. The next inputs to the calculation are the pressure and corresponding saturation temperature of the regenerator. These two values are then inputs to the subroutine WET which returns the values of h_v , S_v , h_{pg} , S_{pg} , S_6 , and h_6 . At this point, the program then determines whether the isentropic expansion to the regenerator pressure is in

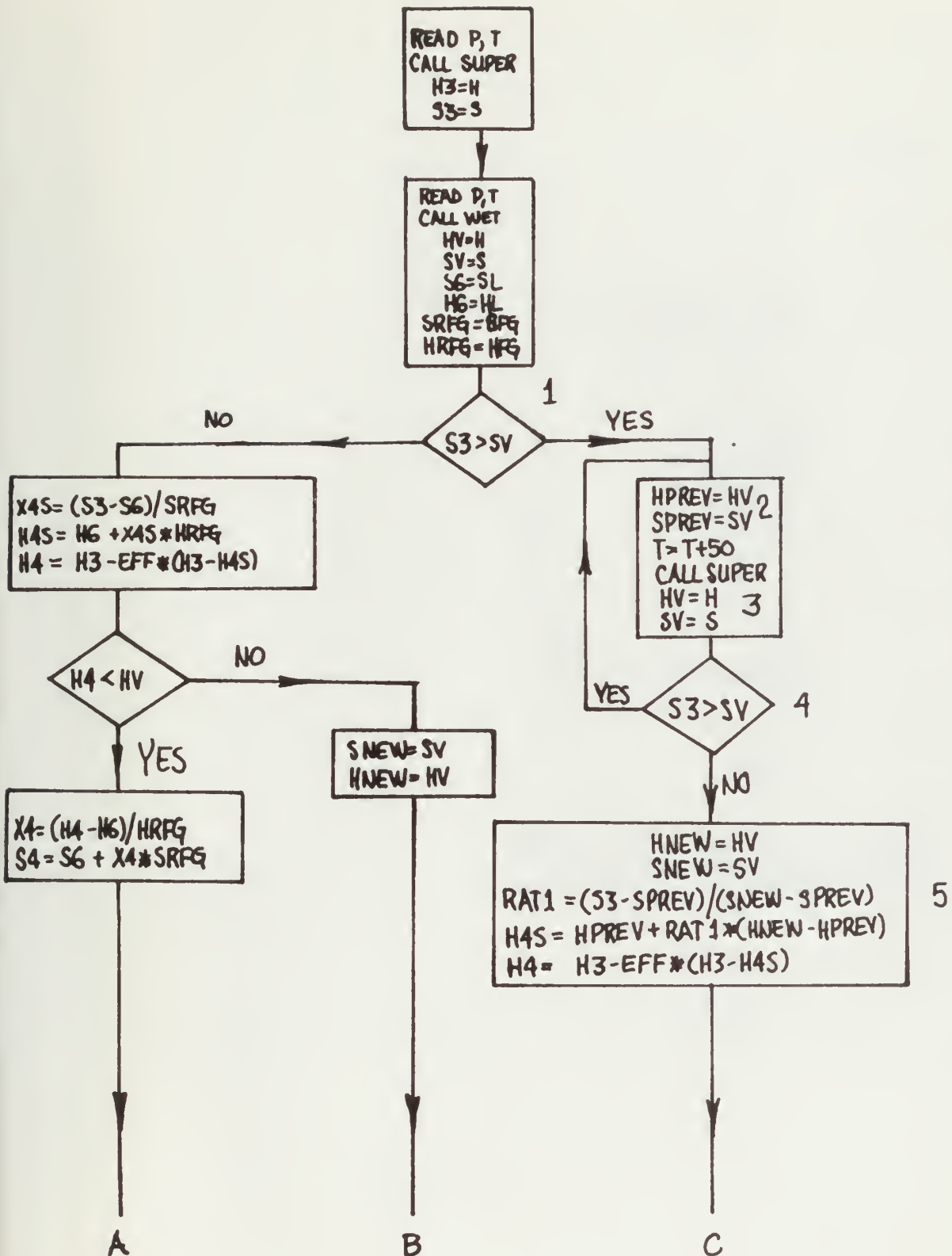


FIGURE D-1 Flow Chart For Determination Of Properties Of Potassium

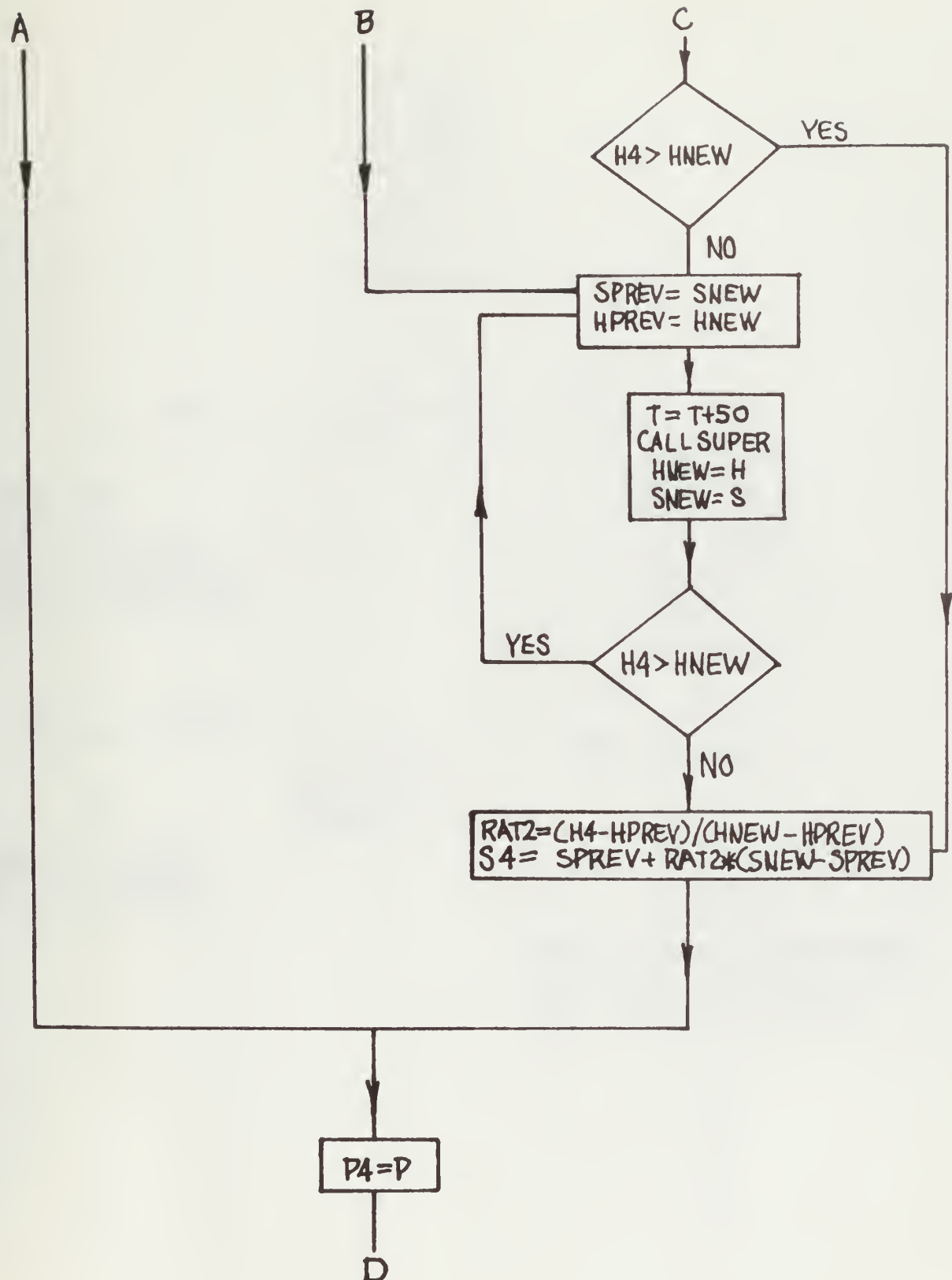


FIGURE D-1 (Continued)

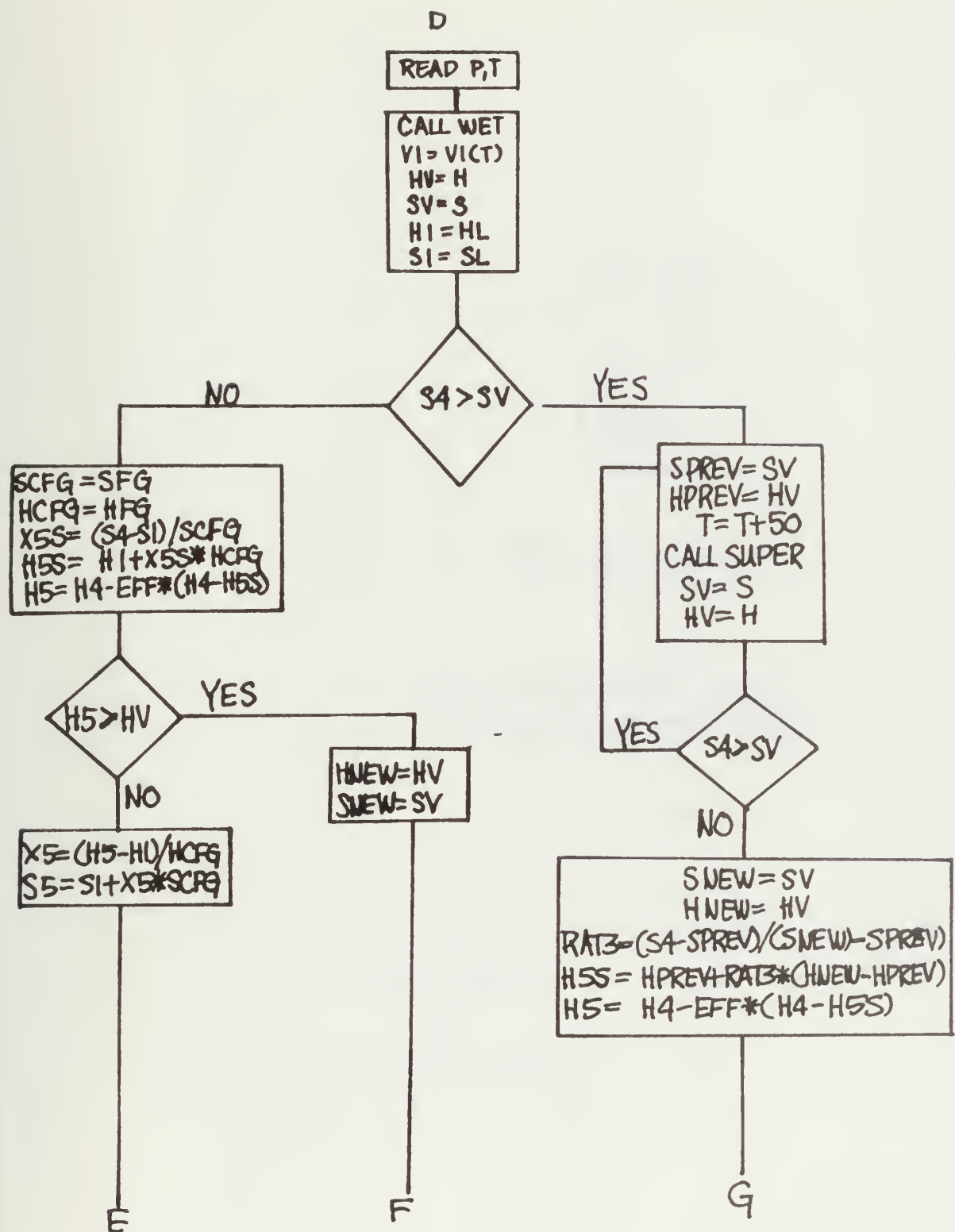


FIGURE D-1 (Continued)

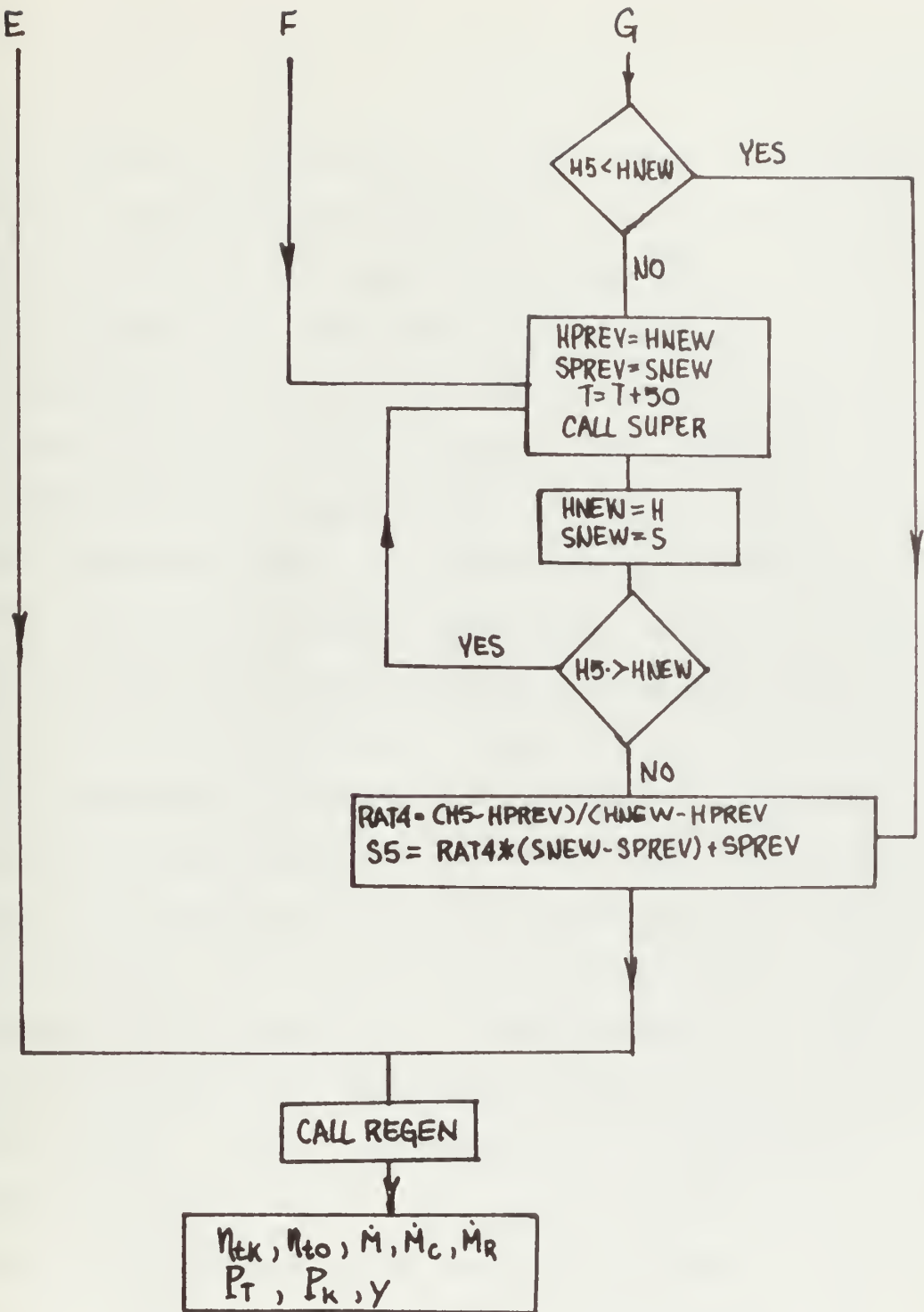


FIGURE D-1 (Continued)

the superheated or in the two phase region. the test at point 1 determines this condition. For isentropic expansion into the two phase region, the result of the test at 1 is negative. For isentropic expansion into the superheated region, the path indicated by the positive result to the test at 1 is taken. It is here that the program searches along the line of constant pressure in 50°F increments until the isentropic value of entropy (S_3) is bracketed between two values. Figure D-2 graphically illustrates this procedure. It is assumed that the line of constant pressure is essentially linear over a 50°F temperature increment in the superheated region. To illustrate the searching procedure, suppose that the program has reached point 2. The values HPREV and SPREV are assigned the values of the saturated vapor enthalpy and entropy. The temperature is then increased by 50°F, and the subroutine SUPER evaluates the superheated enthalpy and entropy. (Point 3 of Figure D-1). The pressure however is not changed. Once again, the value of S_3 is checked to determine if it has been bracketed. This occurs in the test at point 4. A positive result for this test indicates that S_3 has not been bracketed, and the program then adds another 50°F increment to the temperature, determines h and S , and once again tests S_3 .

For the case illustrated in Figure D-2, S_3 is bracketed after two successive increments of temperature addition. Once S_3 has been bracketed, the relationships at point 5 of Figure D-1 can then be used to determine h_4 . The actual value of S_4 is then determined in a similar way, but it is h_4 that is bracketed to determine this value. This method of determining the value of points in the superheated region is used several other times in both the calculation of simple and regenerative cycle points. The next inputs to the calculation are the pressure and temperature of condensation. Using this input, the final expansion point is found. The subroutine REGEN is then called, and the values indicated in Figure D-1 are returned to the main program for printout, and other calculation.

The second law analysis (Section 3-4, Table 3-6) is also calculated in the main program.

Enthalpy

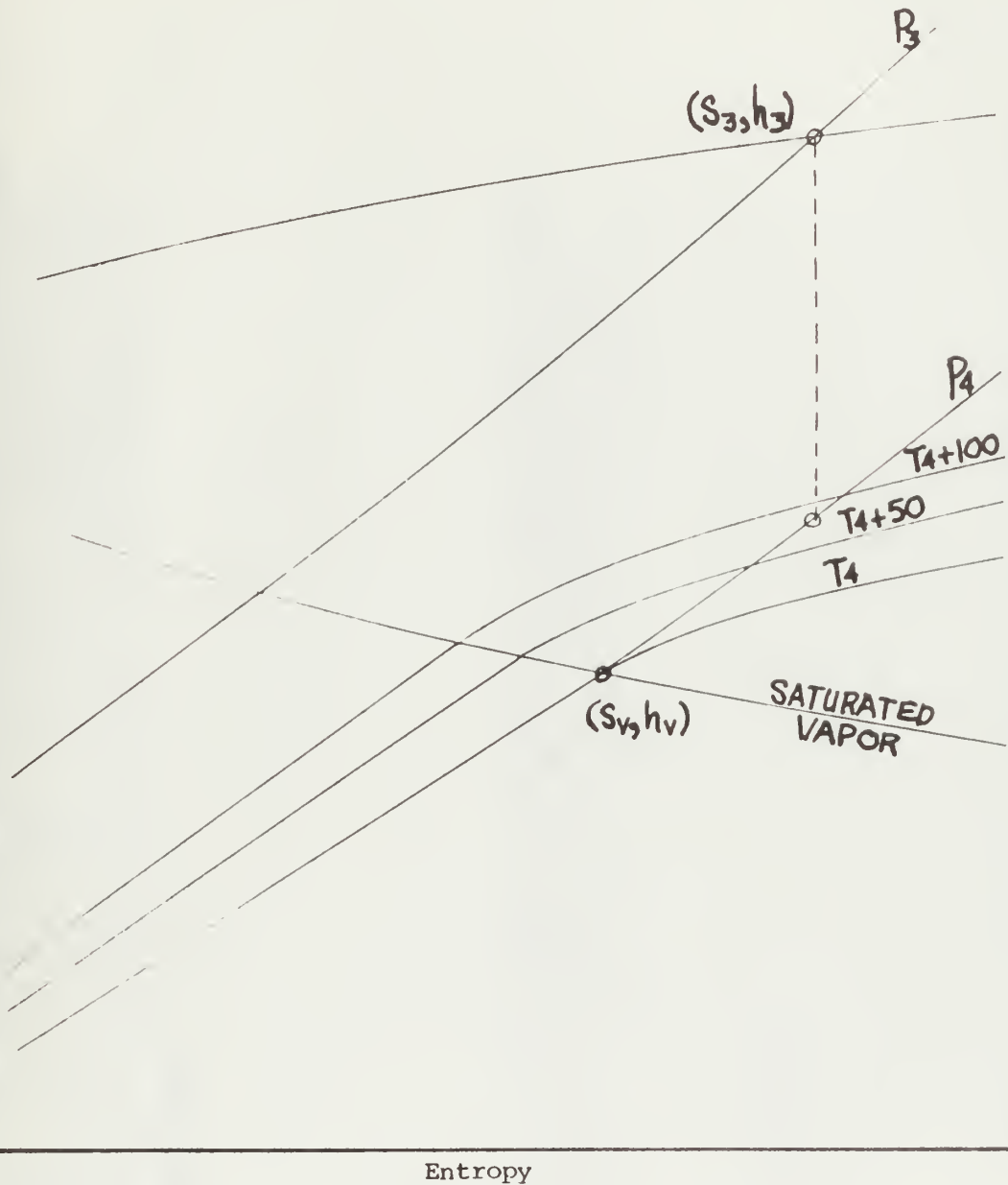


FIGURE D-2 Illustration Of Searching Procedure
Used To Determine Values of Entropy
and Enthalpy of Potassium

C MAIN PROGRAM.
C THE MAIN PROGRAM IS USED TO CALCULATE THE PARAMETERS OF THE TOPPING
C CYCLE, AS WELL AS THE PARAMETERS OF THE POTASSIUM-STEAM BINARY CYCLE.
C THESE PARAMETERS INCLUDE THE THERMAL EFFICIENCY, THE TOPPING CYCLE
C AND BINARY CYCLE ELECTRICAL OUTPUT, THE MASS FLOW RATES IN THE COM-
C PONENTS OF THE TOPPING CYCLE, THE PROPERTIES OF POTASSIUM AT VARIOUS
C POINTS OF THE CYCLE, AND THE CHARACTERISTICS OF THE POTASSIUM CON-
C DENSER.

REAL MDOT, MDOTR, MDOTC

BPAC=1.25

FACTOR=1.0E-9

TATM=549.67

PST=956.327

DR1=0.8

DB=0.375

GR1=100.0

GB=70.0

EPP=0.81

CP=3.41316E6

P AND T ARE THE TOP PRESSURE AND TEMPERATURE OF THE POTASSIUM CYCLE.
KIM IS AN INTEGER WHICH INDICATES WHETHER TO CALCULATE THE VALUES
ONLY FOR THE POTASSIUM CYCLE, OR FOR THE COMPLETE BINARY CYCLE.
IF KIM IS EQUAL TO 1, THEN ONLY THE TOPPING CYCLE CALCULATIONS ARE
PERFORMED.

1 READ,P,T,KIM
PRINT4

QB=7.0022E9

IP(P.EQ.0.0) GO TO 1000

CALL SUPER(P,T,H,S,V)

S3=S

H3=H

P3=P

T3=T

V3=V

READ,I

C THE INTEGER I INDICATES WHETHER THE CYCLE TO BE EVALUATED IS A

C SIMPLE RANKINE CYCLE, OR A REGENERATIVE FEED CYCLE. IF I EQUALS 1,
 C THEN THE CYCLE TO BE EVALUATED IS A REGENERATIVE FEED CYCLE.
 C IF (I.EQ.1) GO TO 200
 C THIS SECTION OF THE PROGRAM EVALUATES A SIMPLE POTASSIUM RANKINE CYCLE.
 C P AND T ARE THE CONDENSING PRESSURE AND TEMPERATURE.
 READ, P,T
 CALL, PRES(P,T)
 PRINT226
 CALL, WET(P,T,H,S,HFG,SPG,HL,SL,V)
 T1=T
 HV=H

$$TT=(T+459.67)/1000.0$$

$$V1=1.0/(56.099-6.9828*TT-0.5942*TT**2.0+0.0498*TT**3.0)$$
 SV=S
 IF (S3.GT.SV) GO TO 411

$$X4S=(S3-SL)/SPG$$

$$H4S=HL+X4S*HFG$$

$$H4=H3-2*PP*(H3-H4S)$$
 IF (H4.GT.HV) GO TO 412
 S1=SL
 H1=HL

$$X4=(H4-H1)/HFG$$

$$S4=X4*SPG+S1$$

$$VFG=V-V1$$

$$V4=X4*VFG+V1$$
 P4=P
 CALL, SIM(H1,H2,H3,H4,P3,P4,QB,CF,V1,DOTM,EFFK,OVEFF,PK,TKW)
 MDOT=DOTM
 P1=P4
 PRINT227,P3,T3,P1,T1
 PRINT225,H1,S1,V1,H2,H3,S3,V3,H4,S4,V4
 PRINT228,MDOT,EFFK,PK,OVEFF
 PRINT285,X4

$$HRK=(H3-H2)*MDOT/PWK*0.001*BFAC$$

$$HRT=(H3-H2)*MDOT/TKW*0.001*BFAC$$
 PRINT350,HRK,HRT


```

IP(KIM.EQ. 1) GO TO 1
DELHK=H4-H1
QIN=HDOT*(H3-H2)
QUAV=MDOT*TATH*(S4-S1)
PKT=PK/0. 98
PT=PKT+PST
GO TO 1001
411 SPREV=SV
HPREV=HV
VPREV=V
T=T+50.0
CALL SUPER (P,T,H,S,V)
SV=S
HV=H
IP(S3.GT.SV) GO TO 411
HNEW=HV
SNEW=SV
VNEW=V
-128-
RAT3=(S3-SPREV)/(SNEW-SPREV)
H4S=HPREV+RAT3*(HNEW-HPREV)
H4=H3-EFF*(H3-H4S)
IP(H4.LT.H NEW) GO TO 413
414 HPREV=HNEW
SPREV=SNEW
VPREV=VNEW
T=T+50.0
CALL SUPER (P,T,H,S,V)
HNEW=H
SNEW=S
VNEW=V
IP(H4.GT.H NEW) GO TO 414
413 RAT4=(H4-HPREV)/(HNEW-HPREV)
S4=SPREV+RAT4*(SNEW-SPREV)
V4=VPREV+RAT4*(VNEW-VPREV)
P4=P
CALL SIM(H1,H2,H3,H4,P3,P4,QB,CF,V1,DOTM,EPPK,OVEFF,PWK,TKW)

```



```

#DOT=DOTW
P1=P4
PRINT279
PRINT227,P3,T3,P1,T1
PRINT225,H1,S1,V1,H2,H3,S3,V3,H4,S4,V4
PRINT 228,HDOT,EFFK,PWK,CVEPP
HRK=(H3-H2)*#DOT/EFFK*0.001*BPAC
HRT=(H3-H2)*#DOT/TKH*0.001*BPAC
PRINT350,HRK,HRT
IF(KIN.EQ.1) GO TO 1
DELHK=H4-H1
QIN=#DOT*(H3-H2)
QUAV=#DOT*TATH*(S4-S1)
PQT=PQT/0.98
PT=PQT+PST
GO TO 1001
4 12 HPREV=HV
SPREV=SV
VPREV=V
T=T+50.0
CALL SUPER (P,T,H,S,V)
HV=S
SV=S
IF(H4.GT.HV) GO TO 412
HNEW=HV
SNEW=SV
VNEW=V
GO TO 413
C THIS SECTION OF THE PROGRAM EVALUATES THE REGRATIVE FEED HEATING
C CYCLE.
C 200 READ,P,T
C P AND T ARE THE VALUES OF THE REGENERATOR PRESSURE AND TEMPERATURE.
C CALL PRES(P,T)
PRINT276
CALL WET(P,T,H,S,HFG,SFG,HL,SL,V)
HV=H

```



```

SV=S
S6=SL
H6=HL
TT=(T+459.67)/1000.0
V6=1.0/(56.099-6.9828*TT-0.5942*TT**2.0+0.0498*TT**3.0)
SRPG=SPG
HRPG=HRPG
1F (S3.GT.SV) GO TO 250
X4S=(S3-S6)/SRPG
H4S=H6+X4S*HRPG
H4=H3-EFF*(H3-H4S)
1F (H4.LT.HV) GO TO 251
SNEW=SV
HNEW=HV
VNEW=V
GO TO 300
251 X4=(H4-H6)/HRPG
S4=S6+X4*SRPG
VPG=V-V6
V4=V6+X4*VPG
PRINT281
GO TO 400
250 HPREV=HV
SPREV=SV
VPREV=V
T=T+50.0
CALL SUPER (P,T,H,S,V)
HV=H
SV=S
1F (S3.GT.SV) GO TO 250
SNEW=SV
HNEW=HV
VNEW=V
RAT1=(S3-SPREV)/(SNEW-SPREV)
H4S=HPREV+RAT1*(HNEW-HPREV)
H4=H3-EFF*(H3-H4S)

```



```

100 IF (HNEW.GT.H4) GO TO 301
300 SPREBV=SNEW
      HPREV=HNEW
      VPREV=VNEW
      T=T+50.0
      CALL SUPER (P,T,H,S,V)
      SNEW=S
      HNEW=H
      VNEW=V
      IF (H4.GT.HNEW) GO TO 300
301 RAT2=(H4-HPREV)/(HNEW-HPREV)
      S4=SPREV+RAT2*(SNEW-SPREV)
      V4=VPREV+RAT2*(VNEW-VPREV)
      PRINT280
400 P4=P
      READ,P,T
      C P AND T ARE THE PRESSURE AND TEMPERATURE OF THE POTASSIUM CONDENSER.
      CALL PRES(P,T)
      T1=T
      CALL WBT (P,T,H,S,HFG,SFG,HL,SL,V)
      TT=(T+459.67)/1000.0
      V1=1.0/(56.099-6.9828*TT-0.5942*TT**2.0+0.0498*TT**3.0)
      HV=H
      SV=S
      S1=SL
      H1=HL
      IF (S4.GT.SV) GO TO 401
      SCPG=SPG
      HCPG=HPG
      X5S=(S4-S1)/SCPG
      H5S=H1+X5S*HCPG
      H5=H4-EPP*(H4-H5S)
      IP (H5.GT.HV) GO TO 402
      X5=(H5-H1)/HCPG
      S5=S1+X5*SCPG
      VPG=V-V1

```



```

V5=V1+X5*VFG
P1=P
CALL REGEN (H1,H2,H3,H4,H5,H6,P3,P1,CF,QB,V1,EPPK,CMDOT,DOTH,RMDOT,
1TKW,OVEPP,PWK,YY)
MDOT=DCTM
MDOTC=CMDOT
MDOTR=RMDOT
PRINT275,H1,S1,V1,H2,H3,S3,V3,H4,S4,V4,H5,S5,V5,H6,S6,V6
PRINT277,P3,T3,P4,P1,T1
PRINT278,MDOT,MDOTR,MDOTC,YY,PWK,EPPK,OVEPP
HAK=(H3-H6)*MDOT/PWK*0.001*BPAC
HRT=(H3-H6)*MDOT/TKW*0.001*BPAC
PRINT286,X5
PRINT350,HRK,HRT
IF(KIN.EQ.1) GO TO 1
DELHK=H5-H1
QIN=MDOT*(H3-H6)
QUAV=MDOTC*TATH*(S5-S1)
PKT=PWK/0.98
PT=PKT+PST
GO TO 1001
4 02 HNEW=RV
SNEW=SV
VNEW=V
GO TO 404
C 4 01 SPREV=SV
HPREV=HV
VPREV=V
T=T+50.0
CALL SUPER (P,T,H,SV)
SV=S
HV=H
IF(S4.GT.SV) GO TO 401
SNEW=SV
HNEW=HV

```



```

VNEW=V
RAT3=(S4-SPREV)/(SNEW-SPREV)
H5S=HPREV+RAT3*(HNEW-HPREV)
H5=H4-EPP*(H4-H5S)
1P(H5-LT.HNEW) GO TO 403
HPREV=HNEW
SPREV=SNEW
VPREV=VNEW
T=T+50.0
CALL SUPER(P,T,H,S,V)
HNEW=H
SNEW=S
VPREV=V
1P(H5.GT.HNEW) GO TO 404
403 RAT4=(H5-HPREV)/(HNEW-HPREV)
S5=SPREV+RAT4*(SNEW-SPREV)
V5=VPREV+RAT4*(VNEW-SPREV)
C
P1=P
CALL REGEN(H1,H2,H3,H4,H5,H6,P3,P1,CP,QB,V1,EPPK,CMDOT,DOTM,RMDOT,
1TKW,OVEFF,PK,YY)
MDOTr=RMDOT
MDOTC=CMDOT
MDOT=DOTM
PRINT279
PRINT277,P3,T3,P4,P1,T1
PRINT275,H1,S1,V1,H2,H3,S3,V3,H4,S4,V4,H5,S5,V5,H6,S6,V6
PRINT278,MDOT,EDOTR,EDOTC,YY,PK,EPPK,OVEFF
HRK=(H3-H6)*MDOT/PK*0.001*BPAC
HRT=(H3-H6)*MDOT/TKW*0.001*BPAC
PRINT350,HRK,HRT
1P(KIM.EQ.1) GO TO 1
DELHK=H5-H1
QIN=MDOTr*(H3-H6)
QUAV=MDOTC*TATM*(S5-S1)
PKT=PK/0.98

```


PT=PKT+PST

GO TO 1001

350 FORMAT('K PLANT HEAT RATE (BTU/KW (E) HR) ',F11.2/)

1 'TOTAL PLANT HEAT RATE (BTU/KW (E) HR) ',F11.2)

276 FORMAT('RANKINE CYCLE WITH REGENERATING FEED HEATERS')

275 FORMAT('0',H1='P7.2.',BTU/LBM S1='P6.4.',BTU/LBM R V

11='P7.2.',PT**3/LBM'/

3 'H2='P7.2.',BTU/LBM'/

2 'H3='P7.2.',BTU/LBM'/

13='P7.2.',PT**3/LBM'/

3 'H4='P7.2.',BTU/LBM S4='P6.4.',BTU/LBM R V

14='P7.2.',PT**3/LBM'/

3 'H5='P7.2.',BTU/LBM S5='P6.4.',BTU/LBM R V

15='P7.2.',PT**3/LBM'/

2 'H6='P7.2.',BTU/LBM S6='P6.4.',BTU/LBM R V

16='P7.2.',PT**3/LBM')

277 FORMAT('0',TURBINE INLET PRESSURE = 'P6.2.',PSI'/

1 'TURBINE INLET TEMPERATURE = 'P7.2.',DEGREES F'/

1 'REGENERATOR PRESSURE = 'P6.2.',PSI'/

1 'CONDENSING PRESSURE = 'P6.2.',PSI'/

1 'CONDENSING TEMPERATURE = 'P7.2.',DEGREES F')

278 FORMAT('POTASSIUM FLOW RATE = 'P12.2.',LBM/HR'/

1 'EXTRACTION FLOW RATE = 'P12.2.',LBM/HR'/

1 'CONDENSER FLOW RATE = 'P12.2.',LBM/HR'/

1 'AMOUNT EXTRACTED FOR REGENERATION IS ',P6.2.', PERCENT'/

2 'POTASSIUM TURBINE ELECTRICAL POWER = ',P7.2.',MW'/

1 'POTASSIUM TURBINE THERMAL EFFICIENCY = ',P6.2.', PERCE

2NT'/

3 'OVERALL THERMAL EFFICIENCY = ',P6.2.', PERCENT')

279 FORMAT('0',FINAL EXPANSION INTO SUPERHEATED REGION OCCURS FOR THE

1 FOLLOWING CONDITIONS')

280 FORMAT('0',EXTRACTION POINT IS IN SUPERHEATED REGION')

281 FORMAT('0',EXTRACTION POINT IS IN WET REGION')

4 FORMAT('1')

285 FORMAT('0',QUALITY AT TURBINE EXHAUST = ',F7.4)

286 FORMAT('0',QUALITY AT TURBINE EXHAUST = ',F7.4)


```

226 FORMAT(' ', 'SIMPLE RANKINE CYCLE')
227 FORMAT('0', 'TURBINE INLET PRESSURE = ', 'P6.2, ' PSI'/
1   ' ', 'TURBINE INLET TEMPERATURE = ', 'P7.2, ' DEGREES F'/
1   ' ', 'CONDENSING PRESSURE = ', 'P6.2, ' PSI'/
1   ' ', 'CONDENSING TEMPERATURE = ', 'P7.2, ' DEGREES F')
225 FORMAT('0', 'H1 = ', 'P7.2, ' BTU/LBM  S1 = ', 'P6.4, ' BTU/LBM R  V
11 = ', 'P7.2, ' PT**3/LBM'/
3   ' ', 'H2 = ', 'P7.2, ' BTU/LBM'/
2   ' ', 'H3 = ', 'P7.2, ' BTU/LBM  S3 = ', 'P6.4, ' BTU/LBM R  V
13 = ', 'P7.2, ' PT**3/LBM'/
3   ' ', 'H4 = ', 'P7.2, ' BTU/LBM  S4 = ', 'P6.4, ' BTU/LBM R  V
14 = ', 'P7.2, ' PT**3/LBM')
228 FORMAT(' ', 'POTASSIUM FLOW RATE = ', 'P12.2, ' LBM/HR'/
1   ' ', 'POTASSIUM TURBINE THERMAL EFFICIENCY = ', 'P6.2, ' PERCE
2NT'/
2   ' ', 'POTASSIUM TURBINE ELECTRICAL POWER = ', 'P7.2, ' kW'/
3   ' ', 'OVERALL THERMAL EFFICIENCY = ', 'P6.2, ' PERCENT')
C THIS SECTION OF THE PROGRAM ESTIMATES THE SIZE OF THE STREAM
C AND REHEATER.
1001 WI=1420.81
G=GR1
VIS=1.674E-5
TK=T1
TIN=551.7
TOUT=1000.0
PR=1.01
THCON=.03495
HD=262.3
DI=DR1
CALL REHEAT(WI,DI,G,VIS,TK,TIN,TOUT,PR,HD,N,AL,THCON)
AR1=A
ALB1=AL
R1K=WI*HD/DELHK
R1ST=WI
NR1=N
BOILER SIZE

```



```

RI=1793.22
DI=DB
G=GB
VIS=5.796E-5
TIN=550.1
TOUT=1000.0
PR=0.95
THCON=0.3043
HI=545.1
HO=1421.7
CALL BOILER(WI,DI,G,VIS,TK,TIN,TOUT,PR,THCON,HI,HO,N,A,AL)
AB=A
ABL=AL
RBK=WI*(HO-HI)/DELHK
BST=WI
NB=N
PRINT2000,BST,R1ST,RBK,R1K,NB,NR1,ABL,ALR1,AB,AR1,DB,DR1
2000 FORMAT('0','22X','STEAM BOILER','8X','REHEATER','/
1      ','STEAM (LBM/SEC) ','P12.2,8X,P12.2/
1      ','K (LBM/SEC) ','P12.2,8X,P12.2/
1      ','TUBES ','I12,8X,I12/
1      ','LENGTH (FT) ','P12.2,8X,P12.2/
1      ','AREA (FT**2) ','P12.2,8X,P12.2/
1      ','DIAM (IN) ','F12.3,8X,P12.3)
C THIS SECTION OF THE PROGRAM PERFORMS THE SECOND LAW ANALYSIS OF THE
C BINARY CYCLE.
QAV=QB-QUAV
QUIN=QAV-PST*CPF
BQUIPT=QUIN/(1000.0*PT)
ETAI=(PKT*CPF+QAV)/QIN*100.0
PCTDEC=(ETAI-OVEPP)/ETAI*100.0
QIN=QIN*FACTOR
QB=QB*FACTOR
QUAV=QUAV*FACTOR
QUIN=QUIN*FACTOR
PRINT2010,QIN,QB,QUAV,QUIN

```



```

2010 FORMAT('0','HEAT ADDITION (BTU/HR*E-9) ',F8.
12/   ' , 'HEAT REJECTED BY K CYCLE (BTU/HR*E-9) ',F8.
12/   ' , 'UNAVAILABLE ENERGY DUE TO ENVIRONMENT (BTU/HR*E-9) ',F8.
12/   ' , 'INCREASE IN UNAVAILABLE ENERGY (BTU/HR*E-9) ',F8.
12) PRINT2011,RQUIPT,PT,OVEPP,PCTDEC
2011 FORMAT(' ','RATIO-UNAVAILABLE ENERGY TO POWER(BTU/KW HR) ',F8.
12/   ' , 'TOTAL POWER OUTPUT (MW MECH) ',F8.
12/   ' , 'OVERALL EFFICIENCY(PERCENT) ',F8.
12/   ' , 'DECREASE IN EFFICIENCY DUE TO INCREASE IN ',F8.
12) TENAV=1183.155
      DTOT=(T1+459.67-TENAV)/(T1+459.67)
      PRINT2013,ETOT
2013 FORMAT(' ','DELTAT ON T = ',F7.4)
      AT=AB+AR1
      PPA=AT/(PT*0.9735)
      PRINT2012,PPA
2012 FORMAT(' ','K CONDENSER AREA PER KW = ',F9.2,' PT**2/KW')
      GO TO 1
1000 STOP
      END

```


SUBROUTINE REGEN(H1,H2,H3,H4,H5,H6,P3,P1,CP,QB,V1,EPPK,CHDOT,DOTh,
C THE SUBROUTINE REGEN EVALUATES THE PARAMETERS FOR A TIPPING CYCLE WHICH
C IS A REGENERATIVE FEED HEATING CYCLE.

```
1RDOT,TKH,CVEPP,PK,YY)
H2=(P3-P1)*V1*0.18509+H1
Y=(H6-H2)/(H4-H2)
EPPK=(H3-H4)+(1.0-Y)*(H4-H5-H2+H1)/(H3-H6)
CHDOT=QB/(H5-H1)
DOTh=CHDOT/(1.0-Y)
RDOT=DOTh-CHDOT
HKK=(H3-H4+(1.0-Y)*(H4-H5-H2+H1))*DOTh
PK=HKK*0.9800/CP
EPPK=(H3-H4)+(1.0-Y)*(H4-H5-H2+H1)/(H3-H6)
TKH=PK*937.2
OVEPP=TKH*CP/(DOTh*(H3-H6)*0.9800)
Y=100.0*Y
EPPK=100.0*EPPK
OVEPP=100.0*OVEPP
      RETURN
      END
```


PGM 6

```
SUBROUTINE SIM(H1,H2,H3,H4,P3,P4,OB,CP,V1,DOTM,EPPK,OVEPP,PKW,TKW)
C   THE SUBROUTINE SIM EVALUATES THE PARAMETERS OF THE BINARY CYCLE FOR
C   A STOPPING CYCLE WHICH IS A SIMPLE RANKINE CYCLE.
C
H2=H1+V1*(P3-P4)*0.18509
EPPK=(H3-H4-H2+H1)/(H3-H2)
DOTM=OB/(H4-H1)
WKK=(H3-H4-H2+H1)*DOTM
PKW=WKK*0.9800/CF
TKW=PKW+937.2
OVEPP=TKW*CP/(DOTM*(H3-H2)*0.9800)
EPPK=100.0*EPPK
OVEPP=100.0*OVEPP
RETURN
END
```


Thesis

165504

P364 Pesar

An evaluation of the
potassium-steam bi-
nary cycle.

3 SEP 76

DISPLAY

Thesis

165504

P364 Pesar

An evaluation of the
potassium-steam bi-
nary cycle.

thesP364
An evaluation of the potassium-steam bin



3 2768 001 98007 1
DUDLEY KNOX LIBRARY

□